SECOND-ORDER LIMIT-SWITCHED LOOP

By

© S.K. TANG

A Thesis
Submitted to the School of Graduate Studies
in Partial Fulfilment of the Requirements
for the Degree
Master of Engineering

McMaster University

April 1979

SECOND-ORDER LIMITED-SWITCHED LOOP

MASTER OF ENGINEERING (1979)
(Electrical Engineering)

McMASTER UNIVERSITY
Hamilton, Ontario

TITLE: Second-Order Limit-Switched Loop

AUTHOR: Siu-Keung Tang

B.Sc. (West Virginia Institute of Technology, 1976)
B.A. (York University, 1975)
Dipl. (Hong Kong Polytechnic, 1970)

SUPERVISOR: Dr. D.P. Taylor

NUMBER OF PAGES: x, 118

ABSTRACT

Time Division Multiple Access (TDMA) or burst mode operation of a communication system requires that synchronization be achieved within an alloted preamble time or else the entire data burst may be lost. A conventional phase-locked loop occasionally exhibits a prolonged lock-up time known as hangup, especially when the initial phase error falls within the neighbourhood of 180 degrees, and is therefore not suitable for synchronization of this type of system. The main purpose of this work is to extend the investigation of a modified phase-locked loop which is termed a limit-switched loop (LSL). The LSL offers a faster lock-up time and lower probability of hangup. The transient probability density function (pdf) of the phase error for a first-order LSL and the steady-state pdf of the phase error for the second-order LSL have been obtained, using Fokker-Planck techniques. Simulations and experimental methods have been used to obtain the probability of hangup on a low frequency model which also reveals the optimum range for the switching time.

ACKNOWLEDGEMENTS

The author wishes to express his deep gratitude to his supervisor, Dr. D.P. Taylor, who suggested the research topic and for his valuable advice and fruitful suggestions during the course of this investigation.

Special thanks to Miss Anissa Lee for her understandings and encouragement necessary to accomplish this work.

In addition, I would like to thank Miss Pat Dillon of the Word Processing Centre for typing this thesis.

TABLE OF CONTENTS

TABLE OF CONTENTS (continued)

TABLE OF CONTENTS (continued)

LIST OF ILLUSTRATIONS

LIST OF ILLUSTRATIONS (continued)

LIST OF ILLUSTRATIONS (continued)

CHAPTER 1

INTRODUCTION

1.1 Introduction

Narrow-band, tuned filters have been used instead of phase-locked loops in many time division multiple access (TDMA) carrier recovery subsystems. This is because phase-locked loops sometimes exhibit a prolonged lock-up or acquisition time which is referred to as the hangup effect and which severely degrades communication system performance. However, tuned filters have their own defects and the phase-locked loop has certain advantages over the tuned filters particularly in steady-state operation. A phase-locked loop is therefore preferred if the hangup problem can be solved. In this thesis, a modified phase-locked loop which can greatly reduce the probability of hangup is investigated.

1.2 TDMA Basis

Communication via satellite has the advantage of multiple access capability, that is, several users, separated by long distances can simultaneously communicate with each other. The multiple access scheme known as FDM/FDMA (frequency division multiplex/ frequency division multiple access) has been used for many years. This scheme provides excellent quality and service, but has an inefficient working flexibility. Any changes in an established FDMA communications link or in link transmission capacities may affect all users. There is also a bandwidth-power relationship problem. In order to conserve bandwidth and to prevent interference between different channels, the travelling wave tube (TWT) amplifier of a satellite transponder cannot operate at or near saturation. Thus optimum power efficiency cannot be achieved [1].

Recently satellite TDMA has gained worldwide attention because of its high efficiency. Several satellite earth stations can share a common transponder by transmitting periodic bursts of signal in a sequential and non-overlapping mode, wherein a periodic time slot is preassigned to each station.

Some of the major advantages of the TDMA are listed below [2,3]:

1. No intermodulation products are developed within the satellite transponder due to amplifier nonlinearity.
2. Higher satellite power efficiency can be achieved since only one carrier exists at any given instant, and the transponder may be operated in saturation.
3. The frequency plan is simplified since all earth stations use the same transmit and receive frequency.

4. Higher system flexibility is achieved. The capacity of each earth station can be changed rapidly and easily by reassignment of time slot and/or burst lengths to meet traffic variations.
5. TDMA is directly compatible with developing terrestrial digital voice and data networks.

Synchronization is required in a TDMA system so that bursts will not overlap with each other. Failure to obtain accurate synchronization will greatly decrease communication efficiency and cause high rates of error in those parts of bursts where overlap occurs.

Burst synchronization can be subdivided into the acquisition process and the normal or tracking operation [4]. Acquisition is the process of entering into an assigned time slot without interfering with other bursts already present in the system. Normal operation is the process of maintaining synchronization after the success of the acquisition process.

A typical TDMA frame and burst format [5] is shown in Fig. 1.1. During the acquisition process the preamble bits (carrier and bit timing recovery bits, unique word, station identification code) are transmitted. This preamble burst is placed at the centre of the assigned time slot. The syncrhonizer will then upon successful acquisition automatically align the preamble burst to the starting

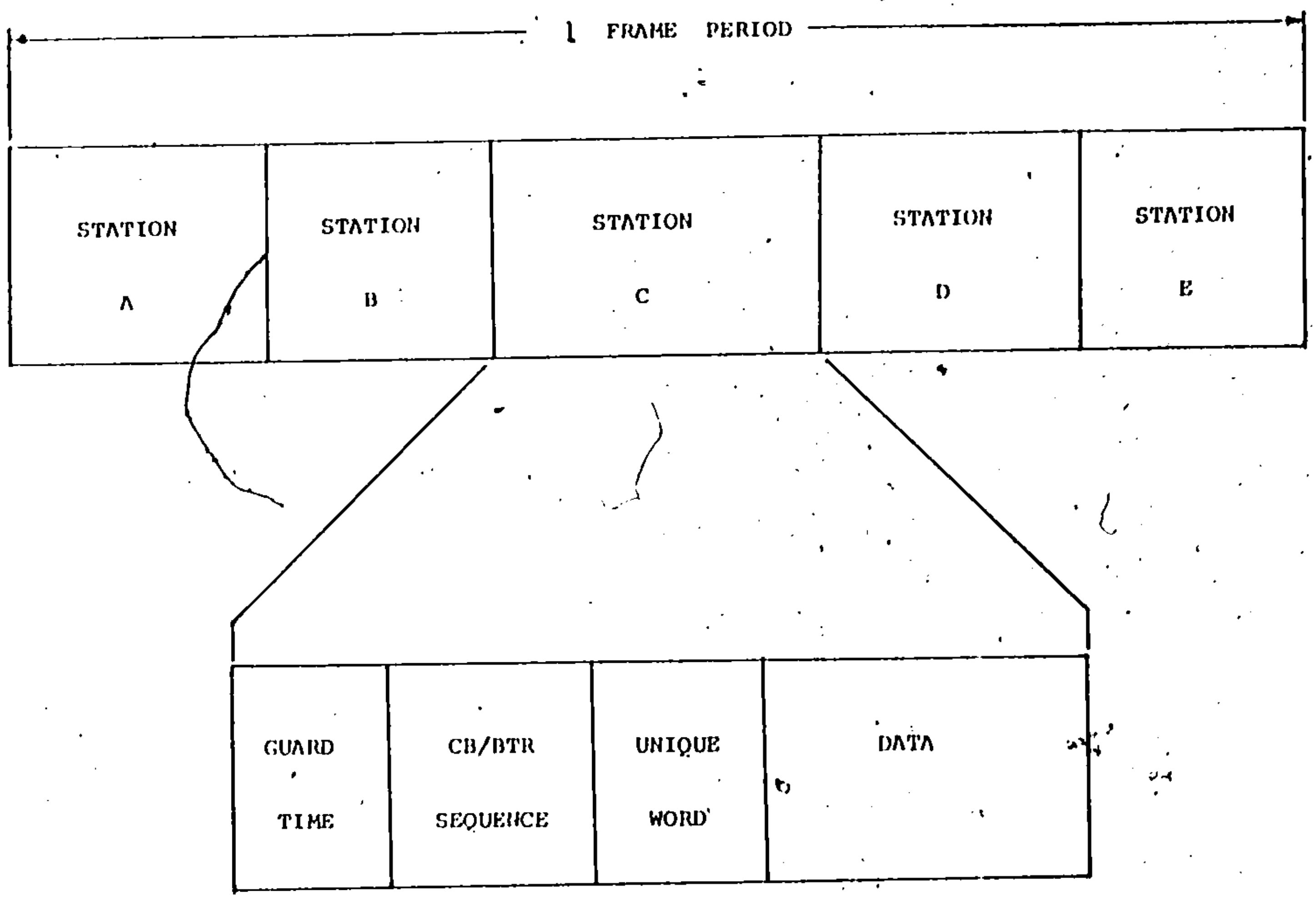

Figure 1.1 Typical TDMA frame and burst formats

position of the time slot. The information bits are then added to each burst and normal operation starts. In normal operation, timing control is achieved by comparing in phase the detected station identification code and the local station unique word. Any timing error is then corrected. This phase-error detection-correction holds the system in continuous synchronization. Carrier phase control is achieved by synchronizing the receiver local oscillator and clock to the carrier phase and bit timing sequence in the burst preamble. Therefore it is apparent that if synchronization is not achieved within the alloted preamble the burst is lost. This causes impulses or "clicks" in voice traffic, and in data transmission, large blocks of data are lost.

1.3 Hangup Effect

Conventional phase-locked loops sometimes exhibit a prolonged lock-in or phase acquisition time, especially when the initial phase error falls in the vicinity of 180 degrees, the unstable null of the phase detector characteristic. This is known as the hangup effect [6]. This hangup effect becomes a severe problem in burst mode digital communications where fast and accurate acquisition is required. The phase-locked loop is required to settle within an alloted synchronization preamble [5] or else the entire data burst may be lost.

Hangup in a phase-locked loop is known to be caused by a weak restoring force and directional equivocation. The restoring force is proportional to the error voltage which is smallest at the two nulls of the phase detector characteristic, as can be seen in Fig. 1.2 which depicts a typical phase detector characteristic. If the initial phase error falls near these unstable nulls, it takes a prolonged time for the loop to move out of this region and hangup is said to have occurred. Noise can be helpful in driving the loop out of its hangup region, however, excessive noise can create a directional equivocation problem. Noise and other disturbances can throw the phase error back and forth across the unstable null for a prolonged period before the error voltage can push the loop out of the hangup region.

Current practice is to use narrow-band, tuned filters to substitute for a phase-locked loop in TDMA synchronizers in order to avoid hangup [7]. The filters must be very precisely tuned to avoid unwanted phase shifts and phase transients, and an automatic frequency control (AFC) device is also required. The resulting equipment becomes overly complex and has certain other unwanted characteristics. Different types of transients are the main drawback of the tuned filters. Phase transients must be allowed to decay to sufficiently small values before satisfactory coherent

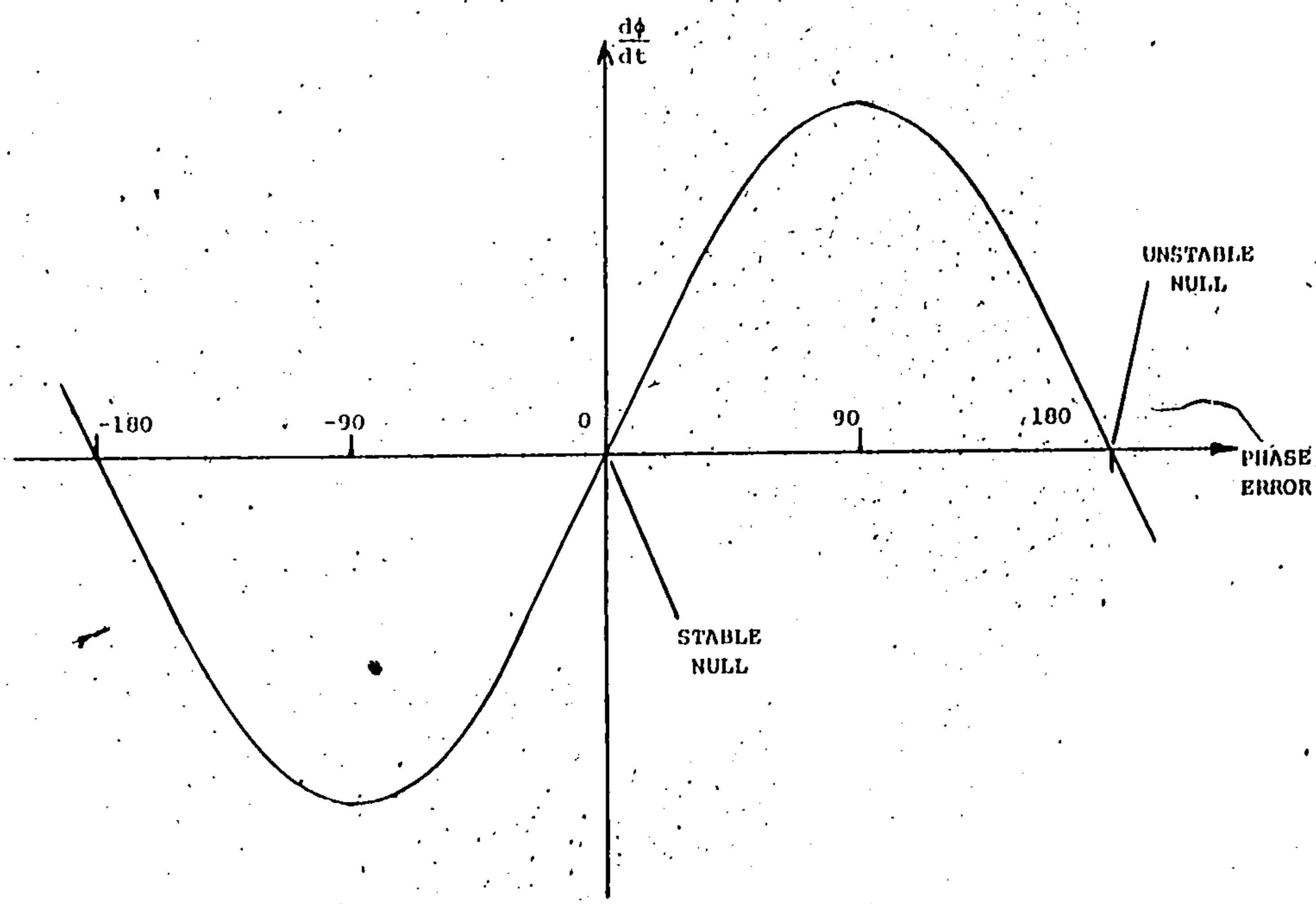

Figure 1.2 Phase-detector characteristic

demodulation or data bit detection can begin. Amplitude transients can be absorbed by a good limiter but a careful design is required to avoid AM-PM conversion in the limiter. On the other hand, a phase-locked loop is simpler to implement and in steady-state it exhibits much superior phase-jitter performance to the tuned filters. Therefore, a hangup-free phase-locked loop should be the optimum choice and it is the purpose of this thesis to investigate such a loop.

1.4 Antihangup Methods

Different ways of eliminating hangup have been suggested [6,7,8,9,10]. Some of these methods are not realizable while others require complex logic control circuits.

It has been suggested that a sawtooth phase detector [8] can eliminate hangups. This is true only in the noiseless case. In real life noise is present in any system, and the phase fluctuations caused by noise can throw the instantaneous phase back and forth across the discontinuity, reducing the rms output of the phase detector. As a result, the discontinuity is replaced by a negative finite slope as shown by dashed lines in Fig. 1.3. Therefore hangup cannot be eliminated but can only be slightly reduced by this method.

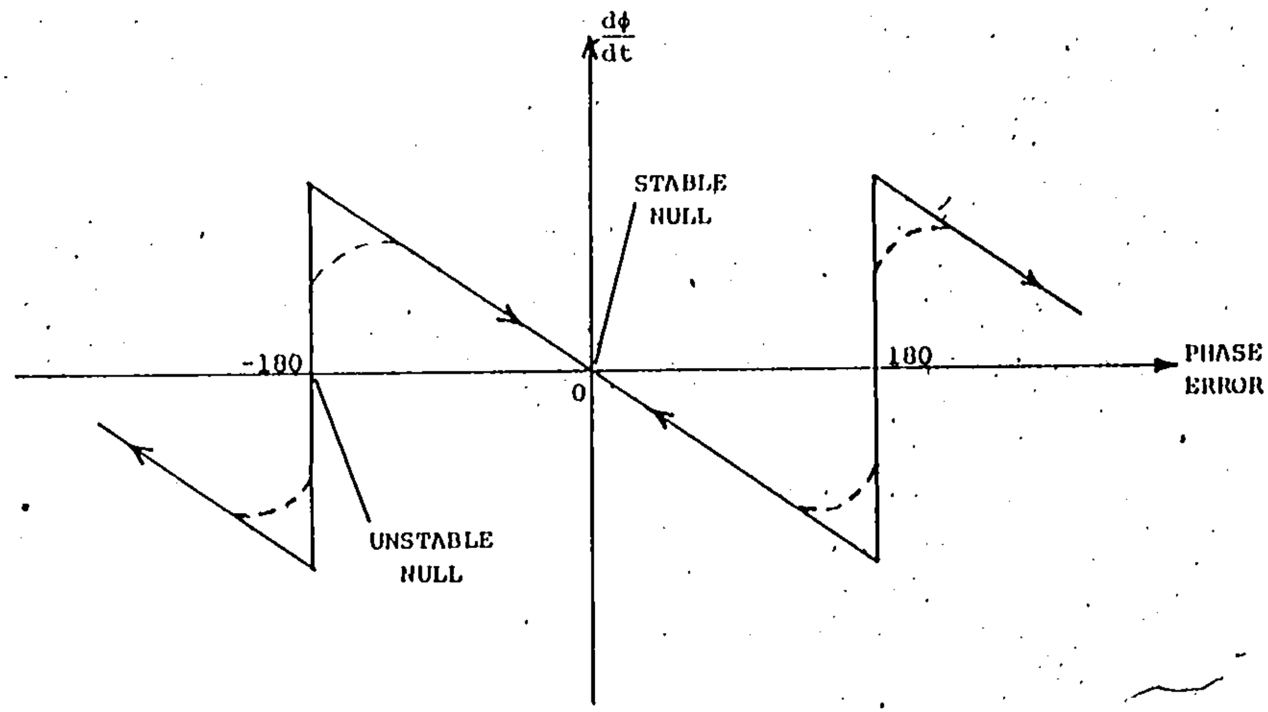

Figure 1.3 Sawtooth phase-detector characteristic

Another is the "kickoff" method [9]. A kickoff pulse is introduced into the loop simultaneously with the introduction of the signal in order to push it out of the hangup region. This method requires a complex control logic to ensure that a correct kickoff pulse is applied at the correct time and in the correct direction. A similar method has been suggested by Gardner [6] in which a large restoring force or slew voltage is applied to the loop whenever the magnitude of the phase error exceeds 90 degrees. This force is shut off whenever the magnitude of the phase error is less than 90 degrees. Such a switching scheme might cause a "bang-bang" situation where the phase error is pushed back and forth across the 90 degree point, and in fact such has been demonstrated by Mariuz [11]. A complex sequential logic is therefore required to prevent reversal of the direction while the slew voltage is turned on. A starting scheme is also required to select a slew direction before applying the slew voltage. This slew voltage is used to slew the phase (that is, offset the frequency) of the voltage-controlled oscillator, VCO.

The sweep method can also be applied to the phase-locked loop to reduce the long pull-in time [10]. Here a sweep voltage is applied to the VCO in order to search for the input frequency. The loop will lock up as the VCO frequency sweeps into the input frequency. In TDMA systems, the frequency of the input signals is known and under tight control (frequency variations are usually less than a few parts in 10^7) by the AFC circuit, and therefore the sweep method does not usually apply here.

The limit-switched loop investigated in this thesis samples the condition of the loop over a predetermined interval and a 180 degrees phase-shift is switched into the loop if hangup is detected. This is equivalent to inverting the loop gain such that the unstable nulls become the stable nulls, as shown in Fig. 1.4. Hangup is therefore eliminated since the hangup region is now changed into the lockup region. The loop will now move towards the previously unstable null until phase-lock is achieved. A certain time is required to elapse before the phase switching decision is made, in order to avoid any possible bang-bang effect across the switching threshold caused by the noise fluctuation.

1.4 Scope of the Thesis

The purpose of this thesis is to extend both theoretically and experimentally the work begun by Mariuz [11] to a second-order loop and to develop a more complete understanding of its transient behaviour. Chapter 2 provides the general operating principles, equations and acquisition behaviour of the first- and second-order limit-switched loop in the absence of noise. Chapter 3

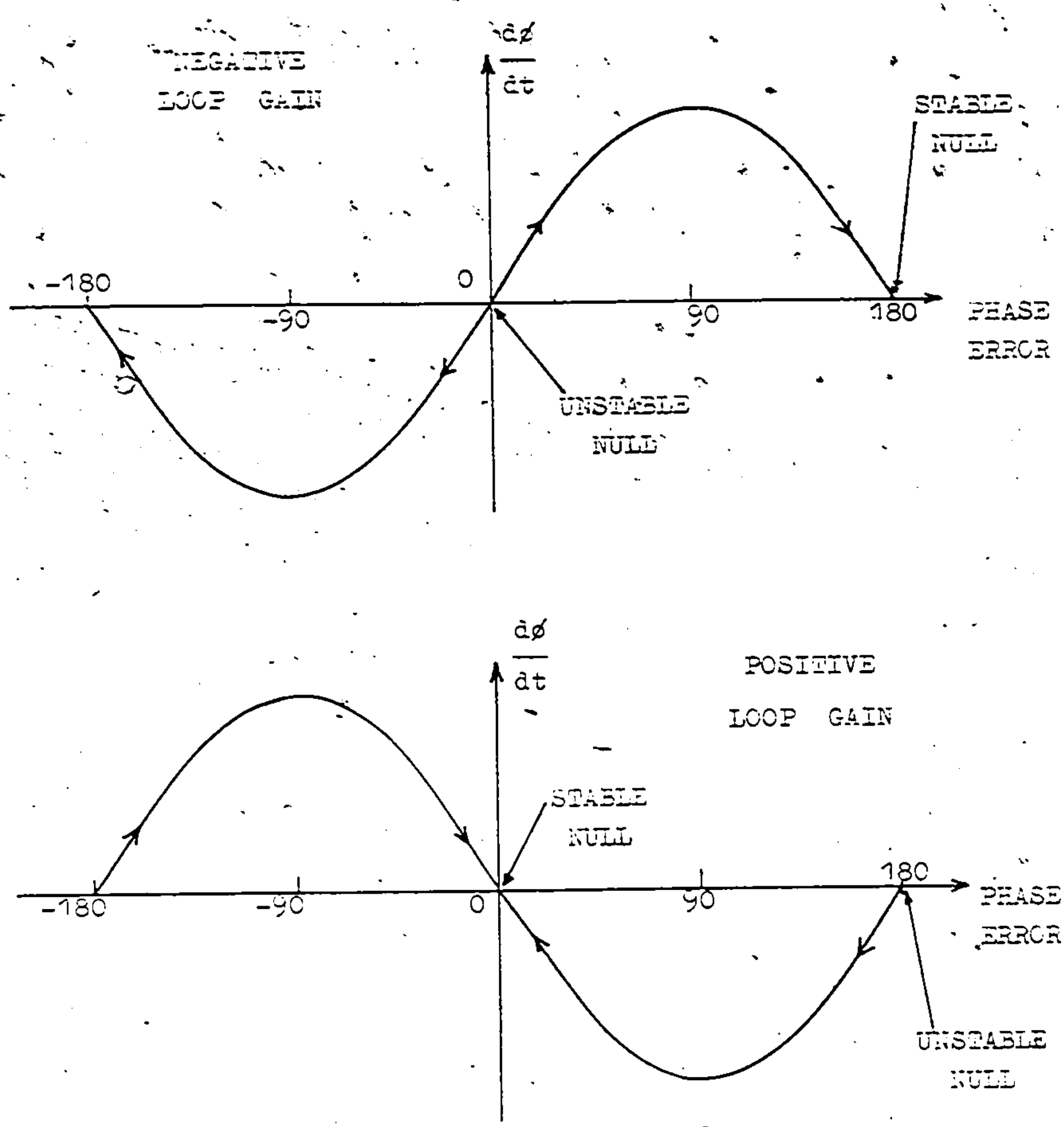

FIG. 1.4 Loop Operating Points

presents a transient analysis of the first-order loop based on the Fokker-Planck equation. Chapter 4 contains a steady-state analysis of the second-order loop and the results obtained are compared with those for a conventional phase-locked loop. Chapter 5 describes a computer simulation method to obtain the probability of hangup and the influences of various loop parameters on the loop performance. Chapter 6 presents an experimental method to obtain the probability of hangup, and this is compared with the computer simulation results. Chapter 7 contains the conclusions reached as a result of the work described in this thesis.

CHAPTER 2

LIMIT-SWITCHED LOOP BEHAVIOUR UNDER NOISELESS CONDITION: LINEAR ANALYSIS

2.1 Introduction

The limit-switched loop equations and operating principles are reviewed. The performance of the limit-switched loop in the absence of noise is presented. This includes analysis of the steady-state phase error and the acquisition behaviour. The resulting simple equations provide a general background to the loop which is helpful both in understanding its operating principles and limitations and in understanding its operation in the presence of noise. The behaviour of the limit-switched loop is analyzed using techniques developed for phase-locked loops. Those with a background in phase-locked loops will find the analysis very easy to follow and straight-forward [12,13].

2.2 First-Order Limit-Switched Loop Equation

The block diagram of the limit-switched loop is shown in Fig. 2.1.

The input signal can be represented by

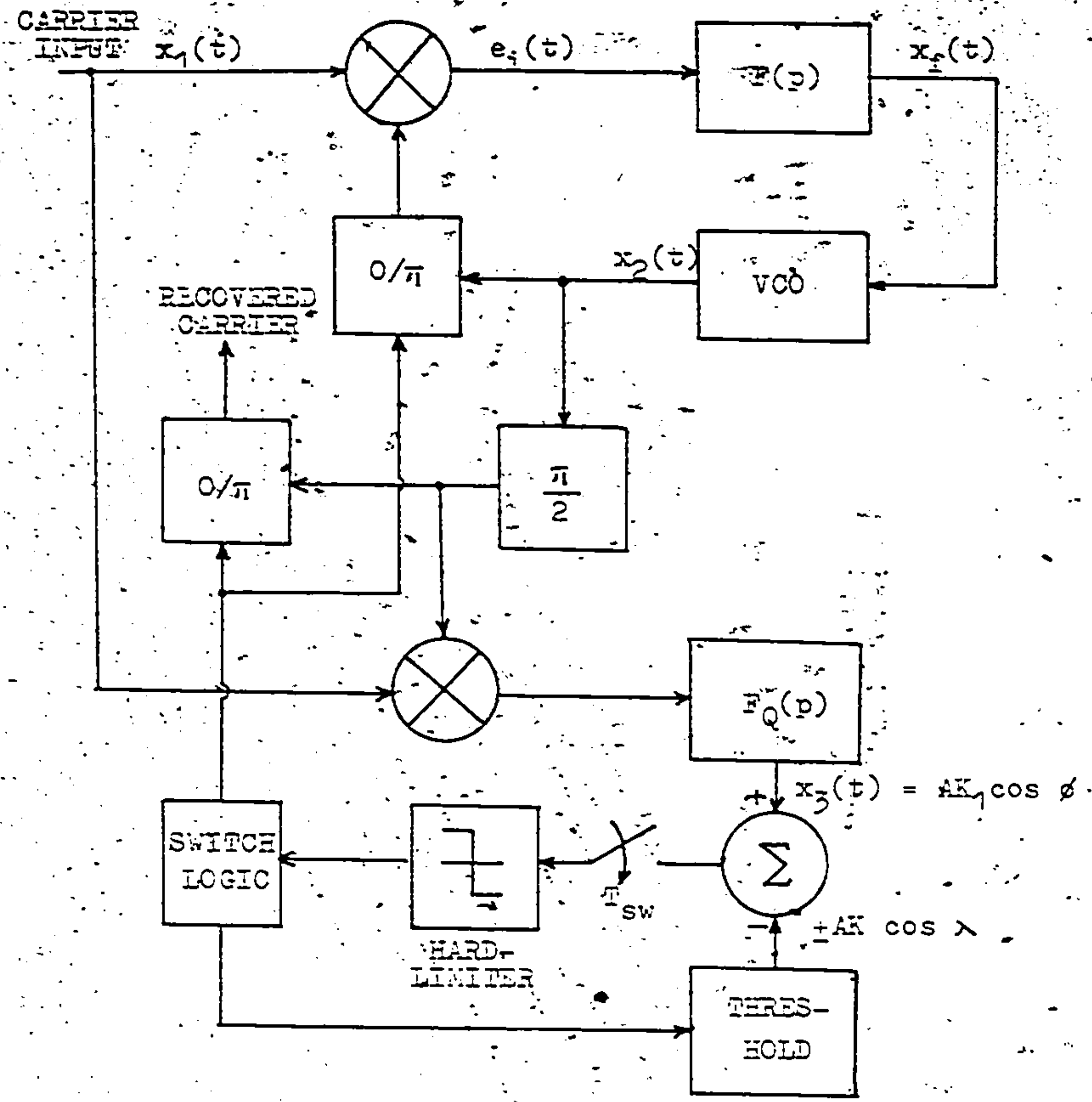

Figure 2.1 The Limit-Switched Loop

Poor Copy

$$x_1(t) = \sqrt{2}\, A \sin(\omega_c t + \theta_1(t))$$

where

A = rms signal amplitude

ω_c = nominal carrier frequency

$\theta_1(t)$ = input phase

Let the VCO output signal be

$$x_2(t) = \sqrt{2}\, K_1 \cos(\omega_c t + \theta_2(t))$$

where

K_1 = rms value of the VCO output

$\theta_2(t)$ = VCO output phase

The output of the low-pass quadrature filter $F_Q(p)$ can then be written as

$$x_3(t) = \{\sqrt{2}\, A \sin(\omega_c t + \theta_1(t))\}\{\sqrt{2}\, K_1 \sin(\omega_c t + \theta_2(t))\}$$
$$= AK_1 \cos \phi(t)$$

where $\phi(t) = \theta_1(t) - \theta_2(t)$, which is defined as the loop phase error.

The difference between the quadrature filter output $x_3(t)$ and the preset switching threshold $AK_1 \cos \lambda$ is used to control the switching logic. The decision threshold λ is taken as $\pm 3\pi/4$ in the non-switch mode and $\pm\pi/4$ in the switched mode.

Defining

$$U(t) \triangleq \cos\phi(t) - \cos\lambda(t)$$

we have

$$x_4(t) = AK_1 U(t)$$

It is clear that $x_4(t)$ will be negative in the hangup region where

$$|\phi| > \lambda$$

and positive otherwise. $x_4(t)$ can then be hard-limited to control the 0 or π phase shifter with a positive value implying a zero phase shift and a negative value implying a 180 degrees phase shift.

The low-pass loop phase detector output can then be denoted by

$$\begin{aligned} e_i(t) &= \{\sqrt{2}\, A \sin(\omega_c t+\theta_1(t))\}\{\sqrt{2}\, K_1 \cos(\omega_c t+\theta_2(t)+S(U))\} \\ &= AK_1 \sin(\phi(t) - S(U)) \\ &= AK_1 \sin\theta(t) \cos(S(U)) \end{aligned}$$

where

$$S(U) \triangleq 0 \qquad |\phi| \leq \lambda$$

$$S(U) \triangleq \pi \qquad |\phi| > \lambda$$

$e_i(t)$ is passed through the loop filter $F(p)$ which results in an output signal

$$e_f(t) = \int_0^t e_i(t-\tau)\ f(\tau)\ d\tau\ .$$

$$= \int_0^t AK_1 \sin\phi(t) \cos(S(U))\ f(t-\tau)\ d\tau$$

Defining

$$\frac{d\theta_2(t)}{dt} \triangleq K_2\ e_f(t),$$

we may therefore write

$$\frac{d\theta_2(t)}{dt} = AK \int_0^t f(t-\tau) \sin\phi(\tau) \cos(S(U))\ d\tau \quad (2.1)$$

where $K = K_1K_2$.

The loop equation then becomes

$$\frac{d\phi(t)}{dt} = \frac{d\theta_1(t)}{dt} - \frac{d\theta_2(t)}{dt} \quad (2.2)$$

Substituting (2.1) in (2.2), we have

$$\frac{d\phi(t)}{dt} = \frac{d\theta_1(t)}{dt} - AK \int_0^t f(t-\tau) \sin\phi(\tau) \cos(S(U))\ d\tau \quad (2.3)$$

or in operator notation

$$\phi(t) = \theta(t) - \frac{AKF(p)\ \sin\phi(t)\ \cos(S(U))}{p} \quad (2.4)$$

where $p = \frac{d}{dt}$ is the linear differential operator.

Equation (2.4) is identical to the loop equation of a convention phase-locked loop except for the switching function cos (S(U)).

In Fig. 2.1 it can be seen that the limit-switched loop consists of a loop phase detector, a loop filter and a VCO which are the main building blocks of a phase-locked loop. Output from the quadrature filter is compared with a threshold every T_{sw} sec. and is then hard-limited to control the 0 or π phase-shifter. It is best to have the settling time T_s of the quadrature filter equal to the switching time T_{sw} [11]. The feedback from the switching logic to the threshold block is to keep track of the status (in non-switch or switched mode) of the loop so as to provide a correct threshold value.

2.3 First-Order Limit-Switched Loop Equation

For the first-order loop $F(p) = 1$, and equation (2.4) then becomes

$$\phi(t) = \theta_1(t) - \frac{AK \sin \phi(t) \cos (S(U))}{p} \qquad (2.5)$$

Let the received signal be a constant frequency ω rad/sec with an initial phase θ_o. Then

$$\theta_1(t) = (\omega - \omega_c)t + \theta_o$$

For small ϕ, $\sin \phi(t) \approx \phi(t)$ and this allows us to linearize equation (2.5). Substituting $\theta_1(t)$ into equation (2.5) and taking the Laplace transform, we obtain, for $|\phi| \leq \lambda$

$$\phi(s) = \frac{\omega - \omega_c}{s(s + AK)} + \frac{\theta_o}{(s + AK)}$$

or

$$\phi(t) = \frac{\omega - \omega_c}{AK} (1 - e^{-AKt}) + \theta_o e^{-AKt} \qquad (2.6)$$

To obtain the steady-state phase error we take the limit of equation (2.6) for large time t to obtain

$$\lim_{t \to \infty} \phi(t) = \frac{\omega - \omega_c}{AK} \text{ radians for } |\phi| \leq \lambda \qquad (2.7)$$

For $|\phi| > \lambda$, the loop gain is inverted and the lock point becomes 180 degrees, and therefore it can be shown that the steady-state phase error becomes

$$\lim_{t \to \infty} \phi(t) = \pi - \frac{\omega - \omega_c}{AK} \text{ radians for } |\phi| > \lambda \qquad (2.8)$$

This indicates that a first-order limit-switched loop can never achieve zero phase error with a constant frequency input which differs from the VCO free-running frequency and an initial phase. It is clear from Fig. 2.2 or equation (2.5) that if $(\omega - \omega_c) > AK$, no stable lock points exist and the loop starts skipping cycles and will never achieve phase lock [14].

2.4 Acquisition Behaviour of First-Order Loop

Equation (2.5) can be written as

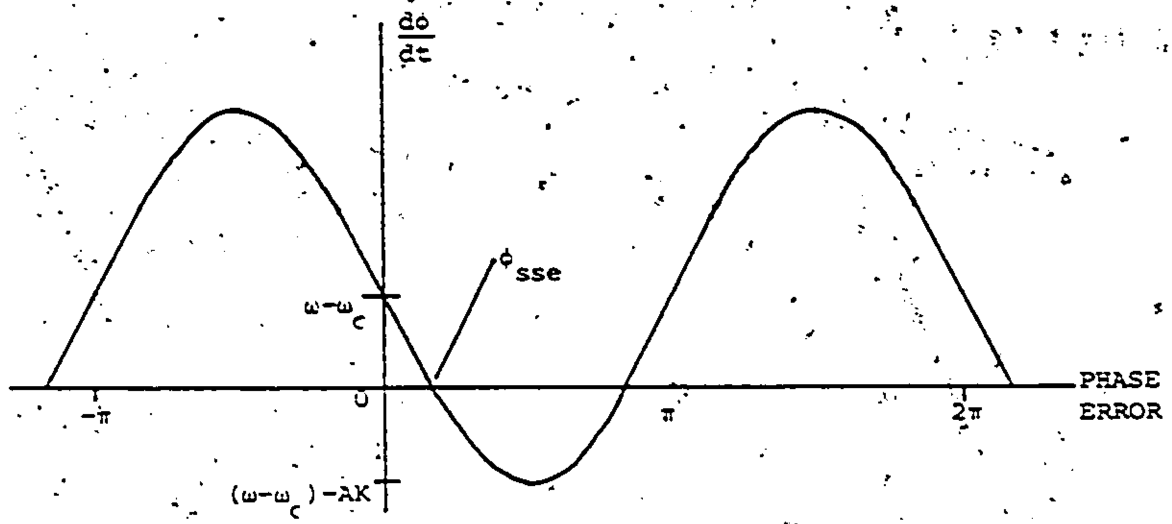

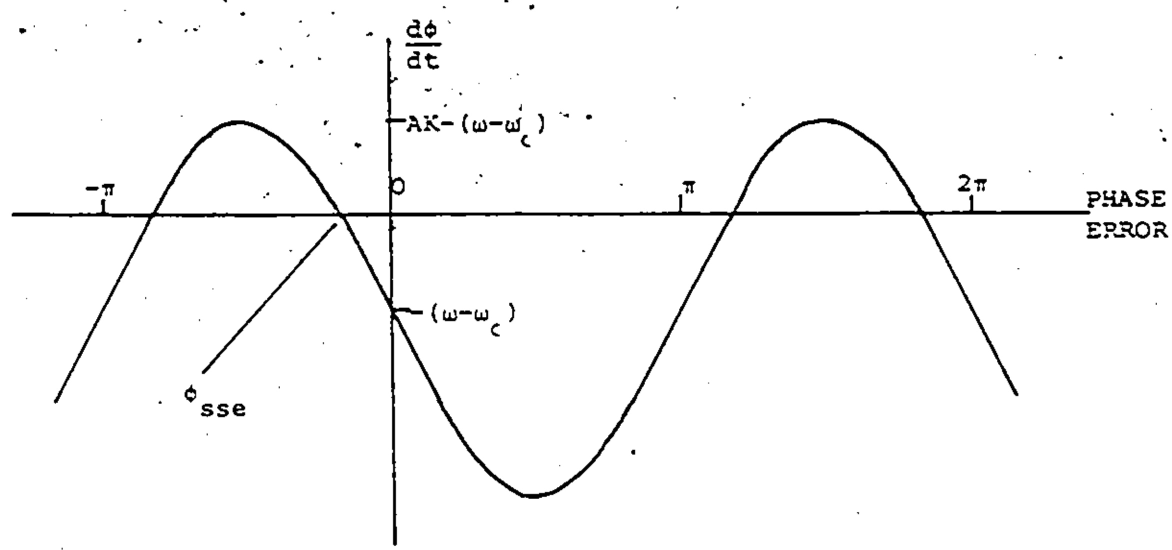

Figure 2.2 System Trajectories for First-Order Loop

Poor Copy

$$\frac{d\phi(t)}{dt} = \frac{d\theta_1(t)}{dt} - AK \sin \phi(t) \cos (S(U))$$

Assuming zero detuning and rearranging, we have

$$dt = \frac{d\phi(t)}{- AK \sin \phi(t) \cos (S(U))} \tag{2.9}$$

For $|\phi| \leq \lambda$, the time required for the loop to achieve lock is obtained by integrating (2.9),

$$t_{acq,\phi=\phi_o} = \int_{\phi}^{\phi_L} \frac{d\phi(t)}{-AK \sin \phi(t)}$$

$$= \frac{- \ln [\tan(\phi_L/2) \cot (\phi_o/2)]}{AK} \tag{2.10}$$

where

ϕ_o = initial phase error

ϕ_L = lock point phase error

Equation (2.10) is identical to that for a conventional phase-locked loop.

The phase angle at which the maximum lock time occurs can be obtained from (2.10). Substitute $t_{acq} = t_{max}$, the maximum lock-up time and $\phi_o = \phi_{t_{max}}$, the phase angle at t_{max} in (2.10), after rearranging, we have

$$\phi_{t_{max}} = 2 \tan^{-1} (\tan(\phi_L/2)\ e^{AKt_{max}})$$

where $t_{max} = T_{sw} + t_{acq,\phi=\lambda}$

For $|\phi_o| > \phi_{t_{max}}$, we may write the total lock-in or acquisition time as

$$t_L = T_{sw} + t_{acq,\phi=180^\circ-|\phi_o|} \tag{2.11}$$

and for $|\phi_o| < \phi_{t_{max}}$ as

$$t_L = t_{acq,\phi=|\phi_o|} \tag{2.12}$$

The relation between the lock-up time and the initial phase error is plotted in Fig. 2.3 using (2.11) and (2.12). It is clear that under noiseless condition, the optimum value of λ for shortest average acquisition time is 90 degrees.

The transient phase error is shown in Fig. 2.4. The trajectories below the threshold (135 degrees) at T_{sw} will lock to 0 degree while the trajectories above the threshold at T_{sw} will lock towards 180 degrees. It can be seen that the limit-switched loop reduces the lock-up time drastically compared with the conventional phase-locked loop under noiseless operation, when the initial phase errors are in the vicinity of 180 degrees.

2.5 Second-Order Limit-Switched Loop Equation

For a second-order loop with a perfect integrator, we have

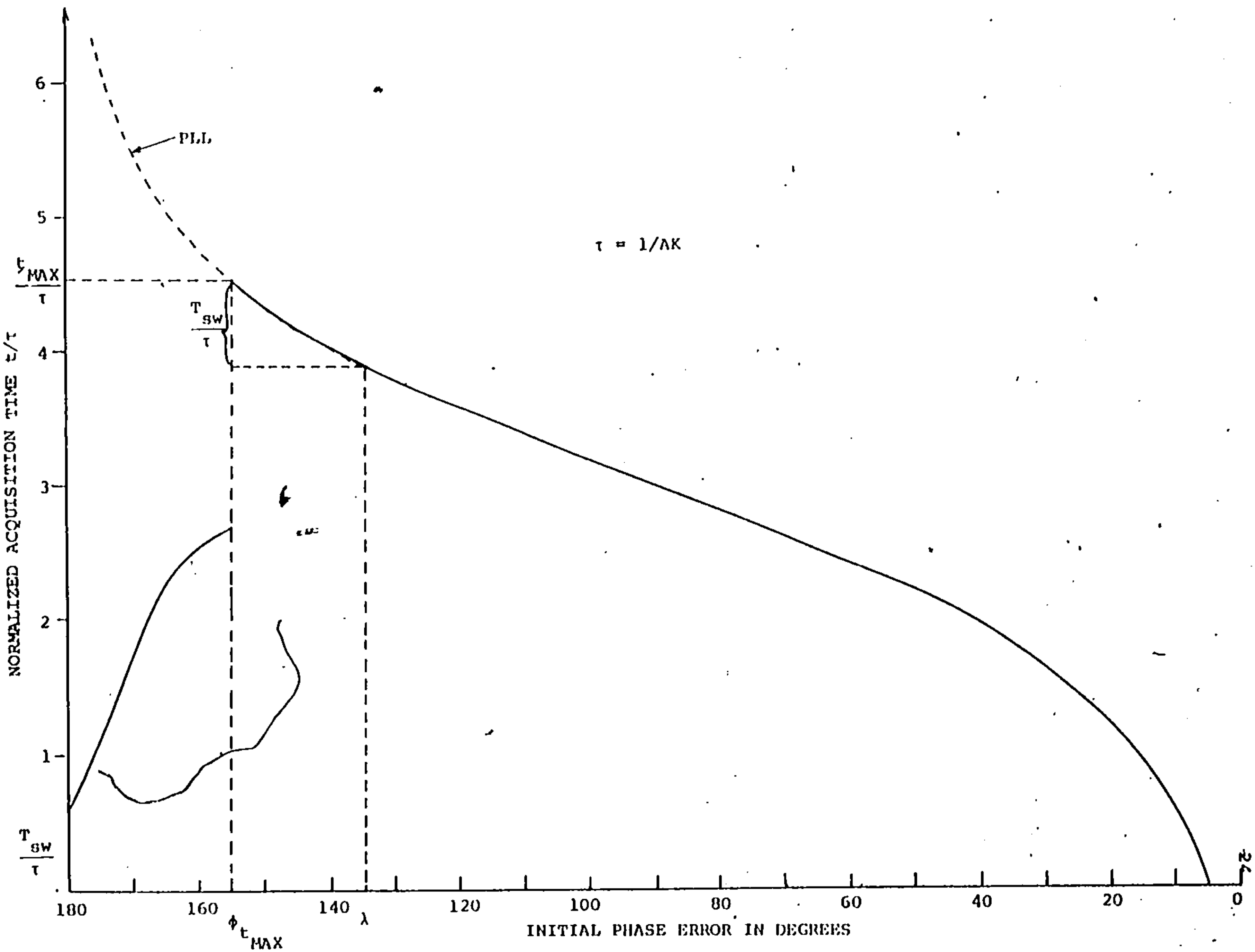

Figure 2.3 Noise-free acquisition times for a first-order limit-switchedbloop

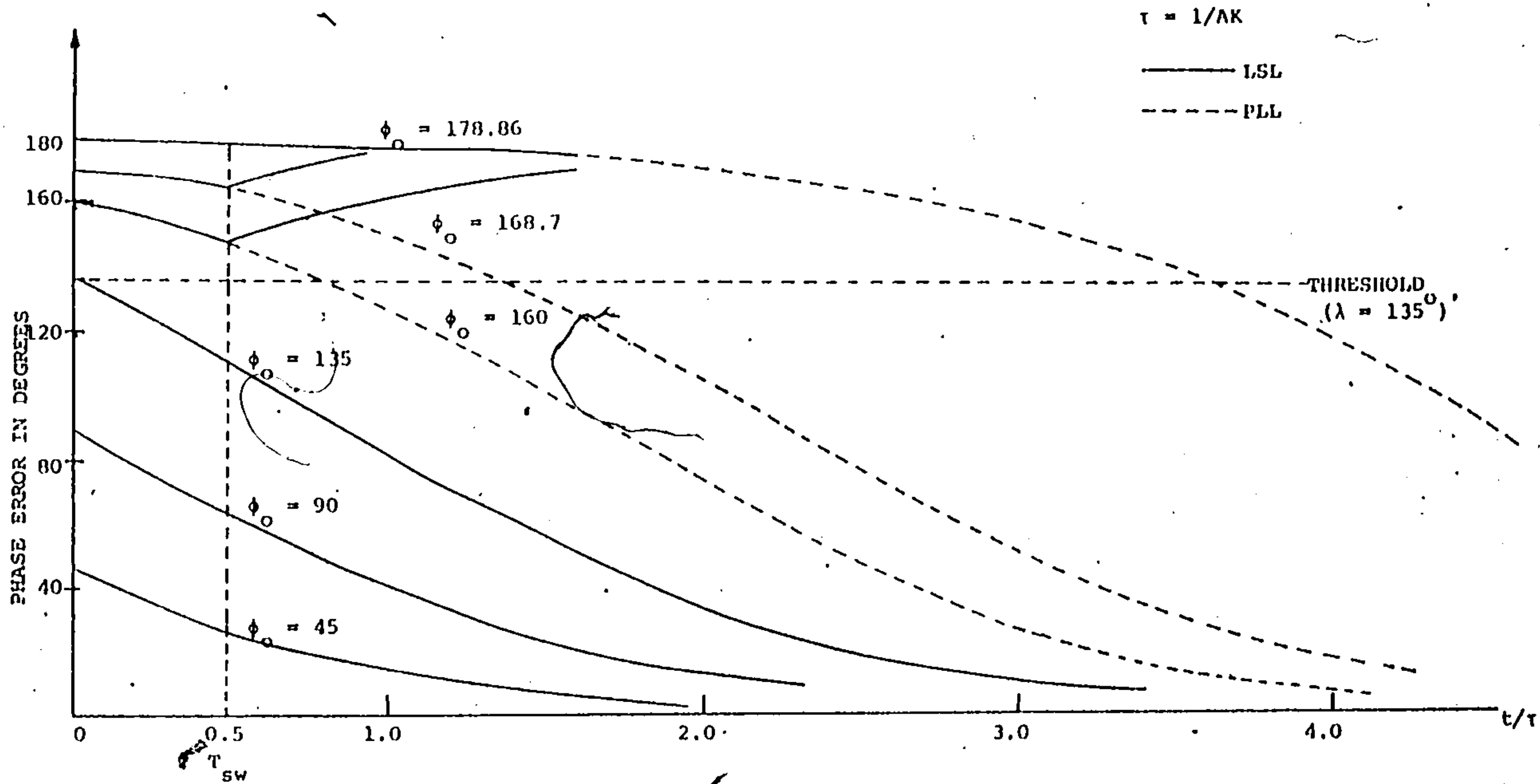

Figure 2.4 Transient phase error for a first order loop

$$F(s) = 1 + \frac{a}{s} \tag{2.13}$$

Taking the Laplace transform of (2.5) and substituting (2.13) into it, we obtain

$$\phi(s) = \frac{s\left(\frac{\omega - \omega_c}{s^2} + \frac{\theta_o}{s}\right)}{s \pm AK\left(1 + \frac{a}{s}\right)}$$

$$= \frac{(\omega - \omega_c) + \theta_o s}{s^2 \pm AKs \pm aAK} \tag{2.14}$$

Applying the final value theorem, (2.14) becomes

$$\lim_{t \to \infty} \phi(t) = \lim_{s \to o} s\phi(s) = 0 \qquad \text{for } |\phi| \leq \lambda \tag{2.15}$$

$$= \pi \qquad \text{for } |\phi| > \lambda \tag{2.16}$$

Equation (2.15) and (2.16) indicate that a second-order loop with a perfect integrator can achieve lock with no steady-state error in the presence of an initial frequency offset.

In real life, integrators are not perfect and the transfer function of the filter becomes

$$F(s) = \frac{s + a}{s + \varepsilon}$$

Using the same approach, we have

$$\phi(s) = \frac{s(s + \varepsilon)}{s^2 + (AK + \varepsilon)s + aAK}\left(\frac{\omega - \omega_c}{s^2} + \frac{\theta_o}{s}\right)$$

and its steady-state error is

$$\lim_{t\to\infty} \phi(t) = \lim_{s\to 0} \phi(s) = \frac{\varepsilon(\omega - \omega_c)}{aAK} \text{ radians for } |\phi| \leq \lambda \quad (2.17)$$

$$= \pi - \frac{\varepsilon(\omega - \omega_c)}{aAK} \text{ radians for } |\phi| > \lambda \quad (2.18)$$

It can be seen that (2.17) and (2.18) are the steady-state error for a first-order loop attenuated by the factor ε/a. By choosing a small value of ε and a large value of a, the imperfect integrator can be made to approach very closely to the perfect integrator case.

2.6 Acquisition Behaviour of Second-Order Loop

Substituting (2.13) into (2.4), we have

$$\frac{d\phi(t)}{dt} = \frac{d\theta(t)}{dt} \mp AK\left(1 + \frac{a}{d/dt}\right) \sin\phi(t) \quad \begin{array}{l} -\text{ve for } |\phi| \leq \lambda \\ +\text{ve for } |\phi| > \lambda \end{array} \quad (2.19)$$

Differentiating through, (2.19) becomes

$$\frac{d^2\phi}{dt} = \mp AK \cos\phi \frac{d\phi}{dt} \mp aAK \sin\phi \quad (2.20)$$

Letting $t = \tau/AK$, $a' = a/AK$, $\dot{\phi} = d\phi/dt$, (2.20) can be written as

$$\ddot{\phi} = \mp \dot{\phi} \cos\phi \mp a' \sin\phi \quad (2.21)$$

or

$$\frac{d\dot{\phi}}{dt} = \mp \cos\phi \mp \frac{a'\sin\phi}{\dot{\phi}} \quad (2.22)$$

By plotting $\dot{\phi}$ versus ϕ, we can obtain a family of curves known as phase plane trajectories [13]. We can see from (2.22) that the equation is periodic in ϕ with period 2π and that the trajectories become sinusoidal if $\dot{\phi}$ is large. The phase plane tranjectories for (2.22) are shown in Fig. 2.5. The trajectories are traversed from left to right in the upper half plane and vice versa in the lower half plane. It can be seen that as the trajectory traverses from $-\pi$ to $+\pi$, there is a small decay and the rate of decay will increase until the value of $\dot{\phi}$ is below the line A-A. The loop will then stop skipping cycles and phase lock will be rapidly achieved. During each cycle of 2π, the value of $\dot{\phi}$ decreases for any initial value of $\dot{\phi}$, therefore the pull-in range of a second-order loop with a perfect integrator is infinite. The points at even multiples of π are stable points and the points at odd multiples of π are unstable points (saddle points) or vice versa when the loop is in the switched mode.

For a conventional phase-locked loop, the points at or near a saddle-point separatrix exhibit a prolonged phase-lock acquisition time and this is where the hangup occurs. A separatrix diagram is shown in Fig. 2.6. It can be seen that any initial phase error that falls on a separatrix will never achieve phase-lock under noiseless condition, and it will jitter back and forth across the ϕ axis under high SNR conditions. For a limit-switched loop, the saddle point

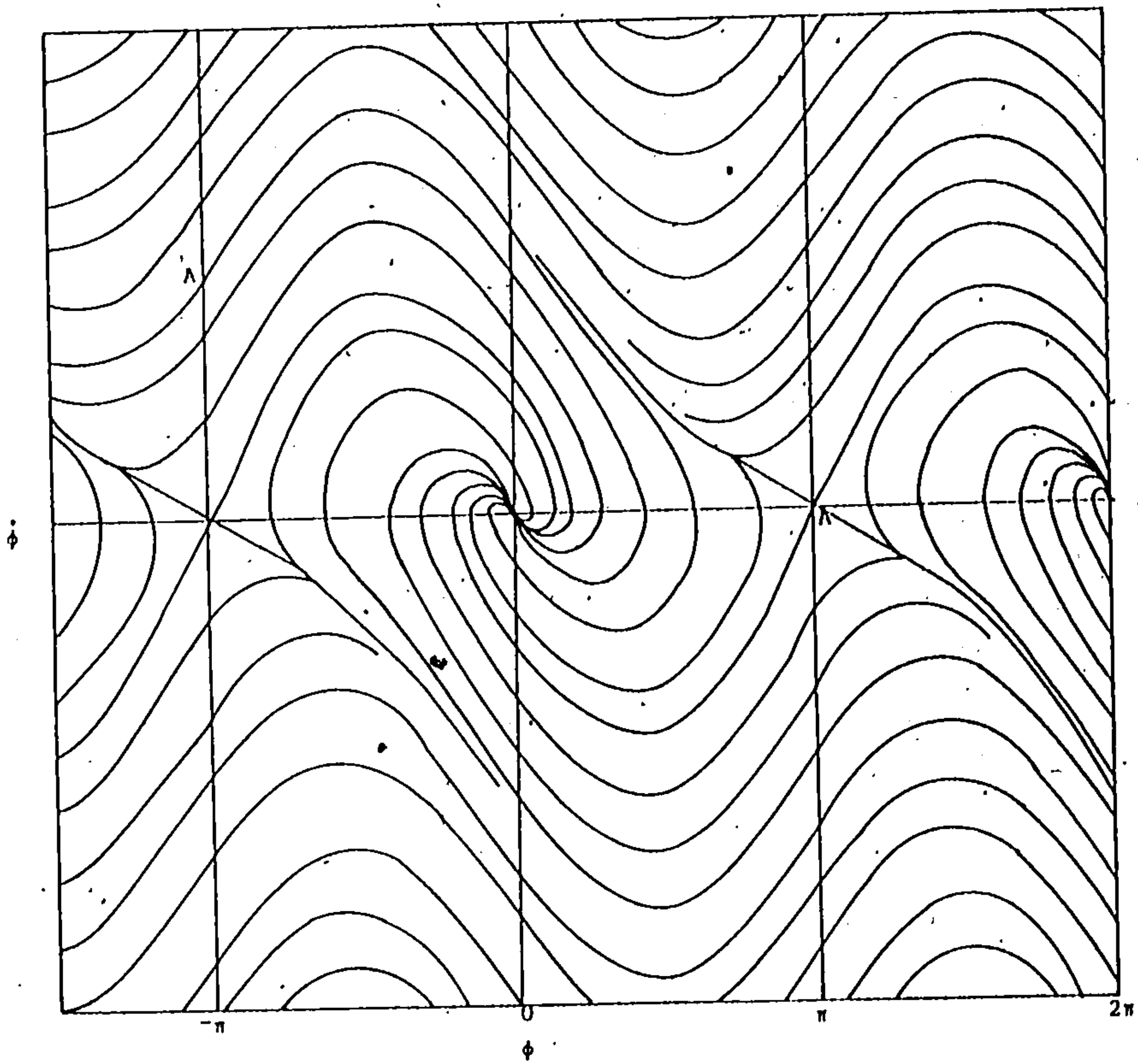

Figure 2.5 Phase plane trajectories for second-order loop

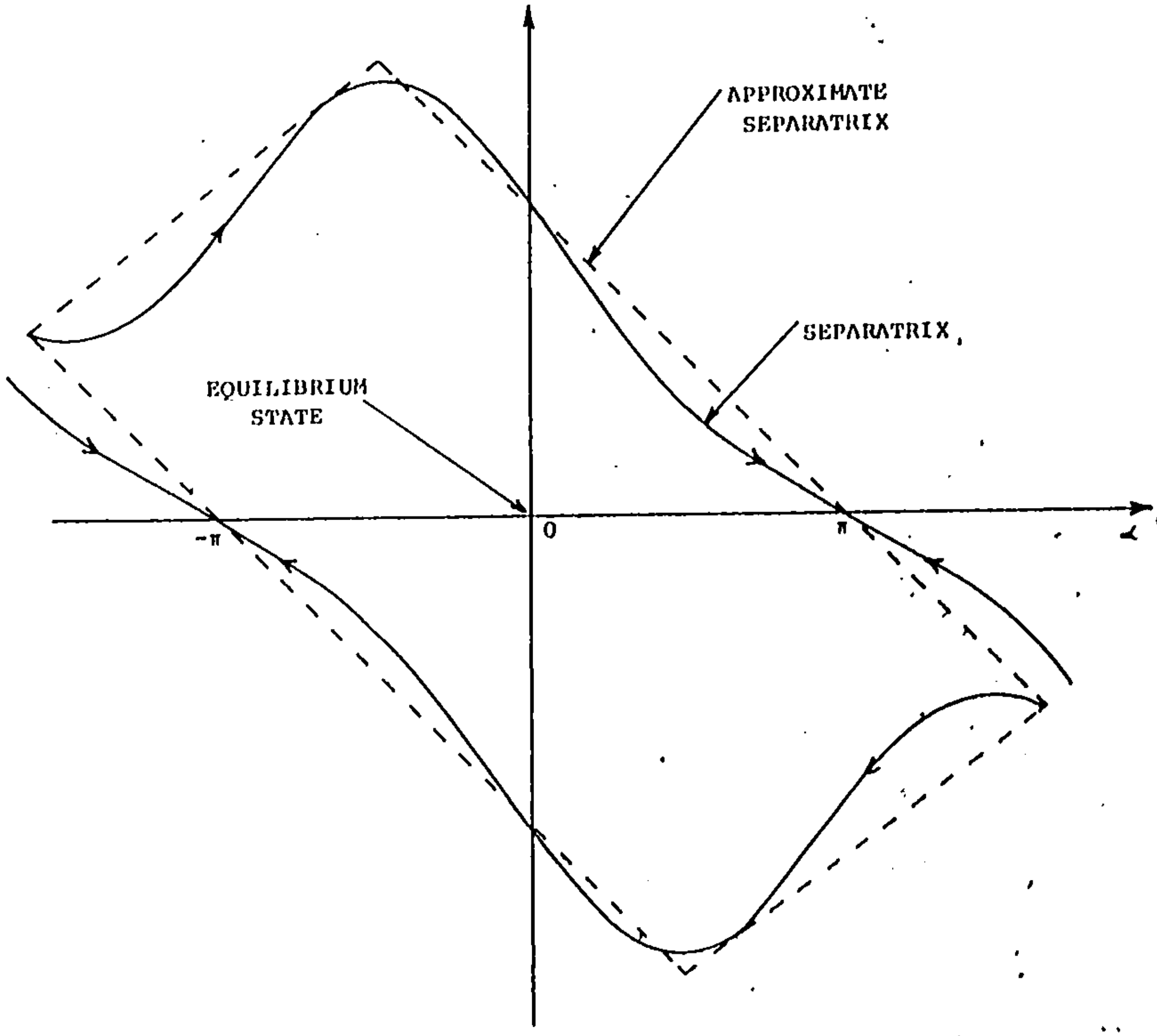

Figure 2.6 Separatrices of phase portrait

separatrix will be switched into a stable point if hangup is detected at T_{sw} and the loop will be phase-locked within a short time interval after that.

2.7 Conclusion

In the absence of noise, the limit-switched loop can be thought of as the combination of two phase-locked loops separated 180 degrees apart with their hangup portions chopped off. This combination results in a hysteresis loop as shown in Fig. 2.7. Analysis of a hysteresis loop seems impossible with the presently available mathematical tools, but it is clear from the figure that no hangup regions exist.

In practice, the second-order loop is the one being most widely used. This is because the second-order loop has many advantages over the first-order loop while the third-order loop has a stability problem in low SNR operations. In the first-order loop, only the loop gain K can be adjusted, if it is necessary to have a large loop gain the bandwidth must also be large. Therefore, narrow bandwidth and good tracking are incompatible in the first-order loop. Other major advantages of the second-order loop over the first-order loop are lower steady-state phase errors and higher tolerable frequency offset. The values of the steady-state error and the maximum tolerable frequency

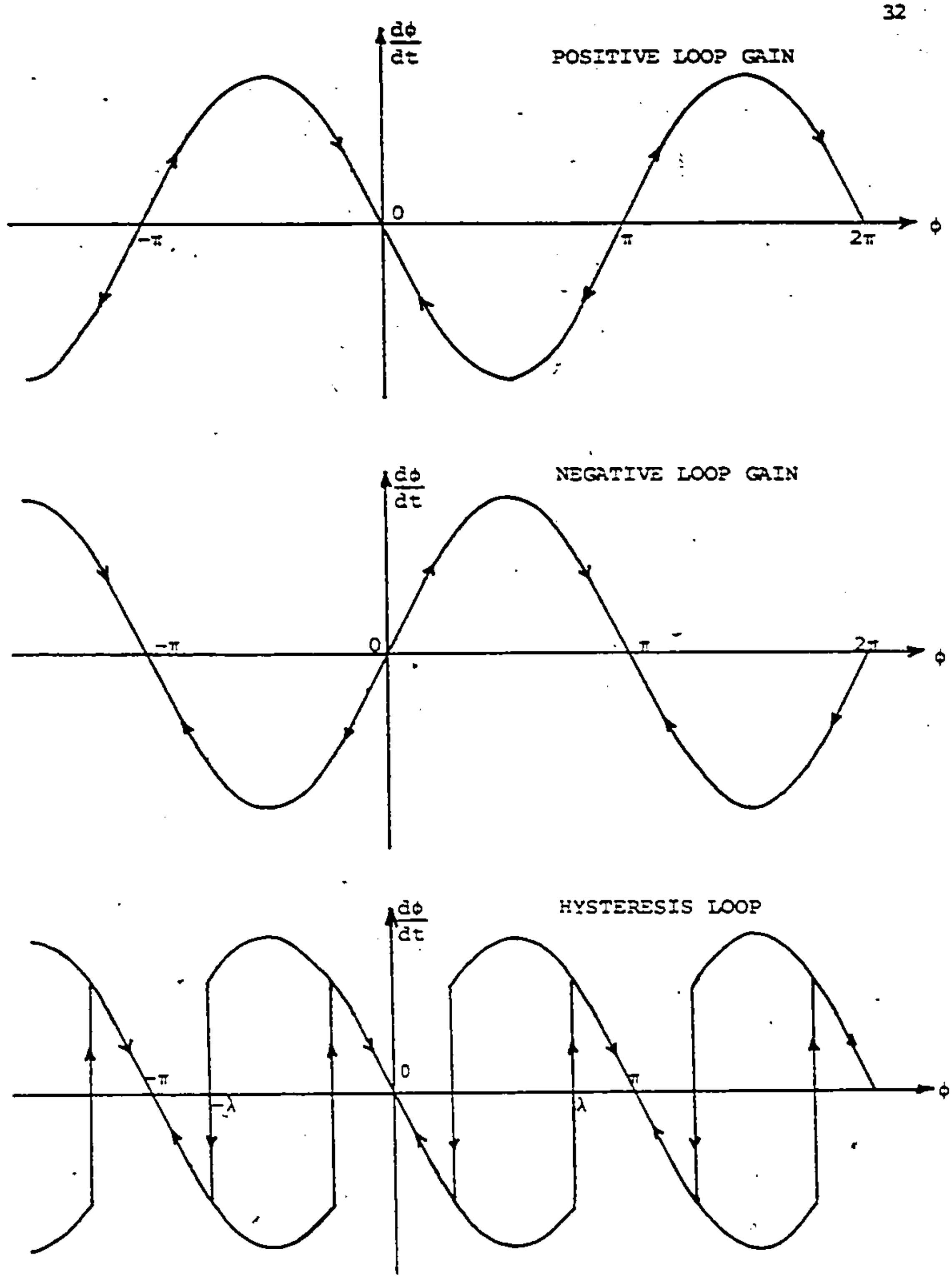

Figure 2.7 Hysteresis loop characteristic

offset (before cycle slipping would occur) are listed in Fig. 2.8.

INPUT $\theta(t) = (\omega t + \theta_o)$	STEADY-STATE ERROR		MAXIMUM TOLERABLE FREQ. OFFSET	
	NON-SWITCH MODE	SWITCHED MODE	NON-SWITCH MODE	SWITCHED MODE
FIRST-ORDER LOOP	$\frac{(\omega - \omega_c)}{\Lambda K}$	$\pi - \frac{(\omega - \omega_c)}{\Lambda K}$	ΛK	ΛK
SECOND-ORDER LOOP WITH PERFECT INTEGRATOR	ZERO	π	INFINITE	INFINITE
SECOND-ORDER LOOP WITH IMPERFECT INTEGRATOR	$\frac{\varepsilon(\omega - \omega_c)}{\Lambda K}$	$\pi - \frac{(\omega - \omega_c)}{\Lambda K}$	$\frac{a\Lambda K}{\varepsilon}$	$\frac{a\Lambda K}{\varepsilon}$

Figure 2.8 Steady-state error and frequency offset limitations of first-, second-order limit-switched loop

CHAPTER 3

TRANSIENT ANALYSIS OF THE FIRST-ORDER LIMIT-SWITCHED LOOP

3.1 Introduction

The behaviour of both the first-order and second-order limit-switched loops in the absence of noise has been investigated in Chapter 2. The analysis is by no means complete without considering the effect of noise on the performance of the loop. This chapter deals specifically with the transient behaviour of the first-order loop in the presence of noise. The steady-state behaviour of the first-order loop in noise has already been developed by Mariuz [11]. Here, a time dependent probability density function of the phase error is obtained by the Fokker-Planck technique. The Fokker-Planck equation is normalized to a dimensionless form and the probability density function of the phase error is obtained by the method of finite differences and successive approximations.

3.2 Limit-Switched Loop Equations in the Presence of Noise

A narrow bandpass filter is usually added in front of the receiver to reduce the noise level. The additive noise $n'(t)$ at the output of this filter is assumed to be a zero-mean Gaussian process whose spectral density is essentially flat over the frequency range of the receiver with a value of $N_o/2$ watts/Hz, and symmetrical about the centre frequency $\pm\omega_c$.

The bandpass noise may be represented by [12]

$$n'(t) = \sqrt{2}\, n_1(t) \cos \omega_c t - \sqrt{2}\, n_2(t) \sin \omega_c t \tag{3.1}$$

where $n_1(t)$ and $n_2(t)$ are the in-phase and quadrature noise components respectively. The signal plus noise input can therefore be written as

$$\sqrt{2}\, \{A \sin (\omega_c t + \theta_1(t)) + n_1(t) \cos \omega_c t - n_2(t) \sin \omega_c t\} \tag{3.2}$$

The VCO input to the phase-detector is

$$x_1(t) = \sqrt{2}\, K_1 \cos (\omega_c t + \theta_2(t) + S(U)) \tag{3.3}$$

The low-pass output of the phase-detector is the product of (3.2) and (3.3) with the double-frequency terms deleted, which then yields

$$e_i(t) = AK_1 \sin (\phi(t) - S(U)) + K_1 n_1(t) \cos (\theta_2(t) - S(U)) + K_1 n_2(t) \sin (\theta_2(t) - S(U)) \tag{3.4}$$

Let

$$n(t) = n_1(t) \cos(\theta_2(t) - S(U)) + n_2(t) \sin(\theta_2(t) - S(U)) \tag{3.5}$$

Substituting (3.5) into (3.4), we have

$$e_i(t) = K_1(A \sin \phi(t) \cos S(U) + n(t)) \tag{3.6}$$

Since

$$e_f(t) = F(p)\ e_i(t) \tag{3.7}$$

(3.7) then becomes

$$e_f(t) = F(p)\ K_1\ (A \sin \phi(t) \cos S(U) + n(t)) \tag{3.8}$$

and

$$\frac{d\theta_2}{dt} \triangleq K_2\ e_f(t) = F(p)\ K(A \sin \phi(t) \cos S(U) + n(t)) \tag{3.9}$$

The loop phase error $\phi(t)$ is defined as

$$\phi(t) \triangleq \theta_1(t) - \theta_2(t) \tag{3.10}$$

Differentiation of (3.10) yields

$$\frac{d\phi(t)}{dt} = \frac{d\theta_1(t)}{dt} - \frac{d\theta_2(t)}{dt} \tag{3.11}$$

Substituting (3.9) into (3.11), we obtain

$$\frac{d\phi(t)}{dt} = \frac{d\theta_1(t)}{dt} - F(p)\ K(A \sin \phi(t) \cos S(U) + n(t)) \tag{3.12}$$

(3.12) represents the nonlinear baseband model of the limit-switched loop. For small phase errors, (3.12) can be approximated by a linear model, with sin $\phi(t)$ replaced by $\phi(t)$. That is

$$\frac{d\phi(t)}{dt} = \frac{d\theta_1(t)}{dt} - F(p)\ K\ (A\ \phi(t)\ \cos S(U) + n(t)) \tag{3.13}$$

3.3 Transient Analysis using Fokker-Planck Technique

For a first order loop, $F(p) = 1$, and (3.12) then becomes

$$\frac{d\phi(t)}{dt} = \frac{d\theta_1(t)}{dt} - K\ (A \sin \phi(t)\ \cos S(U) + n(t)) \tag{3.14}$$

or with the detuning represented as a frequency offset ($\omega - \omega_c$),

$$\frac{d\phi(t)}{dt} = (\omega - \omega_c) - K\ (A \sin \phi(t)\ \cos S(U) + n(t)) \tag{3.15}$$

where ω is the input frequency and ω_c is the VCO free-running frequency.

For white noise we have [14]

$$E[n(t_1)\ n(t_2)] = \frac{N_o}{2}\ \delta\ (t_2 - t_1) \tag{3.16}$$

$n(t_1)$ and $n(t_2)$ are orthogonal and independent, and we can therefore conclude that the solution of the differential equation (3.15) is a Markov process [13] and that the probability density function of $\phi(t)$ must then satisfy the Fokker-Planck equation [15], that is,

$$\frac{\partial p(\phi,t)}{\partial t} = -\frac{\partial}{\partial \phi}\{[(\omega - \omega_c) - AK \sin\phi \cos S(U)]\ p(\phi,t)\} + \frac{K^2 N_o}{4}\frac{\partial^2 p(\phi,t)}{\partial \phi^2} \tag{3.17}$$

with initial condition: $p(\phi,0) = \delta\ (\phi - \phi_o)$ (3.18)

Equation (3.17) can be simplified by normalizing it. Let

$B_L = AK/4$ loop noise bandwidth

$\alpha = \frac{A^2}{N_o B_L}$ signal-to-noise ratio

$\gamma = \frac{(\omega - \omega_c)}{4\ B_L}$ detuning factor

$\tau = 4\ B_L\ t$ normalized time

Equation (3.17) then becomes a dimensionless Fokker-Planck equation

$$\frac{\partial p(\phi,\tau)}{\partial \tau} = \frac{\partial}{\partial \phi}\ [(\sin(\phi)\ \cos S(U) - \gamma)\ p(\phi,\tau)] + \frac{1}{\alpha}\frac{\partial^2 p(\phi,\tau)}{\partial \phi^2} \tag{3.19}$$

For $|\phi| \leq \lambda$, the loop is in its normal operating mode ($S(U) = 0$) as a conventional phase-locked loop. Equation (3.19) then becomes

$$\frac{\partial p(\phi,\tau)}{\partial \tau} = \frac{\partial}{\partial \phi}\ [(\sin\phi - \gamma)\ p(\phi,\tau) + \frac{1}{\alpha}\frac{\partial^2 p(\phi,\tau)}{\partial \phi^2}$$

or

$$\frac{\partial p(\phi,\tau)}{\partial \tau} = \cos\phi\ p(\phi,\tau) + (\sin\phi - \gamma)\frac{\partial p(\phi,\tau)}{\partial \phi} + \frac{1}{\alpha}\frac{\partial^2 p(\phi,\tau)}{\partial \phi^2} \tag{3.20}$$

Equation (3.19) can be evaluated numerically by using the central-difference method to approximate the derivatives, that is,

$$\frac{\partial p(\phi,\tau)}{\partial \tau} = \frac{p(\phi,\tau+\Delta\tau) - p(\phi,\tau)}{\Delta\tau} \tag{3.21}$$

$$\frac{\partial p(\phi,\tau)}{\partial \phi} = \frac{p(\phi + \Delta\phi,\tau) - p(\phi,\tau)}{\Delta\phi} \tag{3.22}$$

$$\frac{\partial^2 p(\phi,\tau)}{\partial \phi^2} = \frac{p(\phi + \Delta\phi,\tau) - 2p(\phi,\tau) + p(\phi - \Delta\phi,\tau)}{(\Delta\phi)^2} \tag{3.23}$$

Substituting (3.21), (3.22), (3.23) into (3.20), we obtain, for $|\phi| \leq \lambda$ (non-switched mode),

$$\begin{aligned} p(\phi,\tau+\Delta\tau|NS) &= p_1(\phi,\tau+\Delta\tau) \\ &= (1 + \Delta\tau \cos\phi)\, p_1(\phi,\tau) + \\ &\quad (\sin\phi - \gamma)\frac{\Delta\tau}{\Delta\phi}[p_1(\phi + \Delta\phi,\tau) - p_1(\phi,\tau)] + \\ &\quad \frac{1}{\alpha}\frac{\Delta\tau}{(\Delta\phi)^2}[p_1(\phi+\Delta\phi,\tau) - 2p_1(\phi,\tau) + p_1(\phi-\Delta\phi,\tau)] \end{aligned} \tag{3.24}$$

For $|\phi| > \lambda$, the loop is in its switched mode ($S(U) = \pi$), and using a similar approach, we have

$$\begin{aligned} p(\phi,\tau + \Delta\tau \mid SW) &= p_2(\phi,\tau + \Delta\tau) \\ &= (1 - \Delta\tau \cos\phi)\, p_2(\phi,\tau) + \\ &\quad \frac{1}{\alpha}\frac{\Delta\tau}{(\Delta\phi)^2}[p_2(\phi+\Delta\phi,\tau) - 2p_2(\phi,\tau) + p_2(\phi-\Delta\phi,\tau)] \end{aligned} \tag{3.25}$$

Equations (3.24) and (3.25) represent the probability density function of the phase error at time t, conditioned on the two operating modes. If we can calculate the probability of occurence of each of the two operating modes, $p_1(\phi,\tau + \Delta\tau \mid NS)$ and $p_2(\phi,\tau + \Delta\tau \mid SW)$ can then be added together according to these two weights, giving the overall probability density function $p(\phi, \tau + \Delta\tau)$.

The initial phase error is assumed to be uniformly distributed. Therefore

$$P(|\phi_o| \le \lambda) = \frac{\lambda}{180}, \tag{3.26}$$

and

$$P(|\phi_o| > \lambda) = \frac{180 - \lambda}{180} \tag{3.27}$$

However, because of the noise, the switching decisions can be wrong and this must be taken into account. Consider the hard-limiter input of the loop,

$$U = AK_1 \cos \phi(t) + K_1 N_Q(t) - AK_1 \cos \lambda$$

It can be seen that the noise can bias the switching function U. It has been found that [11]

$$\begin{aligned} P(\cos S(U) = 1) &= Q[-\sqrt{\alpha_Q} (\cos \phi(t) - \cos \lambda)] \\ &= 1 - Q[\sqrt{\alpha_Q} (\cos \phi(t) - \cos \lambda)] \end{aligned} \tag{3.28}$$

and

$$P(\cos S(U) = -1) = Q[\sqrt{\alpha_Q} (\cos \phi(t) - \cos \lambda)] \tag{3.29}$$

where $P(\cos S(U) = 1)$ and $P(\cos S(U) = -1)$ represent the probability of non-switch and the probability of switching respectively, and α_Q is the quadrature channel SNR.

Defining

$$P(NS) \triangleq P(\cos S(U) = 1)\ P(|\phi_o| \leq \lambda) \qquad (3.30)$$

and

$$P(SW) \triangleq P(\cos S(U) = -1)\ P(|\phi_o| > \lambda) \qquad (3.31)$$

and using (3.30) and (3.31) as the proportional weights, we obtain

$$p(\phi,\tau + \Delta\tau) = p\ (\phi,\tau+\Delta\tau|NS)\ P(NS) + p\ (\phi,\tau+\Delta\tau|SW)\ P(SW) \qquad (3.32)$$

Equation (3.32) can then be solved by a digital computer.

3.4 Numerical Results Obtained by Computer Method

Equation (3.32) can be solved numerically by the method of finite differences and successive approximations. Results were obtained for several low SNRs with zero frequency detuning. Results for high SNRs have not been obtained because the curves tend to crowd towards the centre for high SNRs unless observed for a long interval of time. Errors would then tend to accumulate, making the results meaningless.

A finite difference computer mesh of step-sizes $\Delta\tau = \tau_{n+1} - \tau_n$ and $\Delta\phi = \phi_{m+1} - \phi_m$ is used. For the given initial boundary condition, the phase errors are initially small. Then $\sin\phi$ can be approximated by ϕ and (3.24) and (3.25) can be linearized. $p(\phi,\tau)$ is then very closely Gaussian and it has been shown [16] that with $\gamma = 0$ and

$$\phi_o = 0, \quad \text{for } |\phi| \le \lambda$$

$$p(\phi,\tau) = \left[\frac{\alpha}{2\pi(1 - e^{-2\tau})}\right]^{1/2} \exp\left[-\frac{\alpha\phi^2}{2(1 - e^{-2\tau})}\right] \qquad (3.33)$$

and for $|\phi| > \lambda$

$$p(\phi,\tau) = \left[\frac{\alpha}{2\pi(1 - e^{-2\tau})}\right]^{1/2} \exp\left[\frac{\alpha\phi^2}{2(1 - e^{-2\tau})}\right] \qquad (3.34)$$

(3.33) and (3.34) can then be used to obtain the initial boundary values.

A Gaussian function with mean ϕ_o and standard deviation $\sigma_o = \pi/20$ is used to approximate an impulse function at time τ equal to zero. This is because a finite difference method might have a significant error when acting on the extreme discontinuities of a numerical delta function.

For stable convergence of the numerical algorithm, a criterion of stability for partial difference systems [17] indicates that a sufficient condition for convergence is

$$\Delta\tau < \left(\frac{\alpha}{2}\right) (\Delta\phi)^2$$

Here, $\Delta\phi = \pi/50$ and $\Delta\tau = 0.001\ \alpha$ have been used.

The results were plotted in Fig. 3.1. The curves are symmetrical and so it is necessary only to plot between 0 and 180 degrees. The curves are all normalized to unit area for the modulo-2π probability density function, i.e.,

$$\int_{-\pi}^{\pi} p(\phi,\tau) = 1.$$

It is interesting to note that there is a small buildup of probability of 180 degrees. This is because in the switched mode, 180 degrees becomes the lock-point. The threshold is set at 135 degrees and not at 90 degrees, therefore the buildup at 180 degrees is smaller than the one at 0 degree. If the threshold is set at 90 degrees, the two buildups are expected to be equal [11].

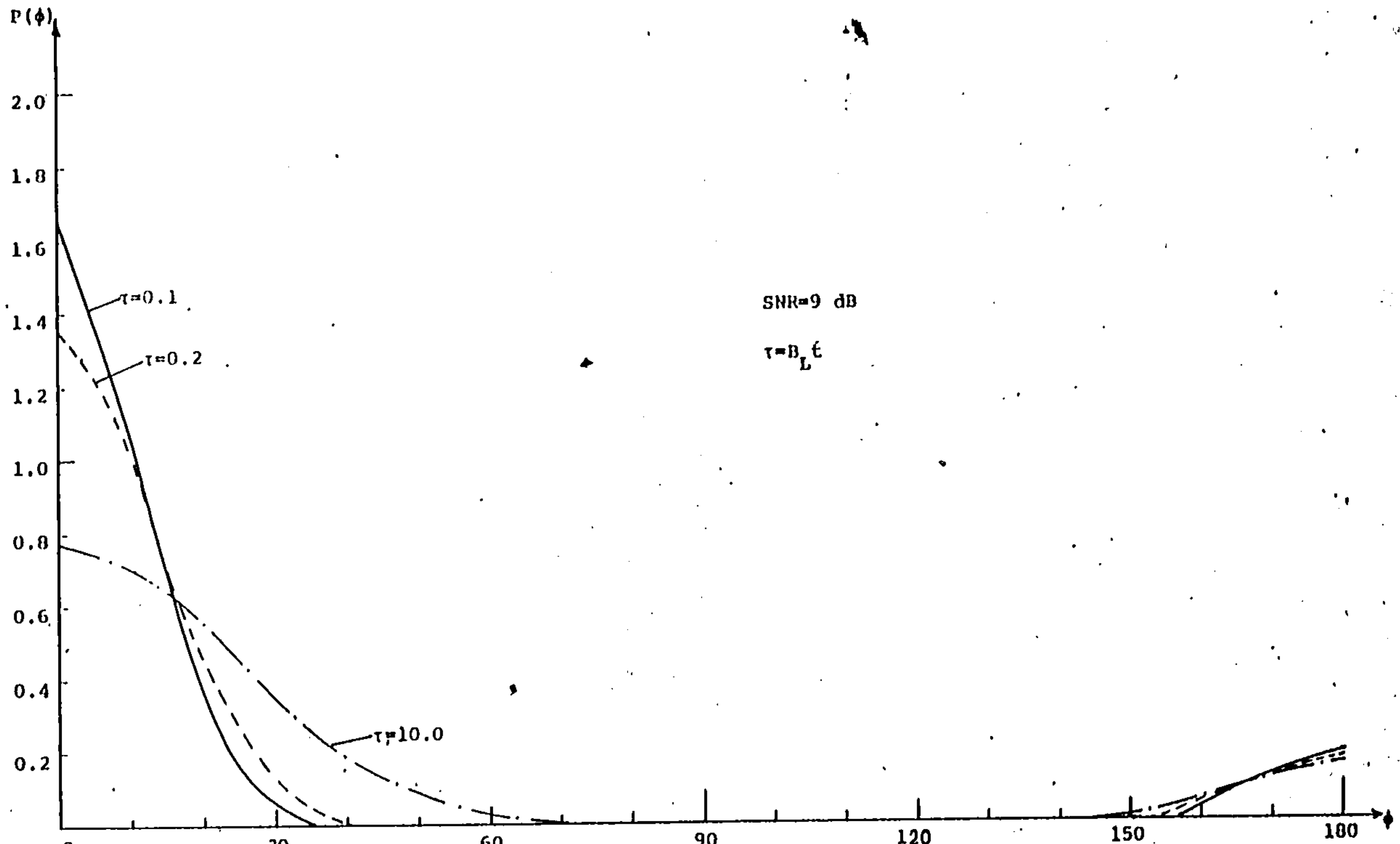

Figure 3.1a Transient behaviour of first-order loop,SNR=9 dB

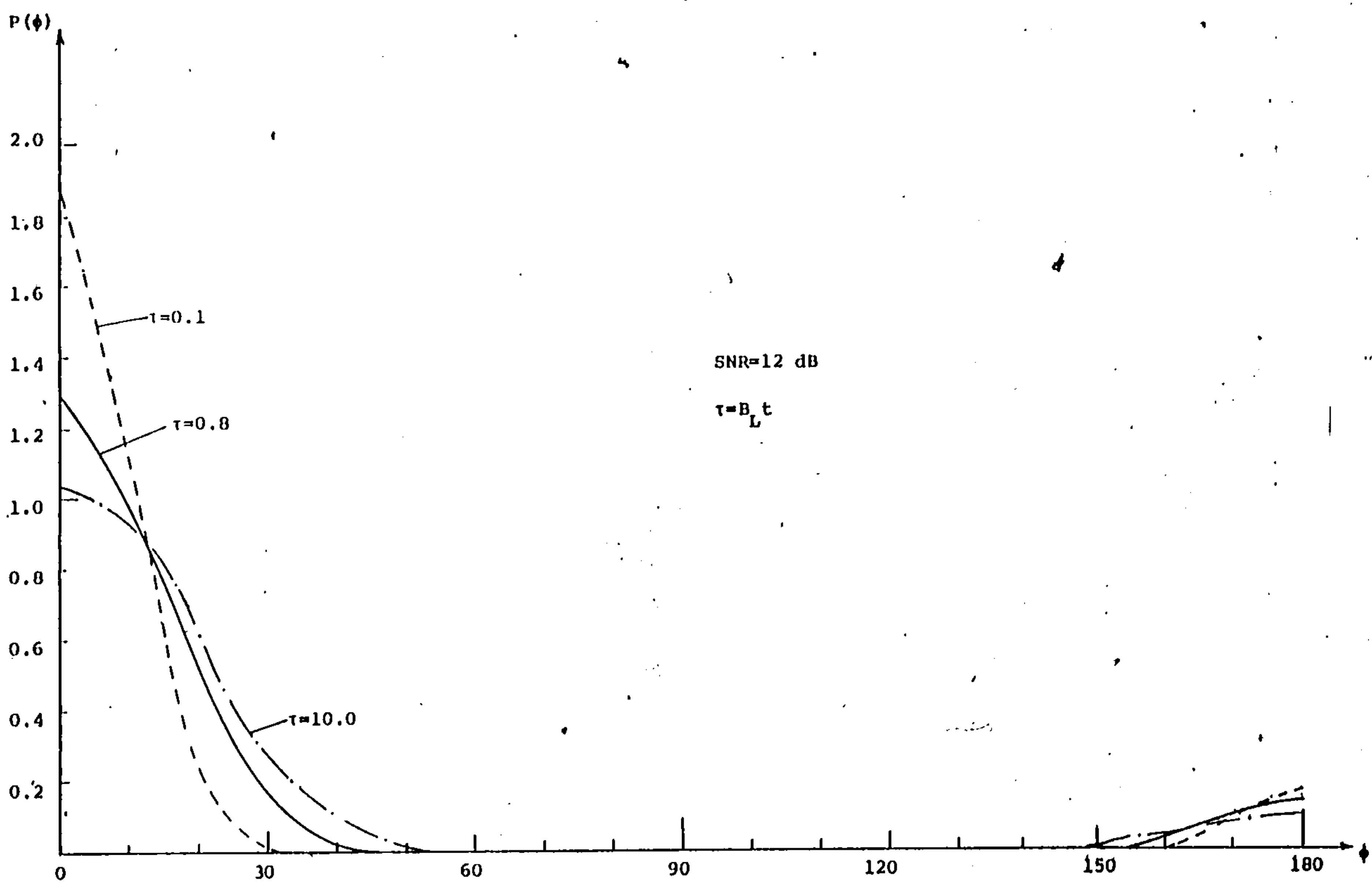

Figure 3.1b Transient behaviour of first-order loop;SNR=12 dB

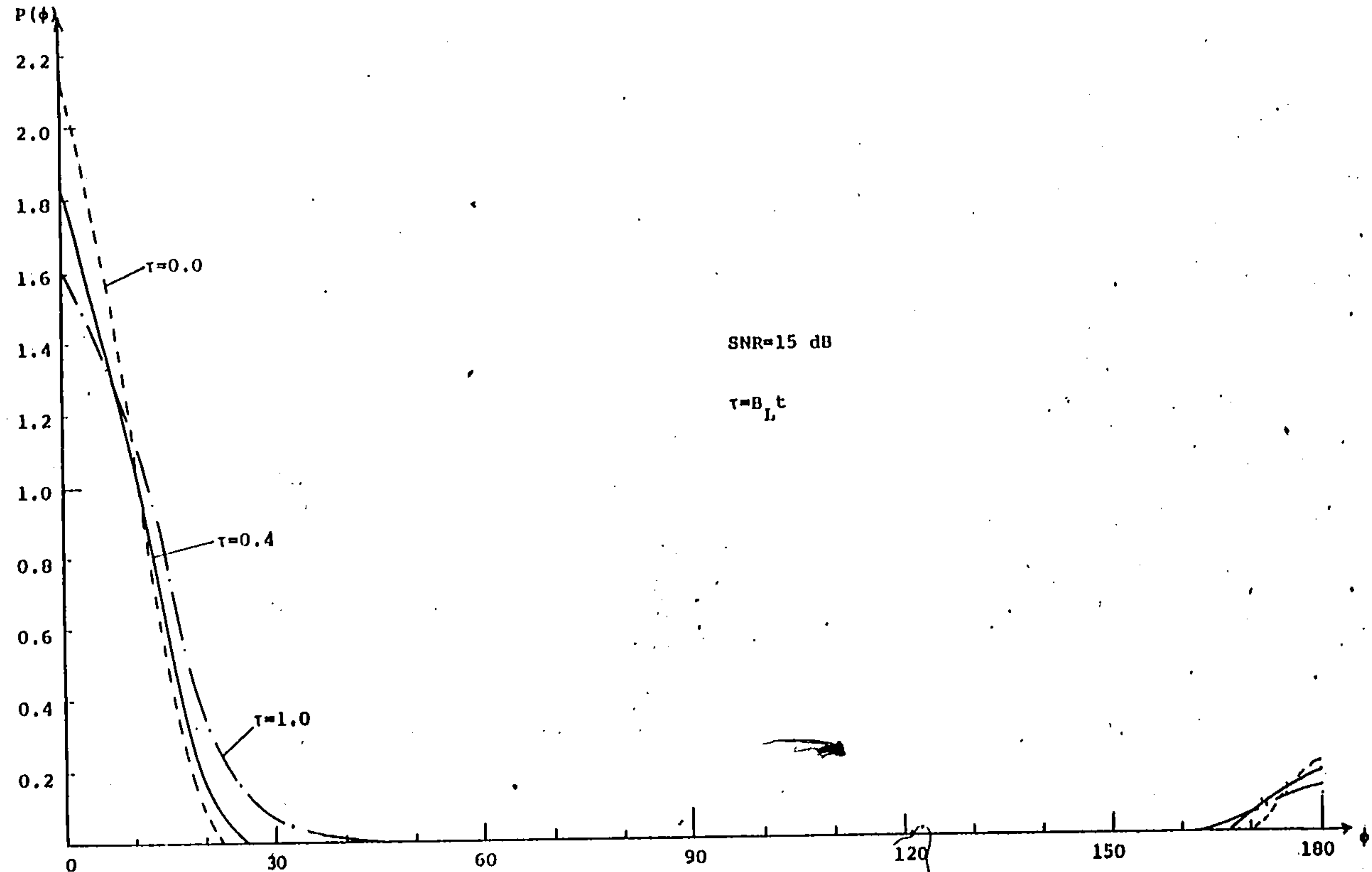

Figure 3.1c Transient behaviour of first-order loop,SNR=15 dB

CHAPTER 4

STEADY-STATE ANALYSIS OF THE SECOND-ORDER LIMIT-SWITCHED LOOP

4.1 Introduction

This chapter is concerned with the noisy nonlinear behaviour of the second-order limit-switched loop. The transient analysis in the presence of noise is mathematically intractable at this time. Therefore only the steady-state analysis is presented. A solution for the stationary, modulo-2π-reduced phase-error probability density function is derived based on the method of Viterbi [13]. The result obtained is a general solution which can be modified to suit different types of loop filter.

4.2 Second-Order Loop in the Presence of Noise

The purpose of the analysis is to obtain the steady-state probability density function of the phase error, and since the steady-state values do not depend on the initial phase error, it is reasonable to assume that both the initial phase error and the frequency detuning are zero. Equation (3.13) can therefore be written as

$$\phi(t) = -\frac{F(s)}{s} K(A \sin \phi(t) \cos S(U) + n(t)) \qquad (4.1)$$

Substituting $F(s) = (1 + \tau_2 s)/(1 + \tau_1 s)$ into (4.1) and rearranging, we obtain

$$s(1 + \tau_1 s)\ \phi(t) = -AK(1 + \tau_2 s) \sin \phi(t) \cos S(U) - K(1 + \tau_2 s)\ n(t) \qquad (4.2)$$

Following Viterbi [13], let

$$\phi(t) = \tau_2 \frac{dx(t)}{dt} + x(t) \qquad (4.3)$$

and substitute (4.3) into (4.2). We then have

$$s(1+\tau_1 s)\ [\tau_2 \frac{dx(t)}{dt} + x(t)] = -AK(1+\tau_2 s) \sin[\tau_2 \frac{dx(t)}{dt} + x(t)] \cos S(U) - K(1+\tau_2 s)\ n(t)$$

which may be written as

$$(1+\tau_2 s)\ [\tau_1 \frac{d^2x(t)}{dt} + \frac{dx(t)}{dt} + AK \sin (\tau_2 \frac{dx(t)}{dt} + x(t)) \cos S(U) + K\ n(t)] = 0 \qquad (4.4)$$

It has been shown in Appendix A that it is sufficient to solve the "reduced" equation

$$\tau_1 \frac{d^2x(t)}{dt} + \frac{dx(t)}{dt} + AK \sin [\tau_2 \frac{dx(t)}{dt} + x(t)] \cos S(U) + K\ n(t) = 0 \qquad (4.5)$$

to obtain the solution for $p(\phi)$.

Defining now a two-dimensional random process

$$y_o(t) \triangleq x(t)$$

$$y_1(t) \triangleq \frac{dx(t)}{dt}$$

We can then obtain two first-order differential equations

$$\frac{dy_o(t)}{dt} = y_1(t)$$

$$\frac{dy_1(t)}{dt} = -\frac{1}{\tau_1}\{y_1(t) + AK \sin[\tau_2 y_1(t) + y_o(t)] \cos S(U) + K\, n(t)\} \tag{4.6}$$

It has been shown [13] that the second-order Fokker-Planck equation corresponding to (4.6) is

$$\frac{\partial p(y_1, y_o, t)}{\partial t} = -y_1 \frac{\partial p(y_1, y_o, t)}{\partial y_o} + \frac{\partial}{\partial y_1} \frac{y_1 p(y_1, y_o, t)}{\tau_1} + \frac{AK}{\tau_1} \sin(\tau_2 y_1 + y_o) \cos S(U)\, p(y_1, y_o, t) + \frac{K^2 N_o}{4\tau_1^{\,2}} \frac{\partial^2 p(y_1, y_o, t)}{\partial y_1^{\,2}} \tag{4.7}$$

with initial condition

$$p(y_1, y_o, 0) = \delta(y_o - y_o(0))\, \delta(y_1 - y_1(0))$$

To obtain an equation in $p(\phi, t)$, let $z = y_o$ and $\phi_o = \tau_2 y_1 + y_o$. Equation (4.7) then becomes

$$\frac{\partial p(\phi,z)}{\partial t} = -\frac{1}{\tau_2}(\phi - z)\left[\frac{\partial p(\phi,z)}{\partial z} + \frac{\partial p(\phi,z)}{\partial \phi}\right] + \frac{\partial}{\partial \phi}$$

$$\left\{\left[\frac{AK\tau_2}{\tau_1} \sin\phi(t) \cos S(U)\right] + \frac{1}{\tau_1}(\phi - z)\, p(\phi,z)\right\} +$$

$$\frac{\tau_2^2 K^2 N_o}{4\tau_1^2} \frac{\partial^2 p(\phi,z)}{\partial \phi^2} \tag{4.8}$$

which characterizes the second-order limit-switched loop.

4.3 Steady-State Probability Density for the Second-Order Loop

Equation (4.8) cannot be solved directly, however, we can obtain a approximation for the density function of ϕ. Since we are interested only in the marginal probability density $p(\phi) = \int_{-\infty}^{\infty} p(\phi,z)\, dz$, we may integrate (4.8) from $-\infty$ to ∞ with respect to z, and we obtain

$$\left(\frac{1}{\tau_1} - \frac{1}{\tau_2}\right)\left\{\frac{d}{d\phi}[\phi p(\phi)] - \frac{d}{d\phi}\int_{-\infty}^{\infty} zp(\phi,z)\, dz\right\} =$$

$$\frac{\tau_2}{\tau_1} AK \frac{d}{d\phi}[\sin\phi \cos(S(U)) p(\phi)] + \frac{K^2 N_o}{4}\left(\frac{\tau_2}{\tau_1}\right)^2 \frac{d^2}{d\phi^2} p(\phi) \tag{4.9}$$

But

$$\int_{-\infty}^{\infty} zp(\phi,z)\, dz = p(\phi)\int_{-\infty}^{\infty} zp(z|\phi)\, dz = p(\phi)\, E[z|\phi]$$

and therefore (4.9) becomes

$$\left(\frac{1}{\tau_1} - \frac{1}{\tau_2}\right) \left\{\frac{d}{d\phi} [\phi p(\phi)] - \frac{d}{d\phi} p(\phi)\, E[z|\phi]\right\} =$$

$$\frac{\tau_2}{\tau_1} AK \frac{d}{d\phi} \{\sin \phi \cos (S(U))\, p(\phi)\} + \frac{K^2 N_o}{4} \left(\frac{\tau_2}{\tau_1}\right)^2 \frac{d^2}{d\phi^2} p(\phi) \tag{4.10}$$

But $z = \phi - \tau_2 y_1$, and therefore averaging over z is the same as averaging over y_1 for fixed ϕ, that is,

$$E[z|\phi] = \phi - \tau_2 E[y_1|\phi]$$

We then have

$$\frac{d}{d\phi} \left\{\left(\frac{\tau_2}{\tau_1} - 1\right) [E[y_1|\phi]] + \frac{\tau_2}{\tau_1} AK \sin \phi(t) \cos S(U) + \right.$$

$$\left. \frac{K^2 N_o}{4} \left(\frac{\tau_2}{\tau_1}\right)^2 \frac{d^2}{d\phi^2}\right\} p(\phi) = 0 \tag{4.11}$$

Equation (4.11) cannot be solved exactly because $E[y_1|\phi]$ requires the joint distribution function of y_1 and ϕ. A workable form of this conditional expectation term can however be obtained by extending the method of Viterbi [13]. Using $\exp(t/\tau_1)$ as an integrating factor and integrating (4.6) from t^+ to a, we then obtain

$$y_1(t^+) = y_1(a) \exp\left(\frac{a - t^+}{\tau_1}\right) + \frac{AK}{\tau_1} \int_{t^+}^{a} \exp \frac{t' - t^+}{\tau_1}$$

$$\sin \phi(t') \cos S(U)\, dt' + \frac{K}{\tau_1} \int_{t^+}^{a} n(t')$$

$$\exp\left(\frac{t' - t^+}{\tau_1}\right) dt' \tag{4.12}$$

Averaging (4.12), conditioned on $\phi(t)$, we note that

$$E[n(t') \mid \phi(t), t' > t] = 0$$

and for fixed (t^+)

$$\lim_{a \to \infty} E[y_1(a) \exp(\frac{a - t^+}{\tau_1}) \mid \phi(t)] = 0$$

Hence letting $\tau = t' - t^+$, (4.12) then becomes

$$E[y_1 \mid \phi] = E(y_1(t) \mid \phi(t))$$

$$= \frac{AK}{\tau_1} \int_0^\infty \exp \frac{\tau}{\tau_1} \cos S(U)\, E[\sin \phi(t + \tau) \mid \phi(t)]\, d\tau \tag{4.13}$$

Since the magnitude of the expectation is always less than one and since τ is several times the inverse of the band-width, that is, τ is very much smaller than τ_1, therefore the term $E[y_1 \mid \phi]$ is small and can be neglected. Equation (4.11) then becomes

$$\frac{d}{d\phi} \{\frac{\tau_2}{\tau_1} AK \sin \phi(t) \cos S(U) + \frac{K^2 N_o}{4} (\frac{\tau_2}{\tau_1})^2 \frac{d^2}{d\phi^2}\} p(\phi) = 0 \tag{4.14}$$

Integrating (4.14) with respect to ϕ we obtain

$$\frac{K^2 N_o}{4} (\frac{\tau_2}{\tau_1})^2 \frac{d}{d\phi} p(\phi) + (\frac{\tau_2}{\tau_1}) AK \sin \phi(t) \cos S(U)\, p(\phi) = C'$$

which may be written as

$$\frac{K^2 N_o}{4} (\frac{\tau_2}{\tau_1}) \frac{d}{d\phi} p(\phi) + AK \sin \phi(t) \cos S(U)\, p(\phi) = C \tag{4.15}$$

Equation (4.15) is a first-order linear differential equation. Solving it over a period ($-\pi \leq \phi < \pi$) with the initial condition $P(\phi,0) = \delta(\phi - \phi_o)$ and the boundary condition $P(\pi,t) = P(-\pi,t)$ for all t,, we then have

$$P(\phi) = D \exp\left[\frac{4A}{KN_o} \left(\frac{\tau_1}{\tau_2}\right) \cos(\phi) \cos S(U)\right] \cdot$$

$$\left\{C \int_{-\pi}^{\phi} \exp\left[-\frac{4A}{KN_o} \left(\frac{\tau_1}{\tau_2}\right) \cos(x) \cos S(U)\right] dx + 1\right\} \tag{4.16}$$

for $-\pi \leq \phi \leq \pi$

Since $\lim_{t\to\infty} P(\pi) = P(-\pi)$, therefore

$$C = \frac{\exp(0) - 1}{\int_{-\pi}^{\pi} \exp\left[-\frac{4A}{KN_o} \left(\frac{\tau_1}{\tau_2}\right) \cos(x) \cos S(U)\right] dx} = 0$$

and because $\int_{-\pi}^{\pi} P(\phi)\, d\phi = 1$, therefore

$$D = \frac{1}{\int_{-\pi}^{\pi} \exp\left[\frac{4A}{KN_o} \left(\frac{\tau_1}{\tau_2}\right) \cos(\phi) \cos S(U)\right] d\phi}$$

$$= \frac{1}{2\pi I_o \left[\frac{4A}{KN_o} \left(\frac{\tau_1}{\tau_2}\right) \cos S(U)\right]} \tag{4.17}$$

Equation (4.16) then becomes

$$P(\phi) = \frac{\exp\left[\frac{4A}{KN_o} \left(\frac{\tau_1}{\tau_2}\right) \cos(\phi) \cos S(U)\right]}{2\pi I_o \left[\frac{4A}{KN_o} \left(\frac{\tau_1}{\tau_2}\right) \cos S(U)\right]} \tag{4.18}$$

If $\tau_1 = \tau_2$ then $F(s) = 1$, that is we have a first-order loop, and $P(\phi)$ is given by

$$P(\phi) = \frac{\exp\left[\frac{4A}{KN_o} \cos(\phi) \cos S(U)\right]}{2\pi I_o \left[\frac{4A}{KN_o} \cos S(U)\right]} \tag{4.19}$$

where $I_o[\cdot]$ is the zero order modified Bessel function. Letting

$$\alpha' = \frac{4A}{KN_o} \cos S(U),$$

we have

$$P(\phi) = \frac{\exp(\alpha' \cos \phi)}{2\pi I_o(\alpha')} \tag{4.20}$$

which agrees with the result obtained by Viterbi [13] except for the switching function $\cos S(U)$.

If we let K and $\tau_1 \to \infty$ such that $K/\tau_1 \to K'$, $F(s)$ becomes $F(s) = (1 + \tau_2 s)/s$, that is, the perfect integrator, and $P(\phi)$ is given by

$$P(\phi) = \frac{\exp\left[\frac{4A^2}{N_o}\left(\frac{1}{AK'\tau + \frac{1}{\tau_2}}\right) \cos(\phi) \cos S(U)\right]}{2\pi I_o \left[\frac{4A^2}{N_o}\left(\frac{1}{AK'\tau_2 + \frac{1}{\tau_2}}\right) \cos S(U)\right]} \tag{4.21}$$

which again agrees with the result of Viterbi [13], but with an additional switching term.

4.4 Numerical Evaluation of the Steady-State Density Function

Equation (4.21) can be written as

$$P(\phi) = \frac{\exp\left[\frac{A^2}{N_o B_L} \cos(\phi) \cos S(U)\right]}{2\pi I_o \left[\frac{A^2}{N_o B_L} \cos S(U)\right]} \tag{4.22}$$

where

$$B_L = \frac{AK + a}{4}$$

$$a = 1/\tau_2$$

$$K = K'/a$$

For $|\phi| \leq \lambda$, (4.22) can be written as

$$P_1(\phi|NS) = \frac{\exp\left[\frac{A^2}{N_o B_L} \cos \phi\right]}{2\pi I_o \left[\frac{A^2}{N_o B_L}\right]} \tag{4.23}$$

and for $|\phi| > \lambda$

$$P_2(\phi|SW) = \frac{\exp\left[-\frac{A^2}{N_o B_L} \cos \phi\right]}{2\pi I_o \left[\frac{A^2}{N_o B_L}\right]} \tag{4.24}$$

Equations (4.23) and (4.24) can again be combined using (3.31) and (3.32) resulting in an overall phase error probability density function of

$$P(\phi) = P_1(\phi|NS)\, P(NS) + P_2(\phi|SW)\, P(SW) \tag{4.25}$$

$P(\phi)$ for three different SNRs has been calculated using (4.25), and the results are shown in Fig. 4.2. The area under each curve is normalized to unity representing a modulo -2π solution. Only values between 0 and 180 degrees are shown because the distribution is an even function.

The bimodal nature of the distribution for a limit-switched loop is shown clearly in Fig. 4.1. The small bumps at 180 degrees indicate that in some cases the loop locks at 180 degrees. The ratio of the magnitudes of the two bumps (at 0 and 180 degrees) depends on the choice of the switching threshold λ, if λ is chosen as 90 degrees, the two bumps should be equal in magnitude. For increasing values of SNR, the area under the curve around the threshold (135 degrees) decreases to insignificant values and the distribution curve becomes sharper near zero degrees, representing a faster acquisition, and smaller steady-state rms phase jitter.

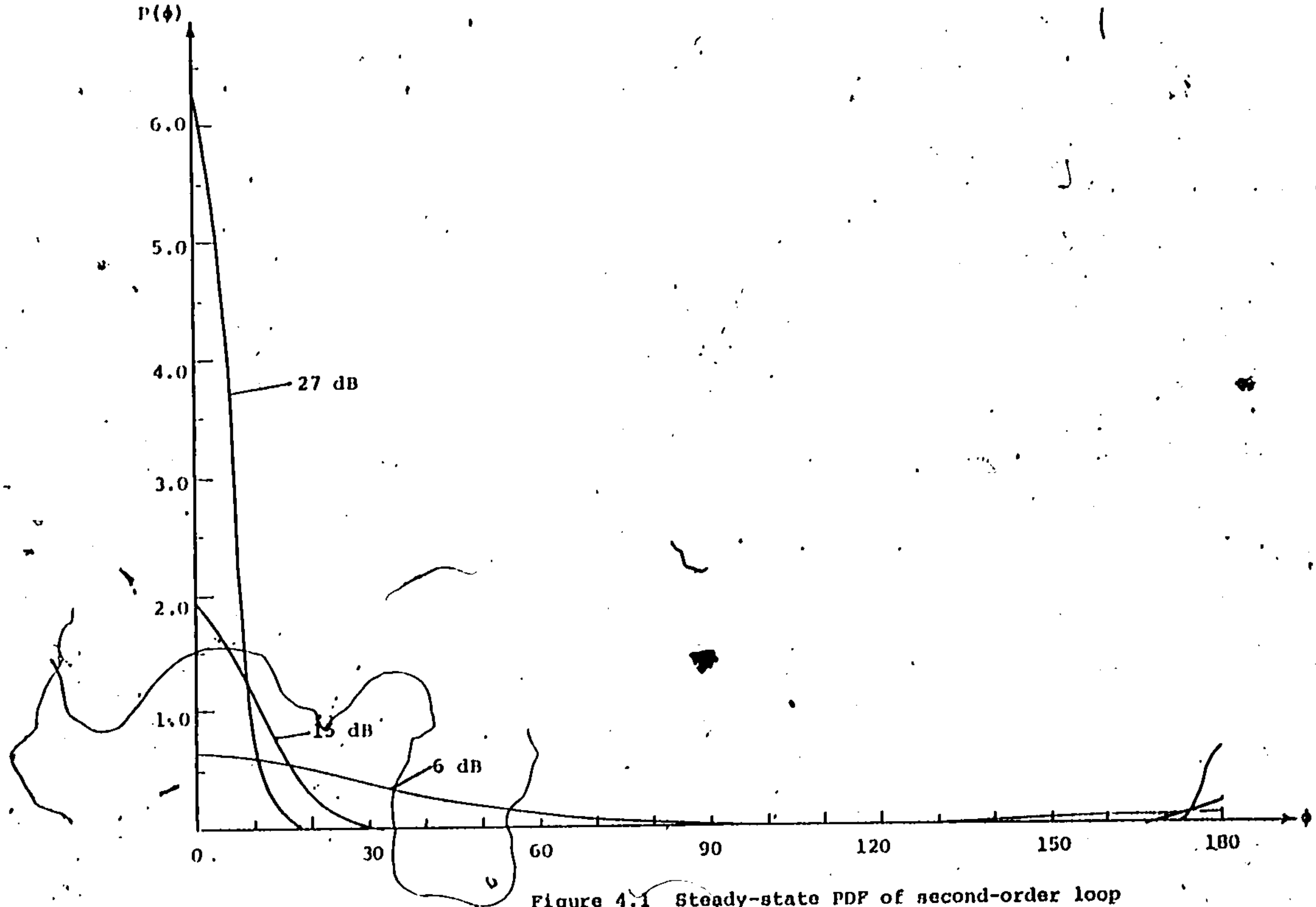

Figure 4.1 Steady-state PDF of second-order loop

CHAPTER 5

STATISTICAL BEHAVIOUR BY COMPUTER SIMULATION

5.1 Introduction

The definition of hangup to be used is discussed and then a computer simulation of the limit-switched loop is developed to obtain the probability of hangup based on this definition. It can be seen from the results of the simulation that the probability of correct switching does not have nearly as much effect on the probability of hangup as the switching time does. The choice of switching time is governed by the noise level. A longer switching time is required under low SNR operation to provide an increased margin against the noise perturbation. Finally, the effect of frequency detuning on the loop is investigated in order to furnish a complete comparison between the limit-switched loop and the conventional phase-locked loop.

5.2 Definitions of Hangup

The hangup region has been loosely defined both in the previous chapters of this thesis and in the literature [6,19] as the regions around the unstable nulls of the phase detector characteristic where occasionally prolonged acquisition time is observed. To obtain the probability of hangup, hangup must be explicitly defined in terms of acquisition time and phase error. This definition of hangup is arbitrarily chosen and can be varied accordingly in time, phase error or both to suit individual requirements. In this chapter, hangup is defined as the situation in which the phase error remains inside the switching region after one loop time constant, where the switching region is defined to lie between -135 and 135 degrees in the nonswitched mode and -45 and 45 degrees in the switched mode. The loop time constant is defined here using normalized time and is equal to real time divided by the open loop gain.

Going back to Fig. 2.4, it can be seen that for a conventional phase-locked loop the phase error ϕ decreases essentially exponentially after it has reached 135 degrees, that is, for $|\phi| \leq 135^{\circ}$. Therefore it is reasonable to assume that once the phase error is out of the ± 135 degrees region, the loop is safe from hangup.

Hangup is most serious when the initial phase error is near the unstable null and special attention should be given to that region. It is clear from Fig. 2.4 that after one time constant, most of the phase error trajectories have dropped below the 135 degrees mark. Exceptions are those trajectories with an initial phase error greater than 160 degrees. This is the reason why 135 degrees and one time constant have been chosen as the parameters on which to base our definition of hangup.

5.3 Design of the Computer Simulation

A computer simulation is developed to evaluate the probability of hangup in a noisy environment. A low-frequency baseband model is used to avoid the requirement of high sampling rate in the simulation and the stringent requirements when building and testing the actual circuit described in Chapter 6. The VCO centre frequency is set at 1.6 KHz and the open loop gain AK is 100. These parameters are the same as those used by Mariuz [11], so that a direct comparison can be made of the results obtained.

The zero mean, Gaussian distributed noise sequence was generated in the computer by RANGAU, a library subroutine available on the CDC 6400 computer. Using a standard deviation of 0.25 at the input of a first-order low-pass filter (f_c 3 dB = 53 Hz, to obtain a noise bandwidth approximately equal to that of the loop) and 10,000 samples points, the resulting average two-sided power spectral density was found to be [11]

$$\frac{N_o}{2} = 1.4 \times 10^{-6} \text{ watts/Hz}$$

Phase lock is defined here to be achieved if the phase error has dropped below 26.93 degrees. This definition of phase lock is arbitrary, however a phase error of 26.93 degrees corresponds to a loss of 1 dB when detecting coherent binary PSK (phase shift keying). That is [19]

$$\text{detection loss} = -10 \log_{10} (\cos^2 26.93)$$
$$= 1 \text{ dB}$$

It should be noted that this too is an arbitrary definition.

A flowchart representing the simulation is shown in Fig. 5.1. The switching portion can be bypassed so that the simulation can be used to model a conventional phase-locked loop. A program listing is included in Appendix B.

A few points are worth noting in obtaining the probability of hangup. First, the loop can fall back into the hangup region after it has moved away from it. This is due to the perturbation caused by noise or to a false switching. Second, the loop may stay in the hangup region for a period equal to or more than two time constants. Therefore, looking at the loop just the once after one time constant is not enough to convey all the information about hangup. The loop should be allowed to operate in a free running mode and hangup tested repeatedly until the loop is locked. Another trial is then initiated until the required number of trials has been reached.

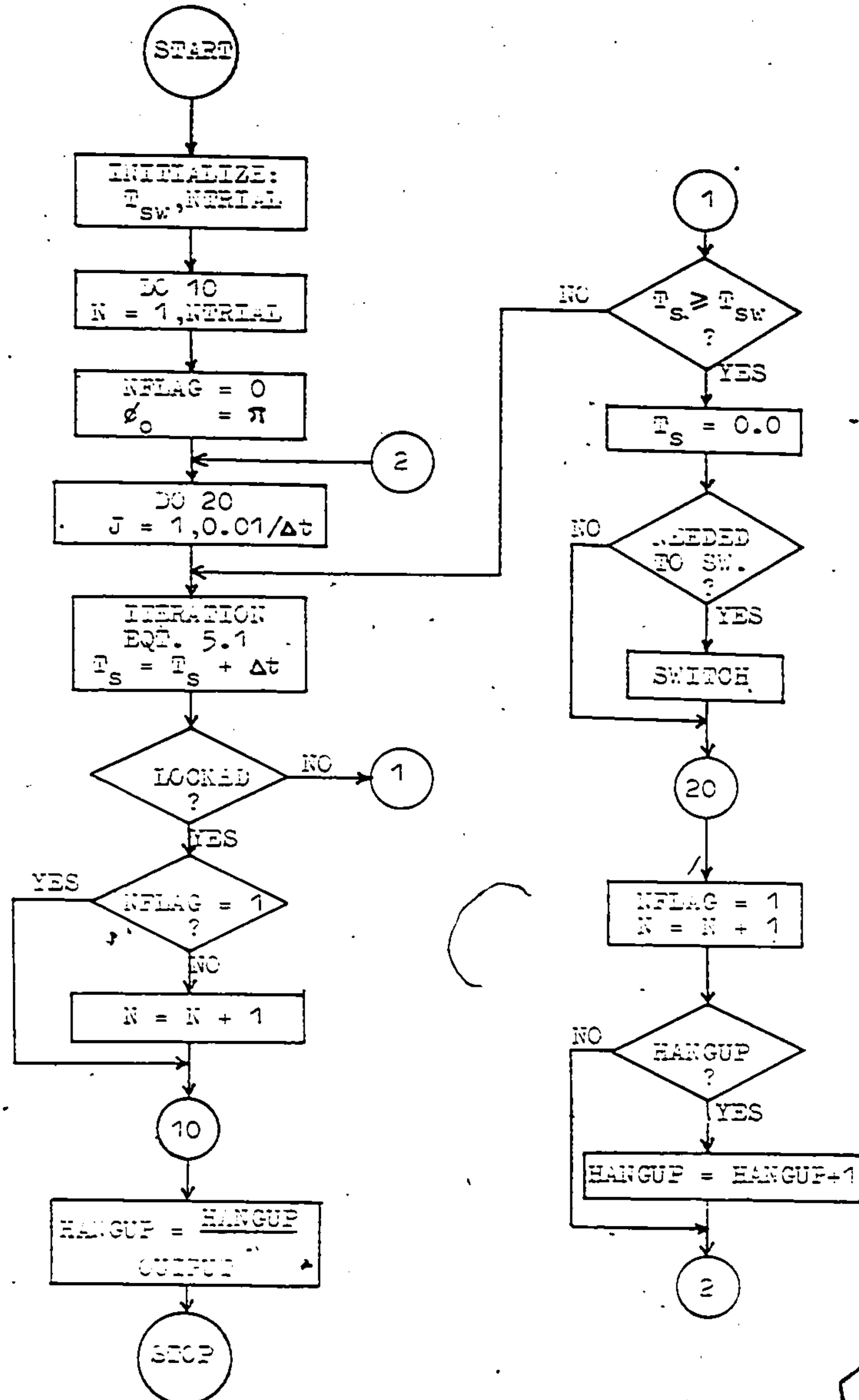

Figure 5.1 Simulation Flowchart

Based on the above, two ways of interpreting the probability of hangup were used. The first way is to allow a maximum of one hangup per trial, ignoring the possibilities of any further hangups. A trial is therefore terminated either by a successful detection of a hangup or when the loop is locked. This arose from the fact that in TDMA operation, the entire burst is lost if a hangup occurs and once this has happened, whether the loop is still in hangup is of no importance anymore. Here, the probability of hangup can be represented as

$$P_1(\text{hangup}) = \frac{\text{number of hangups}}{\text{number of trials}}$$

The second alternative is to repeat testing for hangup at multiples of one time constant until the loop is locked. If a hangup did occur after a testing, and if the loop has one or more chances to switch and switches correctly then the loop should be out of the hangup region at the next test. But for a conventional phase-locked loop, the loop will almost certainly remain in the hangup region at the next test. The probability of hangup is then defined to be equal to the number of hangups divided by the total number of testings.

$$P_2(\text{hangup}) = \frac{\text{number a hangups}}{\text{total number of testings}}$$

For the first-order loop, two sets of simulations were run, first with an initial phase error set at 180 degrees, then with a random initial phase error input. Each individual set of tests consists of three different switching timies and three different SNRs, representing the low, moderate and high SNR situations. A total of eighteen simulations were run. The difference equation of the loop under no frequency offset is

$$\phi(n+1) = \phi(n) - \Delta t\,(AK \sin(\phi(n)) + KV_I(n)) \qquad (5.1)$$

where V_I is the input noise and

$$SNR \triangleq \frac{A^2}{N_o B_L}$$

Δt is set equal to 0.00005 seconds which is more than adequate [18] for stability requirement.

There are four possibilities when a switching decision is made for each trial:

1. P(SW/SHOULD), switching occured, given that ϕ is inside the switching region at T_{sw}.
2. P(SW/SHOULDN'T), switching occured, given that ϕ is outside the switching region at T_{sw}.
3. P(NS/SHOULD), switching did not occur, given that ϕ is inside the switching region at T_{sw}.
4. P(NS/SHOULDN'T), switching did not occur, given that ϕ is outside the switching region at T_{sw}.

The above four possibilities can be condensed into two, the probability of correct switching, P(CORRECT SW) and the probability of incorrect switching, P(INCORRECT SW)

$$P(\text{CORRECT SW}) = P(\text{SW/SHOULD}) + P(\text{NS/SHOULDN'T})$$

$$P(\text{INCORRECT SW}) = P(\text{SW/SHOULDN'T}) + P(\text{NS/SHOULD})$$

The probabilities of hangup obtained are shown in Figs. 5.2 and 5.3 together with the average acquisition time and the probabilities of correct and incorrect switchings. It is obvious that ~~the~~ limit-switched loop has a much lower probability of hangup than the conventional phase-locked loop. The amount of improvement varies according to the switching times. In some cases hangup appears to have been completely eliminated.

Since in TDMA systems it is required to achieve phase lock within a specified time interval, the acquisition time of the loop is also an important factor and therefore it is reasonable to obtain the acquisition time along with the probability of hangup. The results obtained are shown in Figs. 5.4, 5.5 and 5.6 in a form similar to that used by Goldman [19]. The percentage of acquisition simulation times smaller than the time t is plotted against the time t in seconds. Again, the limit-switched loop surpasses the phase-locked loop, especially at high SNR with an initial pahse error of 180 degrees.

A. Limit-Switched Loop

LOOP SNR dB	T_{sw} sec.	P_1 (hangup)	P_2 (hangup)	AVE. ACQ. TIME, sec.	P(CORRECT-SW.)	P(INCORRECT-SW.)
6	0.003	0.02	0.0177	0.00826	0.6345	0.3655
	0.005	0.12	0.08824	0.01417	0.6255	0.3745
	0.009	0.10	0.08065	0.01506	0.5877	0.4123
15	0.003	0.055	0.05761	0.00955	0.5107	0.4893
	0.005	0.1505	0.1108	0.01552	0.6017	0.3983
	0.009	0.100	0.1004	0.01430	0.7491	0.2509
27	0.003	0.00	0.0000	0.00615	0.4950	0.5050
	0.005	0.06	0.0894	0.01095	0.6469	0.3531
	0.009	0.00	0.0000	0.00906	1.0000	0.0000

B. Phase-Locked Loop

LOOP SNR dB	P_1 (hangup)	P_2 (hangup)	AVE. ACQ. TIME, sec.
6	0.25	0.1893	0.02105
15	0.47	0.2527	0.03231
27	0.57	0.3278	0.04741

ϕ_o = 180 degrees

ϕ_{lock} = 0.47 radians

Figure 5.2 Comparisions of first-order LSL and PLL with initial phase error = 180 degrees

A. Limit-Switched Loop

LOOP SNR dB	T_{sw} sec.	P_1 (hangup)	P_2 (hangup)	AVE. ACQ. TIME, sec.	P(CORRECT-SW.)	P(INCORRECT-SW.)
6	0.003	0.05	0.03968	0.00694	0.7340	0.2660
	0.005	0.05	0.04167	0.00703	0.6704	0.3297
	0.009	0.07	0.06897	0.00704	0.6000	0.4000
15	0.003	0.010	0.00885	0.00822	0.8548	0.1452
	0.005	0.030	0.03629	0.00927	0.8436	0.1564
	0.009	0.010	0.00870	0.00920	0.8561	0.1439
27	0.003	0.000	0.0000	0.00796	0.8921	0.1079
	0.005	0.015	0.01754	0.00874	0.9370	0.0630
	0.009	0.000	0.0000	0.00877	0.8944	0.1056

B. Phase-Locked Loop

LOOP SNR dB	P_1 (hangup)	P_2 (hangup)	AVE. ACQ. TIME, sec.
6	0.09	0.1027	0.01087
15	0.05	0.04724	0.01021
27	0.10	0.1151	0.01115

ϕ_o = RANDOM

ϕ_{lock} = 0.47 radians

Figure 5.3 Comparisions of first-order LSL and PLL with random initial phase error

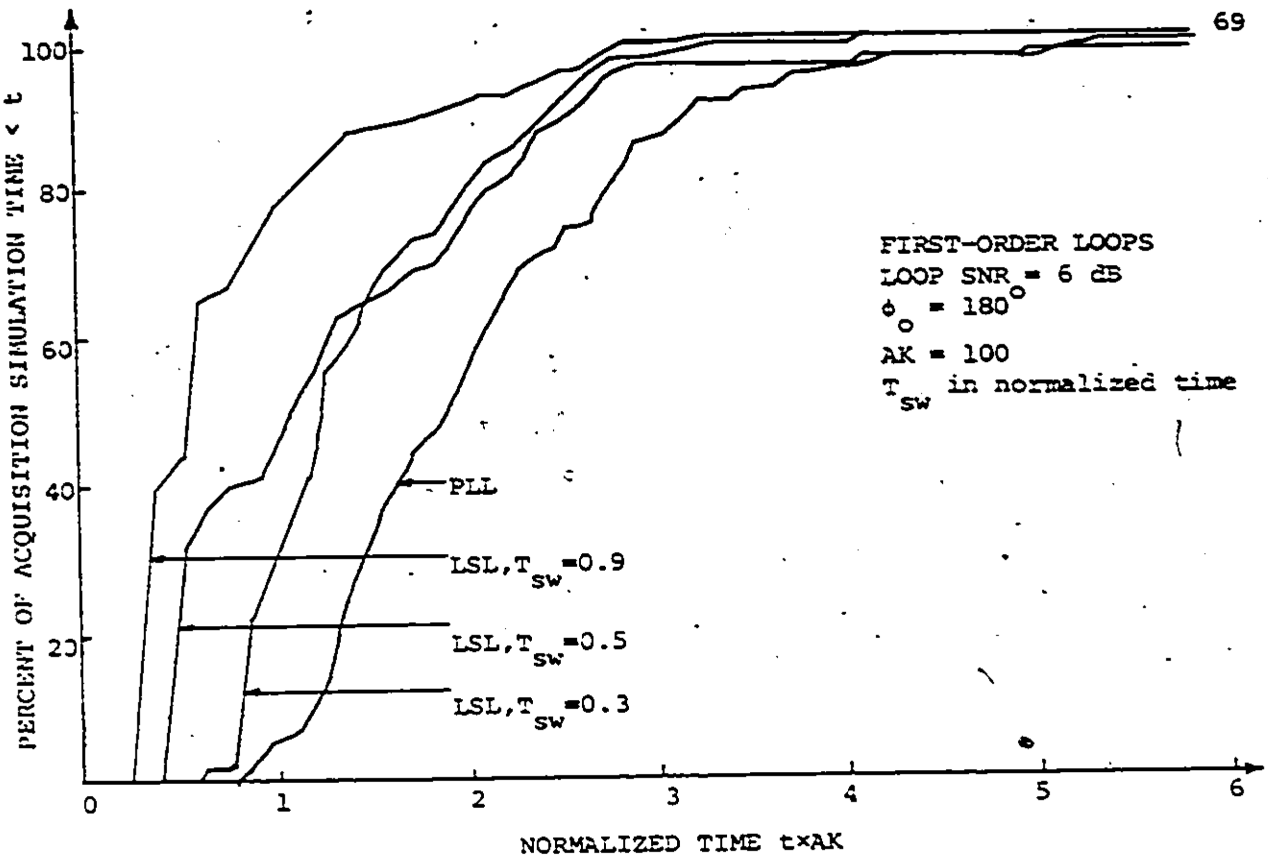

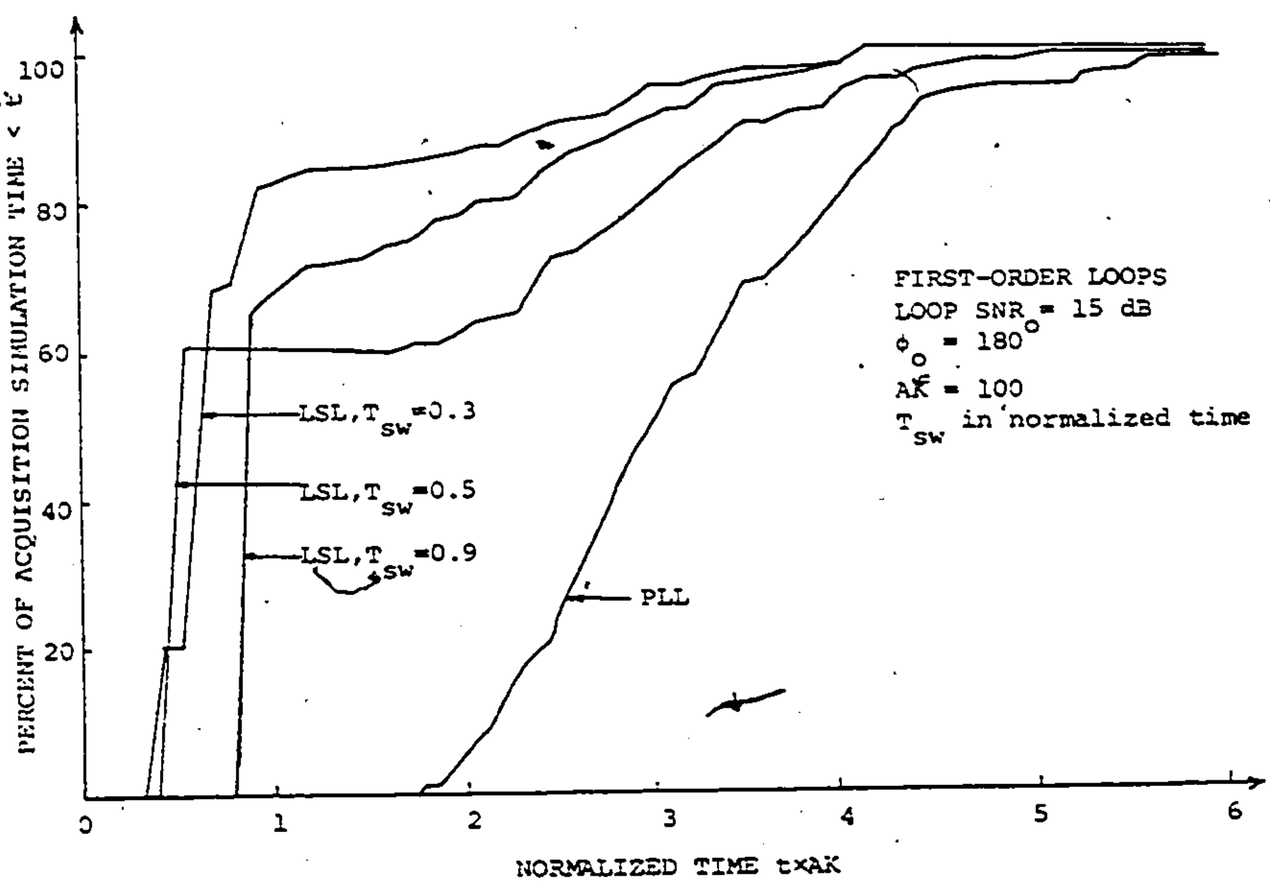

Figure 5.4 Simulation results of phase-lock acquisition time

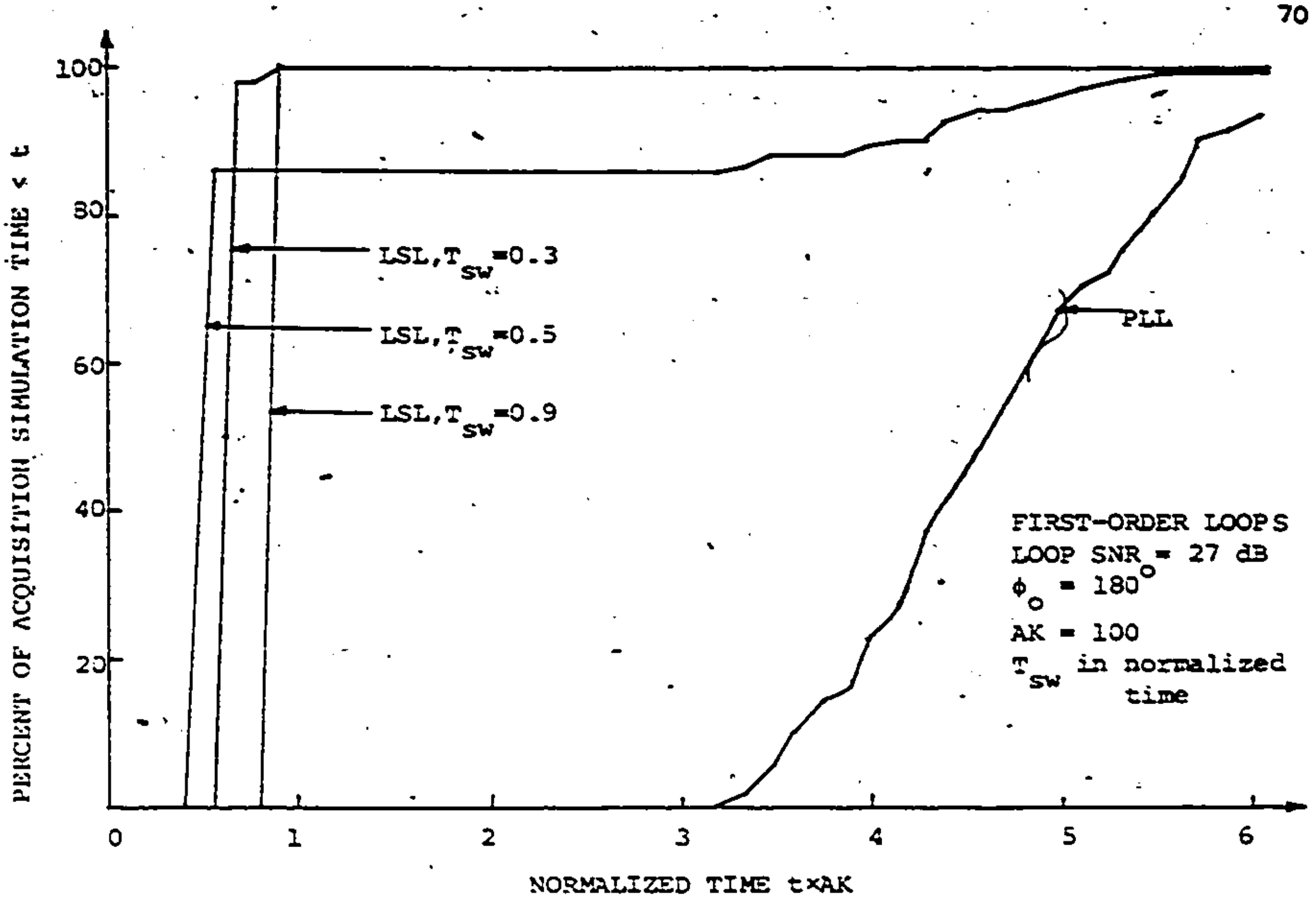

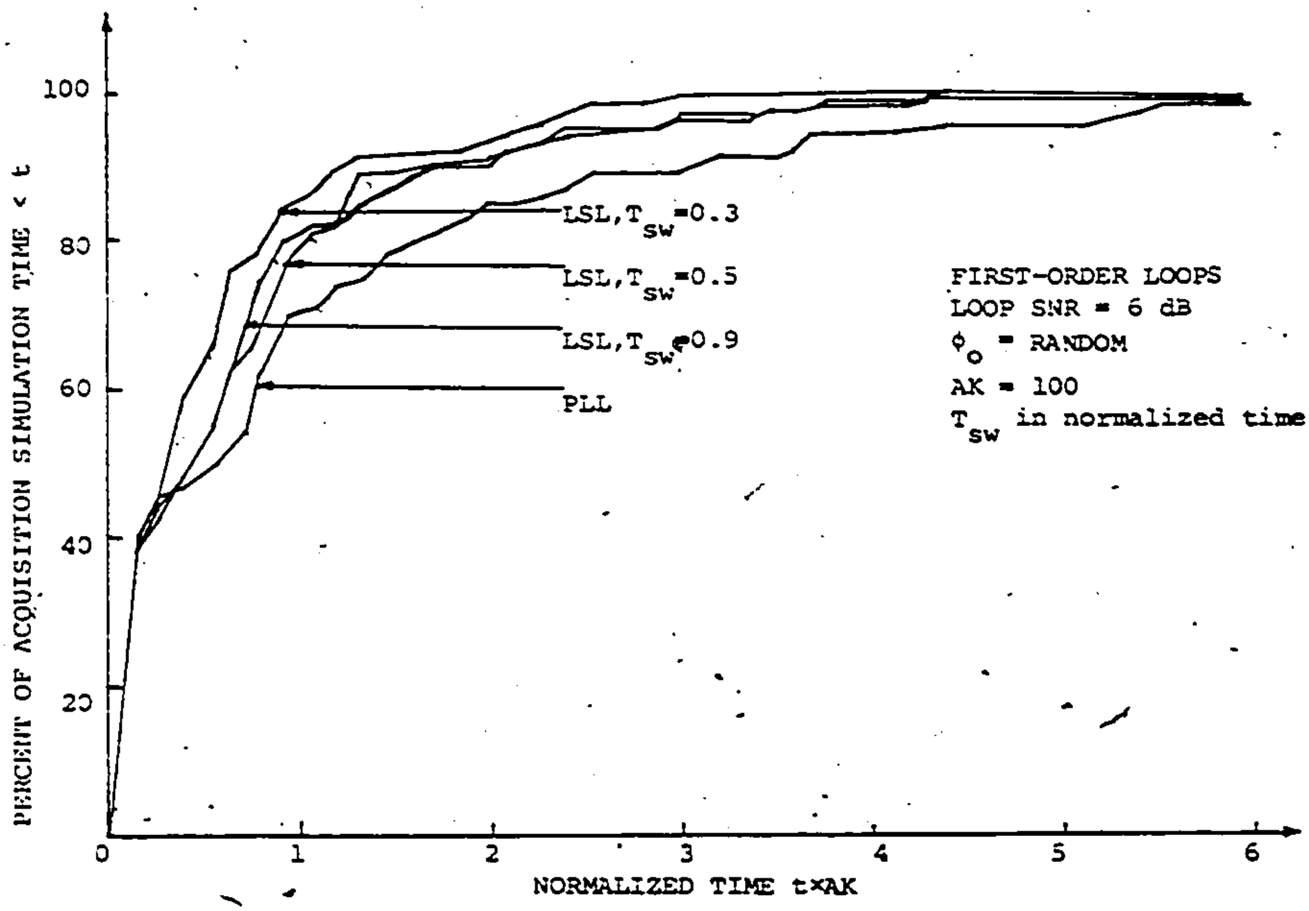

Figure 5.5 Simulation results of phase-lock acquisition time

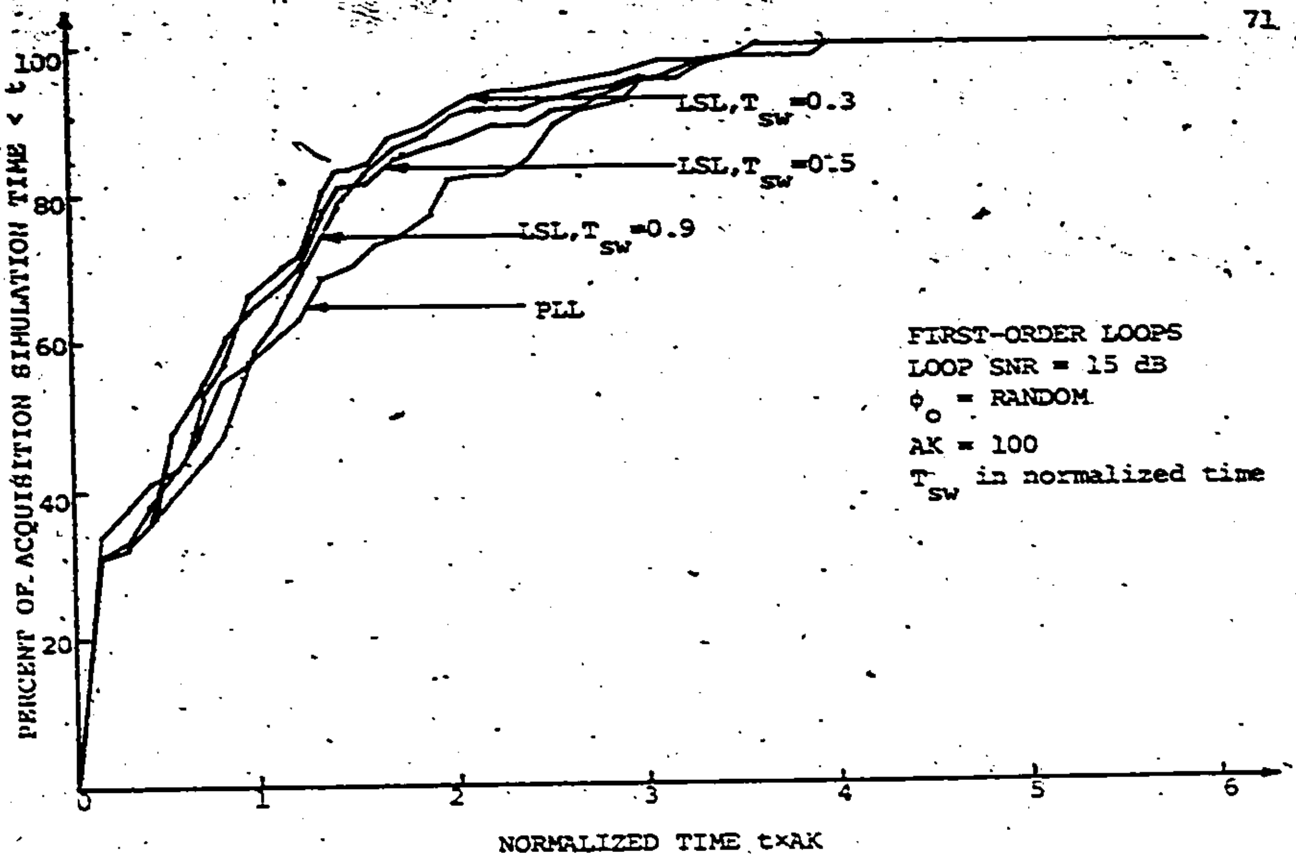

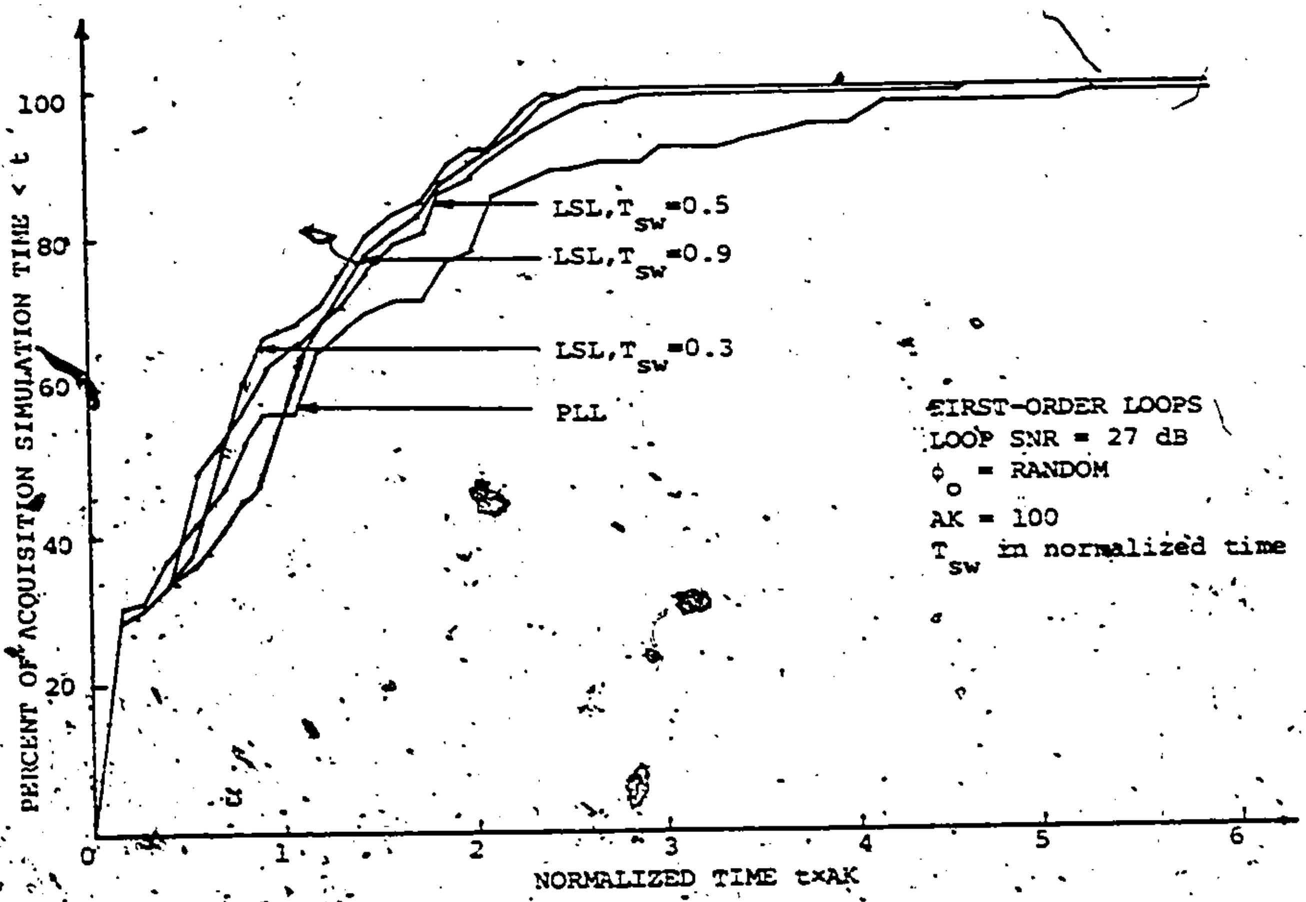

Figure 5.6 Simulation results of phase-lock acquisition time

The nine simulations with an initial phase error of 180 degrees are repeated for the second-order loop. The results are shown in Fig. 5.7 and the acquisition time curves in Figs. 5.8 and 5.9. Similar improvements are observed for the second-order loop.

5.4 Effect of Switching Time

Results from the simulations indicate that the switching time has a very strong effect on the probability of hangup and acquisition time. This can be related to the effect of noise on the switch. A shorter switching time results in a faster acquisition but is more susceptible to noise perturbations.

With the noise represented as

$$n'(t) = \sqrt{2}\, n_1(t) \cos \omega_c t - \sqrt{2}\, n_2(t) \sin \omega_c t$$

The low-pass phase detector output due to the noise alone is

$$v_n(t) = K \{n_1(t) \cos (\theta_2 - S(U)) + n_2(t) \sin (\theta_2 - S(U))\}$$

Assuming θ_2 changes slowly, that is, θ_2 is independent of $n'(t)$, then the mean square noise output becomes

$$\overline{v_n^2(t)} = K^2 \{\overline{n_1^2(t) \cos^2(\theta_2 - S(U)) + n_2^2(t) \sin^2(\theta_2 - S(U))}$$
$$\overline{+ 2\, n_1(t)\, n_2(t) \cos (\theta_2 - S(U)) \sin (\theta_2 - S(U))}\}$$

A. Limit-Switched Loop

LOOP SNR dB	T_{sw} sec.	P_1(hangup)	P_2(hangup)	AVE. ACQ. TIME, sec.	P(CORRECT-SW.)	P(INCORRECT-SW.)
6	0.003	0.02	0.01786	0.00735	0.6161	0.3839
	0.005	0.14	0.1119	0.01382	0.6815	0.3185
	0.009	0.10	0.07914	0.01680	0.6319	0.3681
15	0.003	0.055	0.05976	0.00996	0.5204	0.4796
	0.005	0.20	0.1327	0.01884	0.6208	0.3792
	0.009	0.07	0.06818	0.01388	0.7985	0.2015
27	0.003	0.00	0.0000	0.00611	0.4988	0.5012
	0.005	0.00	0.0000	0.00612	0.9901	0.0099
	0.009	0.00	0.0000	0.00906	1.0000	0.0000

B. Phase-Locked Loop

LOOP SNR dB	P_1(hangup)	P_2(hangup)	AVE. ACQ. TIME, sec.
6	0.30	0.1848	0.02602
15	0.54	0.2395	0.03792
27	0.57	0.3156	0.05349

ϕ_o = 180 degrees

ϕ_{lock} = 0.47 radians

$F(s) = 1 + 50/s$

Figure 5.7 Comparisions of second-order LSL and PLL

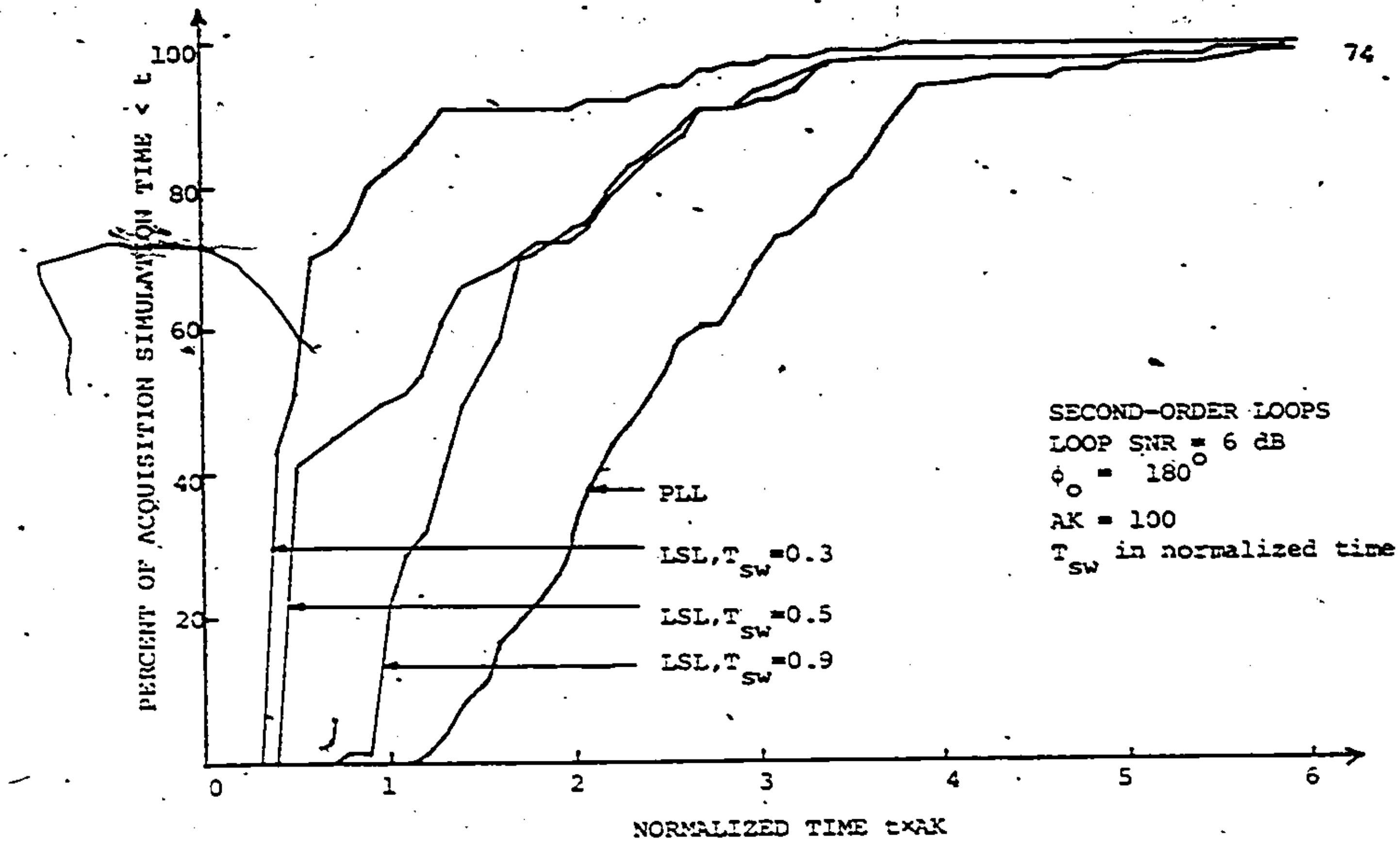

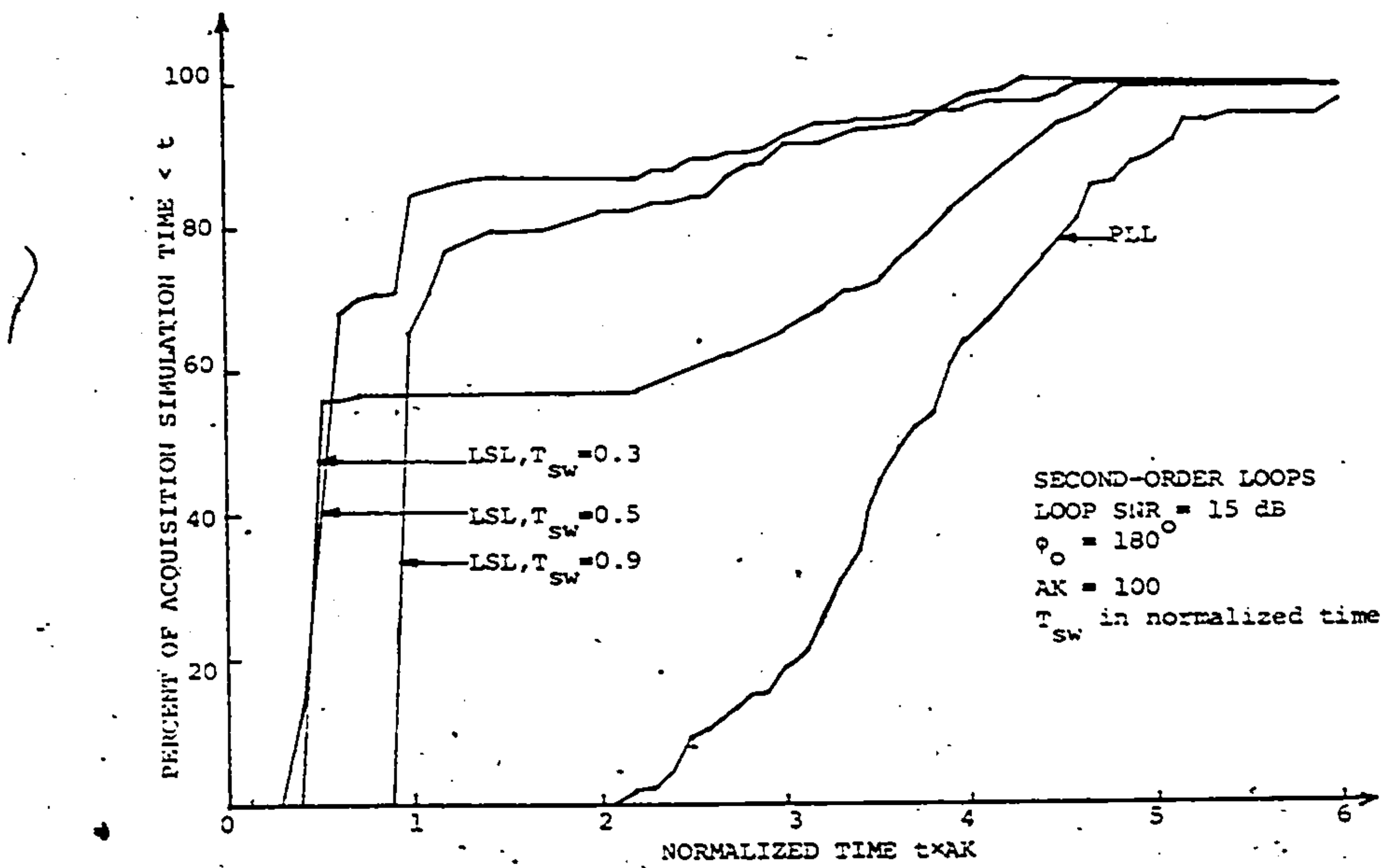

Figure 5.8 Simulation results of phase-lock acquisition time

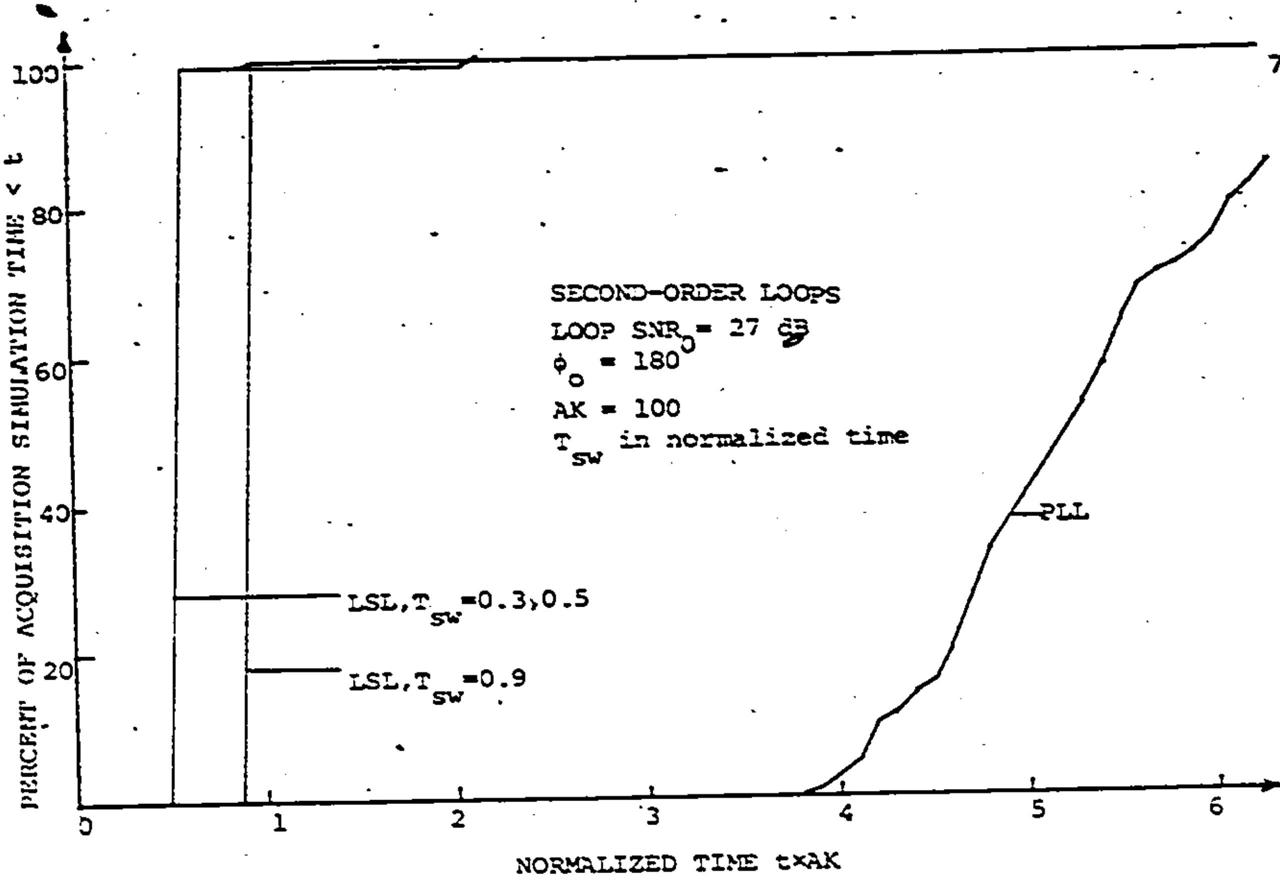

Figure 5.9. Simulation results of phase-lock acquisition time

$$= K^2 \{\overline{n_1^2(t)}\ \overline{\cos^2(\theta_2 - S(U))} + \overline{n_2^2(t)}\ \overline{\sin^2(\theta_2 - S(U))}$$

$$+ 2\ \overline{n_1(t)\ n_2(t)}\ \overline{\cos(\theta_2 - S(U))\sin(\theta_2 - S(U))}\}$$

Since $n_1(t)$ and $n_2(t)$ are independent and

$$\overline{n_1^2(t)} = \overline{n_2^2(t)} = \overline{n^2(t)}$$

therefore

$$\overline{v_n^2(t)} = K^2(\overline{n^2(t)}) \qquad (5.2)$$

Let the amplitude of the input signal be $\sqrt{2}A$ with $\overline{\theta_{ni}^2}$ representing the equivalent mean-square input phase jitter which will produce the same output from the phase detector. Equating the linearized signal output power with the mean-square noise output from (5.2), we have

$$[\sqrt{2}\ AK(\overline{\theta_{ni}^2})^{1/2}]^2 = K^2\ \overline{n^2(t)}$$

or

$$(\overline{\theta_{ni}^2}) = \frac{\overline{n^2(t)}}{2A^2} = \frac{1}{2(SNR)_i} \text{ radians}^2 \qquad (5.3)$$

where $(SNR)_i$ is the input signal-to-noise ratio.

Assuming the loop is preceded by a band-pass filter with bandwidth B_i, then the input noise spectral density is

$$N_i = \frac{\overline{n^2(t)}}{B_i} \text{ watts/Hz}$$

The spectrum of the input noise phase θ_{ni} is a low-pass rectangle with bandwidth $B_i/2$ and a density of

$$\phi = \frac{\overline{\theta_{ni}^2}}{B_i/2} = \frac{1}{B_i(SNR)_i} \text{ radians}^2/\text{Hz} \tag{5.4}$$

The output phase jitter from the VCO is

$$\overline{\theta_{no}^2} = \int_0^{B_i/2} \phi \, |H(j\omega)|^2 \, df = \int_0^{\infty} |H(j\omega)|^2 \, df$$

assuming $B_i >> B_L$.

Let $$B_L = \int_0^{\infty} |H(j\omega)|^2 \, df, \text{ then}$$

$$\overline{\theta_{no}^2} = \phi B_L = \frac{1}{(SNR)_i} \frac{B_L}{B_i} \tag{5.5}$$

Rewriting (2.8) as

$$t_{acq} = \int_{\phi_i}^{\phi_f} \frac{d\phi(t)}{-AK \sin \phi(t) \cos S(U)} \text{ seconds}$$

where ϕ_f = final value of the phase error

ϕ_i = initial value of the phase error

then the time required for the phase error ϕ to change from $(\lambda + \theta_{no})$ to λ is

$$t_{acq} = \int_{\lambda+\theta_{no}}^{\lambda} \frac{d\phi(t)}{-AK \sin \phi(t) \cos S(U)} \text{ seconds} \tag{5.6}$$

The following example will illustrate the relations between the noise level and the switching time T_{sw}.

Let the lopen loop gain, AK = 100, the switching threshold λ equal 135 degrees and the output phase jitter θ_{no} from the VCO be ±10 degrees.

Case 1:

Let $\phi = 134.9^\circ$ at T_{sw}, this implies that no switching is necessary. Suppose the noise level has increased at this point and pushed the phase error ϕ to $\phi = 134.9^\circ + 10^\circ = 144.9^\circ$ it will take $\int_{144.9}^{134.9} \frac{d\phi(t)}{-AK \sin \phi(t)} \approx 0.003$ sec. for the loop to move back to 134.9°, assuming that ϕ is moving in the correct direction. Therefore, the minimum T_{sw} required is 0.003 sec. to maintain the same switching decision or to avoid a "bang-bang" action in the next switching decision.

Case 2:

Let $\phi = 135.1^\circ$ at T_{sw} which implies a switching is necessary and after the switching, ϕ is now moving towards 180°, it will take $\int_{34.9}^{44.9} \frac{d\phi(t)}{AK \sin \phi(t)} \approx 0.003$ sec. for the loop to move the phase error ϕ to 145.1° such that the noise cannot push ϕ to go below 135° ($\phi = 145.1^\circ - 10^\circ = 135.1^\circ$) and causes the loop to switch back to its normal mode in the next switching decision.

Summing up, T_{sw} should be as short as possible under noiseless conditions to minimize the acquisition time. Under the influence of noise, the T_{sw} required can be estimated from (5.6) where θ_{no} is governed by the SNR. The theoretical values of T_{sw} for different SNRs have been calculated, using (5.5) and (5.6) and are listed in Fig. 5.10. It can be seen that T_{sw} is inversely proportional to the SNR, this is because a wider margin is required for the noise perturbation at low SNRs than at high SNRs.

Although a longer T_{sw} gives a higher probability of correct switching, it is suggested that a repeated switching decision will give a lower probability of hangup, provided T_{sw} is not small enough to cause a "bang-bang" effect. This repeated switching decision can be loosely viewed as an analogy to error reduction using repetition coding. The switching decision is quite reliable when the phase error is close to the lock points, therefore, if a correct switching has occured it is very unlikely that an incorrect switching will follow. With T_{sw} set equal to 0.003 sec. the loop has three chances to make a correct decision before hangup is tested at one time constant (0.01 sec.).

One more point to notice is that with the switching threshold λ set at 135 degrees, an incorrect switching does not necessarily result in a hangup or in a longer acquisition time. A simple example will clarify this. Assuming the phase error ϕ is 120 degrees at the point of switching, an incorrect switching will switch the loop to lock at 180 degrees which will require approximately 0.026 seconds (assuming a first order loop with an open loop gain of 100). On the other hand, a correct decision would

Open loop gain AK = 100

Loop noise bandwidth B_L = 25 Hz

Pre-loop bandpass filter noise bandwidth B_i = 628 Hz

INPUT SNR dB	LOOP SNR dB	θ_{no}	T_{sw}, sec.	T_{sw} NORMALIZED
20	34	1.14	2.85×10^{-4}	0.0285
10	24	3.62	9.22×10^{-4}	0.092
6	20	5.75	1.49×10^{-3}	0.149
3	17	8.09	2.16×10^{-3}	0.216
0	14	11.43	3.17×10^{-3}	0.317
-4	10	18.12	5.5×10^{-3}	0.55
-8	6	28.72	1.06×10^{-2}	1.063

Table 5.10 Theorectical Optimum T_{sw}

require 0.037 seconds for the same loop to lock at 0 degrees.

The simulations of the second-order limit-switched loop have been run for nine different switching times for SNRs of 6 dB and 15 dB, the results are presented in Figs. 5.11 and 5.12.

The graph in Fig. 5.12 agrees with the predicted shape. First, the acquisition time goes up as the switching time is increased. Second, the probability of hangup goes up when the switching time is increased beyond its optimum value. It will finally reach a peak at approximately 0.005 seconds and then decreases again. This is because with a switching time greater than or equal to 0.005 seconds (half of one time constant) only one switching can be made before hangup is being tested at one time constant. However, a longer switching time results in a more reliable switching decision, and a more reliable switching decision means a lower probability of hangup when only one switching can be made. Therefore, under the definition of hangup used in this chapter, T_{sw} equals to 0.005 seconds is clearly the worst choice.

If for any particular reasons, the switching time has to be made greater than 0.005 seconds, a switching time of 0.008 seconds or 0.009 seconds is recommended due to the higher probability of correct switching. This will make the

A. SNR = 15 dB, $\phi_o = 180^o$, ϕ_{lock} = 0.47 radians

T_{sw} sec.	P_1(hangup)	P_2(hangup)	P(SW/ SHOULD)	P(SW/ SHOULDN'T)	P(NS/ SHOULD)	P(NS/ SHOULDN'T)	P(CORRECT-SW.)	P(INCORRECT-SW.)
0.001	0.04	0.05882	0.1186	0.00131	0.6597	0.2203	0.3389	0.6611
0.002	0.06	0.07031	0.1913	0.00652	0.5435	0.2587	0.4500	0.5500
0.003	0.055	0.05976	0.2720	0.0000	0.4796	0.2484	0.5204	0.4796
0.004	0.06	0.06796	0.6234	0.01948	0.3117	0.04545	0.6689	0.3312
0.005	0.20	0.1327	0.1601	0.0000	0.3429	0.4107	0.5708	0.4292
0.006	0.13	0.1282	0.5921	0.01974	0.2500	0.1382	0.7303	0.2697
0.007	0.11	0.1102	0.5478	0.00639	0.2293	0.2166	0.7644	0.2356
0.008	0.06	0.06723	0.6641	0.03053	0.1527	0.1527	0.8168	0.1832
0.009	0.07	0.06818	0.5755	0.00719	0.1942	0.2230	0.7985	0.2015

B. SNR = 6 dB, $\phi_o = 180^o$, ϕ_{lock} = 0.47 radians

T_{sw} sec.	P_1(hangup)	P_2(hangup)	P(SW/ SHOULD)	P(SW/ SHOULDN'T)	P(NS/ SHOULD)	P(NS/ SHOULDN'T)	P(CORRECT-SW.)	P(INCORRECT-SW.)
0.001	0.05	0.04016	0.1790	0.05030	0.3462	0.4246	0.6036	0.3964
0.002	0.01	0.00971	0.4299	0.04206	0.3224	0.2056	0.6355	0.3645
0.003	0.02	0.01786	0.3438	0.1295	0.2545	0.2723	0.6161	0.3839
0.004	0.05	0.04464	0.2896	0.1131	0.2489	0.3484	0.6380	0.3620
0.005	0.14	0.1119	0.1855	0.03629	0.2823	0.4960	0.6815	0.3185
0.006	0.11	0.08397	0.2139	0.1642	0.1791	0.4428	0.6567	0.3433
0.007	0.10	0.07813	0.2500	0.1667	0.1548	0.4286	0.6786	0.3214
0.008	0.10	0.07576	0.2403	0.1948	0.1494	0.4156	0.6559	0.3441
0.009	0.10	0.07914	0.1944	0.1806	0.1875	0.4375	0.6319	0.3681

Figure 5.11 Simulation results of second-order LSL for different switching times

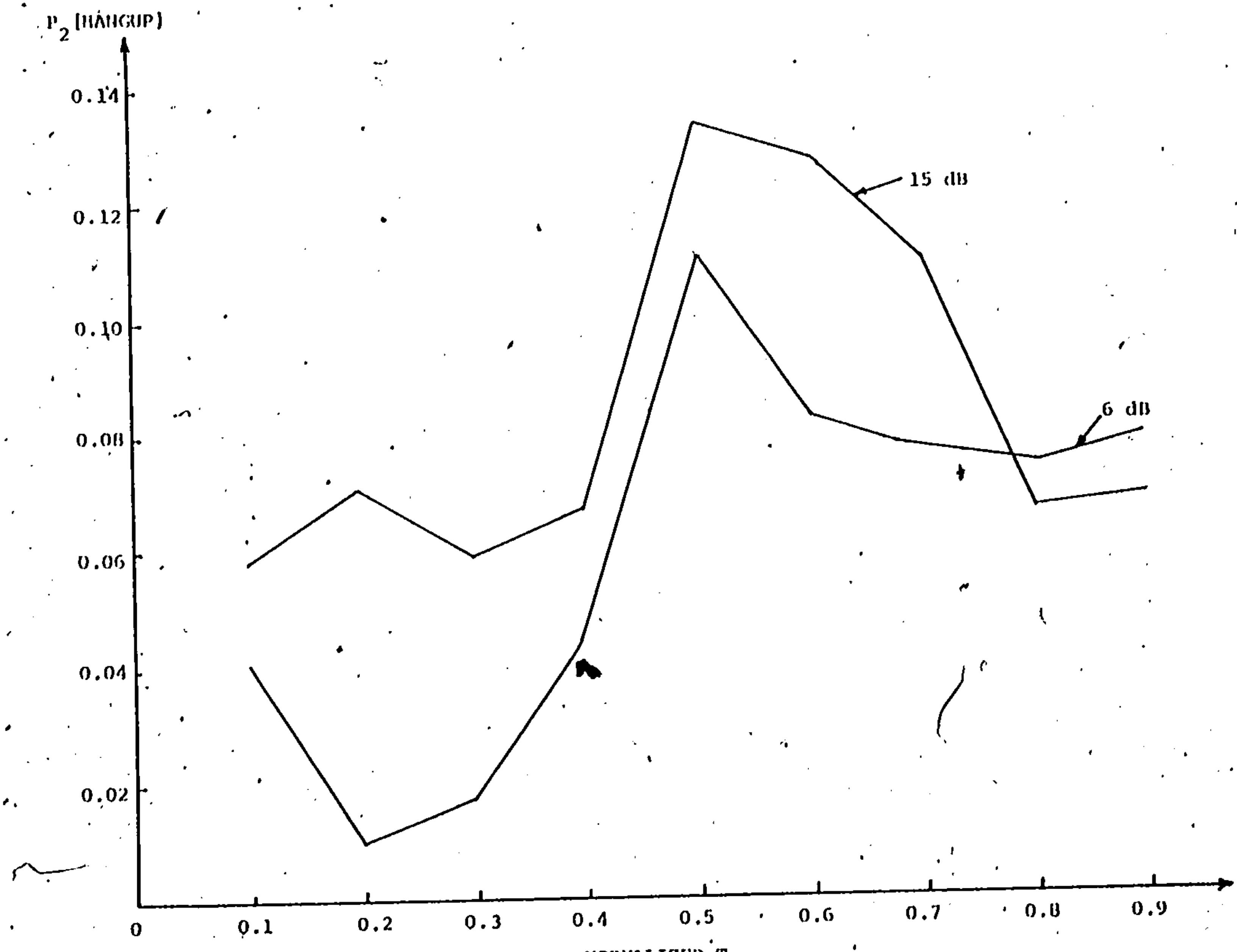

Figure 5.12 Simulation results of second-order LSL for different switching time

performance of the loop more predictable with only a small penalty in slightly increased acquisition time.

5.5 Effect of Frequency Detuning

It has been suggested that an initial frequency offset should prevent hangup because the phase would not be able to dwell at the unstable null. This is incorrect. In a first-order loop, a frequency offset only shifts the locations of the null (see Fig. 2.2) but the unstable null still exists. In a second-order loop hangup will still occur if the initial state is close to a saddle-point separatrix on the phase plane trajectories (see Fig. 2.5). It does not depend on the less likely condition of initial state being close to the saddle-point.

The limit-switched loop was not designed to deal with the problems of frequency offset since in TDMA systems, the magnitude of frequency offset is limited to be no bigger than a few parts in 10^7 by the AFC circuit. However, in order to show that a frequency offset has no significant influence on hangup, a frequency offset of 0.1 B_L has been introduced into an imperfect second-order loop with an open loop gain AK of 100, an imperfect integrator with a 50.5 and $\epsilon = 0.5$. The noise bandwidth B_L of the second-order loop is defined as $B_L = AK(AK + a)/(4(AK + \epsilon))$. The results of the simulations are shown in Fig. 5.13. Out of the five cases,

T_{sw}, sec.	P_2 [HANGUP]	
	FREQ. OFFSET = 0.0 Hz	FREQ. OFFSET = 2.5 Hz
0.001	0.05882	0.008475
0.003	0.05976	0.008547
0.005	0.1327	0.1531
0.007	0.1102	0.05405
0.009	0.06818	0.02326

LOOP SNR = 15 dB

$\phi_o = 180^\circ$

$\phi_{lock} = 0.47$ radians

Figure 5.13 Second-order loop, probability of hangup with frequency detuning only one shows a 15 percent increase in the pobability of hangup, all others are reduced substantially.

5.6 Conclusion

All the previous sections have agreed that the limit-switched loop has a shorter acquisition time and a much lower probability of hangup, especially with an initial phase error of 180 degrees. Those results are all obtained by testing for hangup after one time constant. It will be very useful to know how the probability of hangup changes with respect to time. Figure 5.14 represents the results of 25 simulations, using different switching times and testing for hangup at different time intervals. The SNR used is 15 dB. Here hangup at a particular time has to be redefined as the situation in which the phase error remains inside the switching region at that time. It can be seen that all these curves decrease exponentially with respect to time and the probability of hangup practically goes to zero after two time constants. It is therefore reasonable to conclude that the limit-switched loop is a device with a well-defined characteristic and can be used to replace the phase-locked loop where fast acquisition of phase lock and low probability of hangup are required.

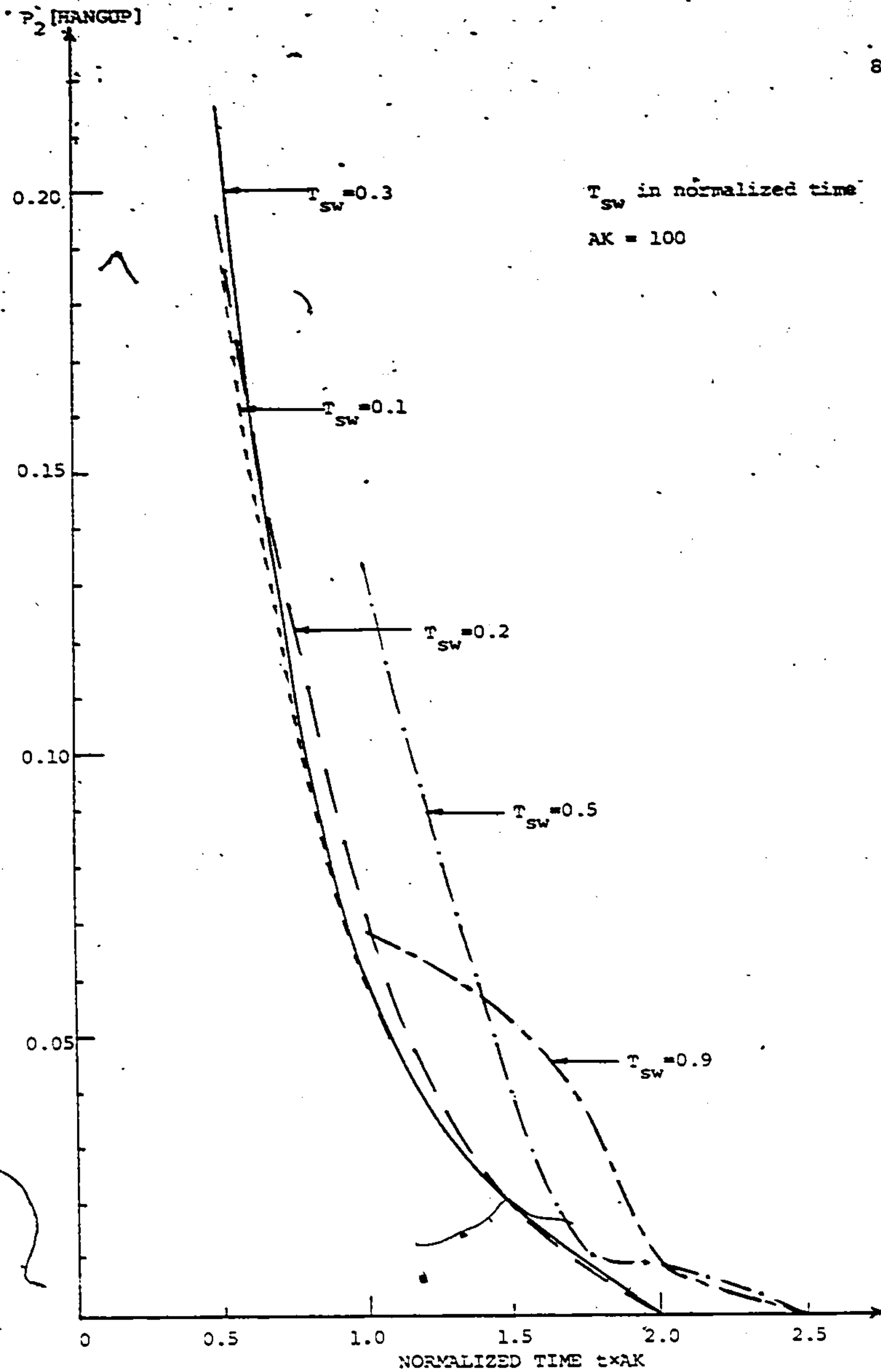

Figure 5.14 Simulation results of probability of hangup using different definitions of hangup

CHAPTER 6

STATISTICAL BEHAVIOUR BY EXPERIMENTAL METHOD

6.1 Introduction

The first-order limit-switched loop was built and tested by Mariuz [11]. His testing concentrated on the reliability of the phase-shifting switch. In this chapter the testing of the second-order limit-switched loop is presented. The testing is concentrated on the measurement of the probability of hangup in the presence of noise rather than on the probability of correct switching. The loop is allowed to free-run until a hangup is detected or phase-lock has been acquired. A new trial is then initiated. The probability of hangup so obtained is compared with the simulation results obtained in Chapter 5. The loop filter used is the proportional-plus-integral control type. This filter is generally used for carrier tracking purposes in the implementation of phase-coherent-communication systems [20].

6.2 The Testing of Hangup

It has been shown in Chapter 5 that a high probability of correct switching does not necessary imply a low probability of hangup. It is the purpose of this experiment to determine the probability of hangup directly rather than in terms of the probability of correct switching. The testing for hangup requires dealing with the loop phase transients. The measurement of the statistical parameters of the loop operating in noise is very difficult and complex [20]. At low or high SNRs, the phase transients become extremely slow or fast respectively. This together with other disturbances made the testings in these two ranges of SNR unrealiable and meaningless, and therefore only results for a SNR of 15 dB have been obtained.

A block diagram of the experimental structure for a second-order loop is shown in Fig. 6.1. The parameters of the loop are identical to those used in the simulation. That is, the open loop gain AK is 100 and the filter transfer function is $(s + a)/(s + \epsilon)$ with a equal to 50.5 and ϵ equal to 0.5. The external VCO and the external gating circuit are used to provide an initial phase error of 180 degrees to the limit-switched loop. The two-phase VCO [21] in the limit-switched loop and the external VCO both have a free-running frequency of 1.6 KHz. With the two switches of the external gating circuit as shown in the figure, the system is in its reset state. The input of the limit-switched loop is grounded and the cos $\omega_c t$ signal is fed to a phase detector. This signal when multiplied by the

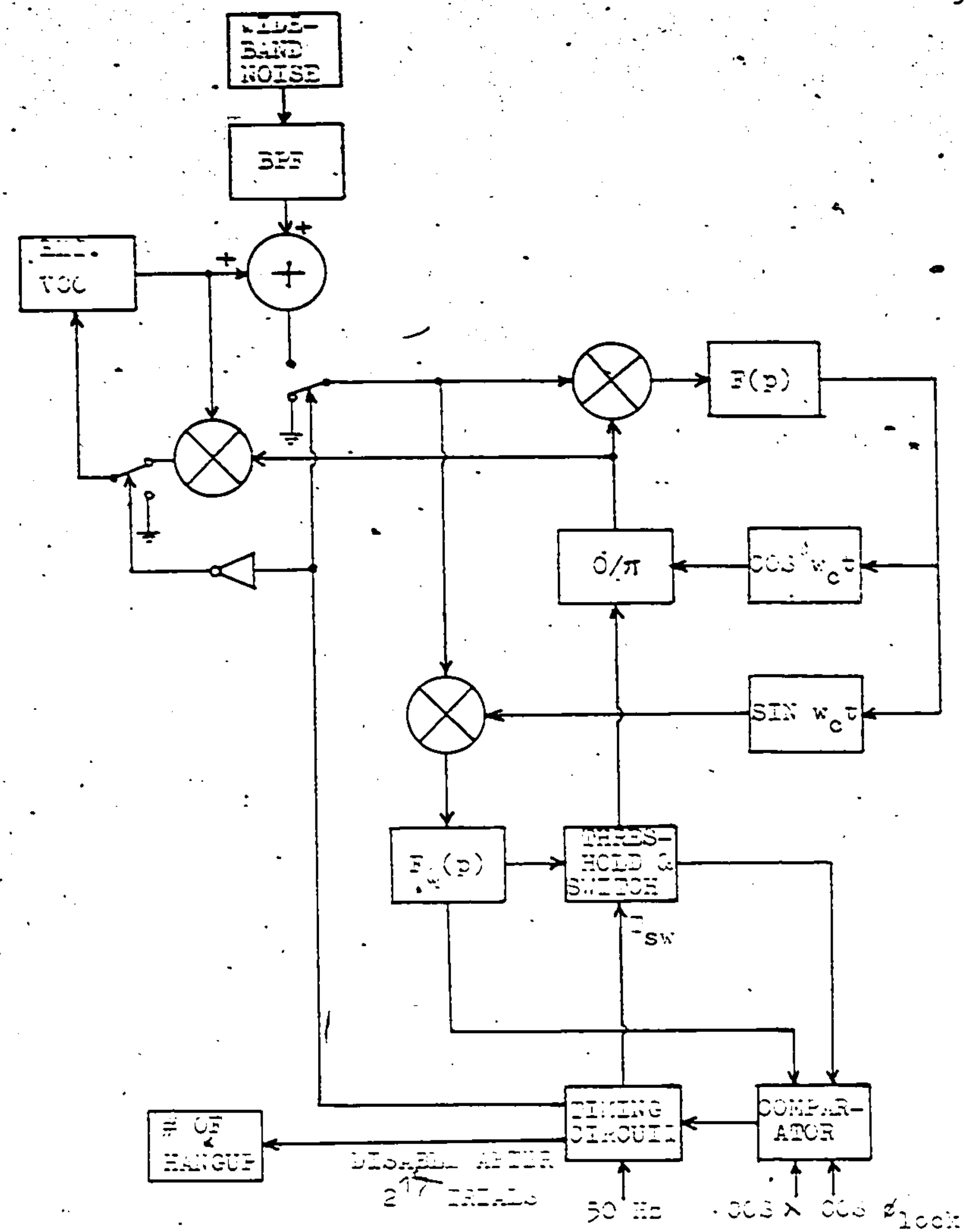

FIG. 6.4 HANGUP TEST CIRCUIT

Poor Copy

external VCO output will force the external VCO to generate $-\sin \omega_c t$. When the system is switched to the set state by the timing circuit, the external VCO input is grounded and the $-\sin \omega_c t$ is input to the limit-switched loop, representing an initial phase error of 180 degrees.

The original definition of hangup is being used in this chapter, that is, hangup is defined as the situation in which the phase error remains inside the switching region after one time constant. The limit-switched loop is allowed to track the input signal until it is locked or until hangup is detected. A timing pulse from the timing circuit allows the loop to switch at multiples of T_{sw} seconds if necessary. In order to detect hangup, output from the quadrature filter is applied to the comparator of the testing circuit after one loop time constant. Occurence of hangup will increase the hangup counter by one and then terminates the trial, while an occurence of phase-lock will only terminate the trial. In both cases a new trial will be initiated until the predetermined number of trials (2^{17} trials) has been reached. Probability of hangup is equal to the number of hangups recorded by the counter divided by the number of trials.

6.3 Design of the Circuits

The loop filter used is the proportional-plus-integral control type. This type of filter is generally used for carrier tracking purpose in the implementation of phase-coherent communication systems. Mechanization of the filter is shown in Fig. 6.2. The transfer function of the filter is

$$F(s) = \frac{s + a}{s + \epsilon}$$

In terms of the loop parameters, it can be easily shown that

$$\omega_n = \sqrt{aAK}$$

$$\xi = \frac{AK + \epsilon}{2\sqrt{aAK}}$$

$$B_L = \frac{AK(AK + a)}{4(AK + \epsilon)} \qquad (6.1)$$

where ω_n, ξ, B_L are the undamped natural frequency, the damping factor and the equivalent one-sided loop noise bandwidth respectively.

The approximations in (6.1) are valid if a is made much greater than ϵ. In most practical designs the loop filter zero is chosen to be located at or near the natural frequency ω_n and ϵ is chosen to be much smaller than the open loop gain AK of the loop.

The parameter values associated with the experimental

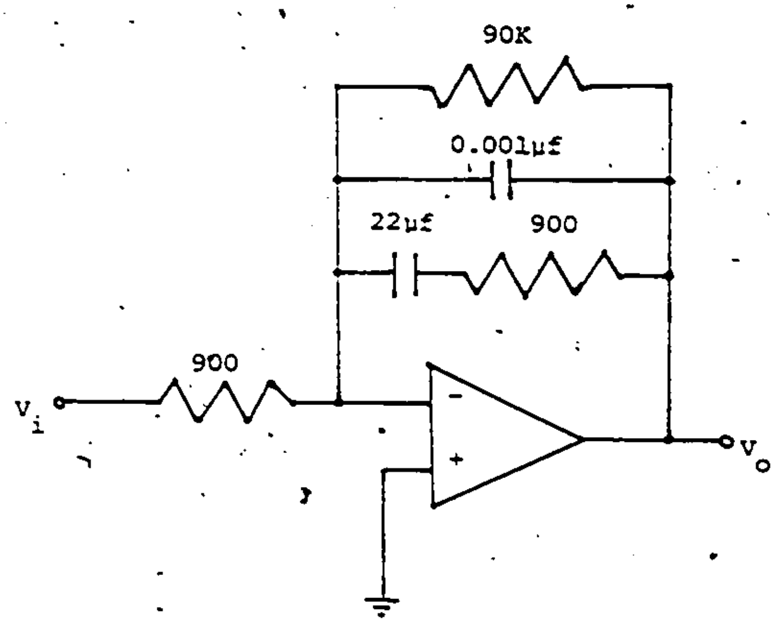

Figure 6.2 Loop filter

loop considered in this paper are $\omega_n = 71.1$ rad./sec., $\xi = 1/\sqrt{2}$, $B_L = 37.4$ Hz.

The second-order Butterworth low-pass filter [22] used as the quadrature filter is shown in Fig. 6.3. The settling time of the filter is given by [23],

$$t_s = \frac{4}{\xi_f \omega_h} \text{ sec.}$$

where ω_h is the 3 dB high frequency cut-off point and is equal to,

$$\omega_h = \frac{1}{R_3 C} \text{ Hz}$$

The low-frequency voltage gain A_{vo} of the operational amplifier and the damping factor ξ_f of the filter are related by,

$$A_{vo} = 3 - 2\xi_f$$

where

$$A_{vo} = \frac{R_2 + R_1}{R_2}$$

The threshold comparator and switching logic circuit used in [11] have been modified and are shown in Fig. 6.4. Consider the condition when Q is LOW, the loop is in its normal mode with 0 degree as the lock-point. The comparator output will be HIGH and causes a switching if $\cos\phi$ is smaller than or equal to $\cos\lambda$, that is, if ϕ falls between

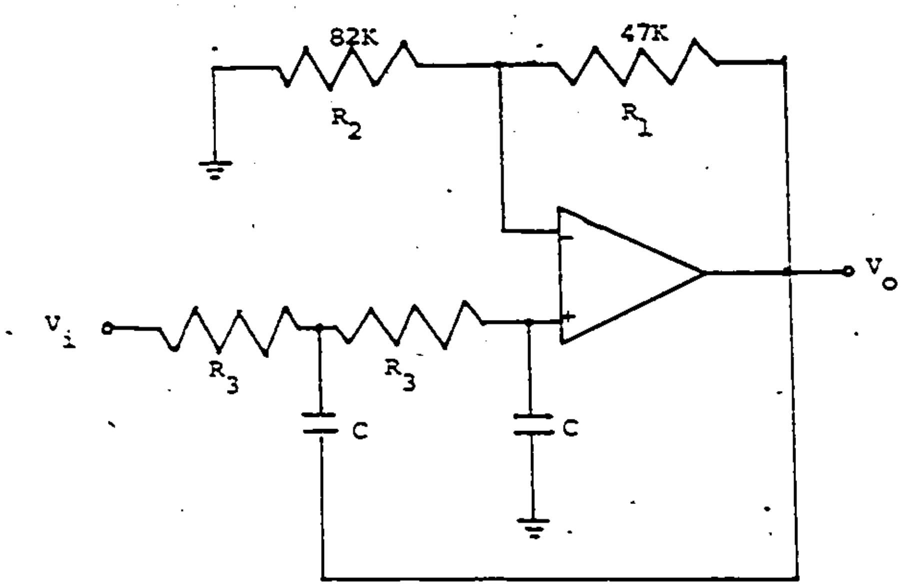

T_{sw},sec.	R_3,KΩ	C,µf
0.001	180	0.001
0.002	330	0.001
0.003	270	0.002
0.004	330	0.002
0.005	470	0.002
0.006	100	0.01
0.007	100	0.012
0.008	150	0.01
0.009	150	0.012

Figure 6.3 Quadraturature filter with settling times

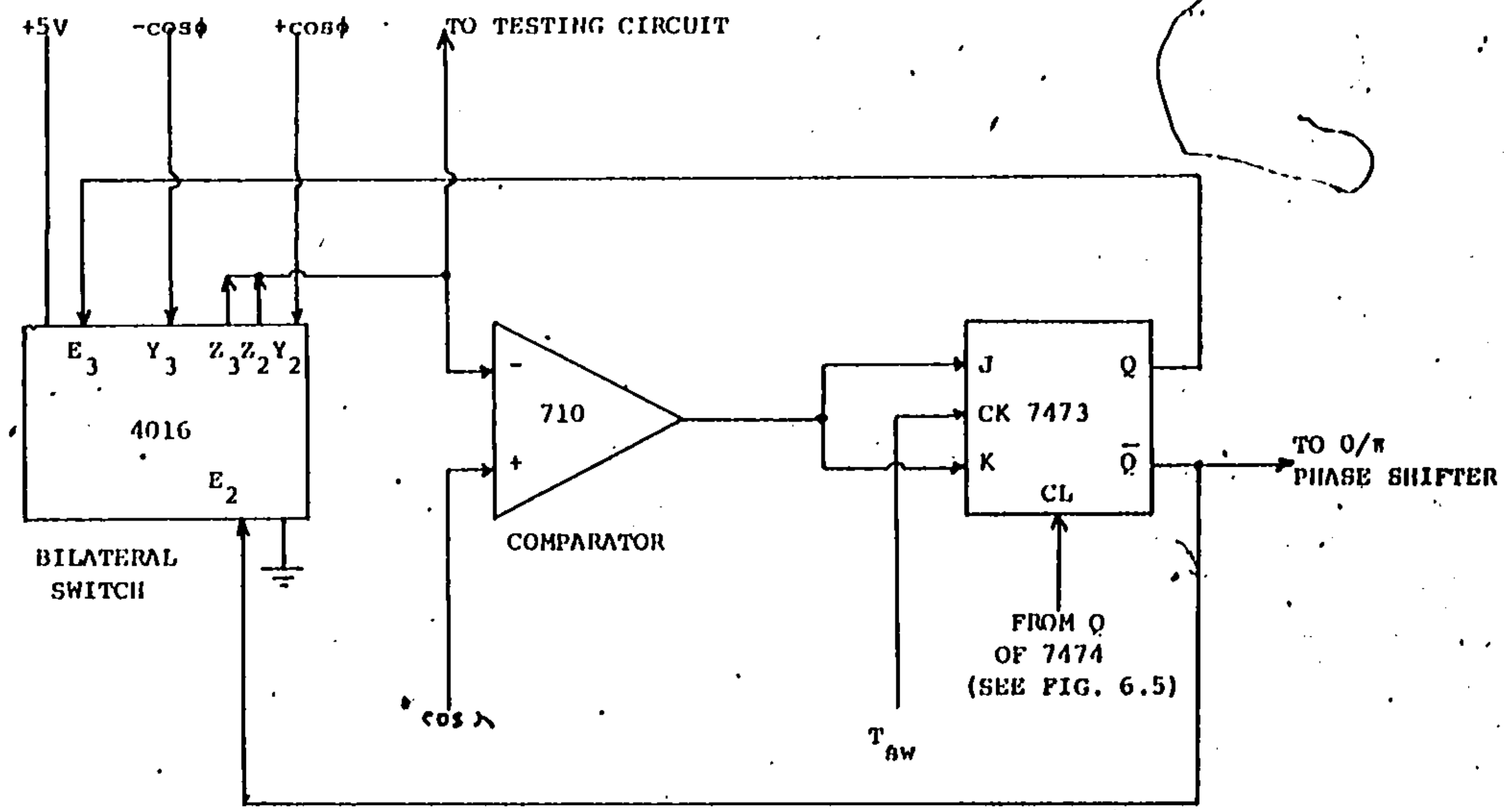

Figure 6.4 Threshold comparator and switching logic circuit

135 and 180 degrees. When Q is HIGH, the loop is in the switched mode with 180 degrees as the lock-point. The comparator output will be HIGH and cause a switching back to the normal mode if $-\cos\phi$ is smaller than or equal to $\cos\lambda$, that is, if ϕ falls between 0 and 45 degrees. In either case, a HIGH in the comparator output represents a hangup and will toggle the flip-flop to the opposite state when it is clocked. The clock frequency is set equal to the reciprocal of the switching time T_{sw} required. The feedback paths from the outputs $(Q,\bar{Q})$ of the flip-flop are required in order to keep track of the operating mode (in switched or nonswitched mode) of the loop so as to provide a correct phase error ($+\cos\phi$ or $-\cos\phi$) to the comparator input.

The threshold comparator and switching logic circuit described by Mariuz [11] tend to give ambiguous switching decisions which in turn will not give correct counts of hangup. When Q is LOW, the loop is operating in its normal mode, $-\cos\phi$ will appear at the positive comparator input, and $+\cos\lambda$ will appear at the negative comparator input. The flip-flop will toggle if $-\cos\phi$ is greater than or equal to $\cos\phi$. Any phase error between 45 to 180 degrees will satisfy this condition and cause a switching. Similarly, when Q is HIGH, the loop is operating in its switched mode, $-\cos\phi$ will appear at the negative comparator input and $-\cos\lambda$ will appear at the positive comparator input. The flip-flop will then toggle if $-\cos\phi$ is smaller than or equal to $-\cos\lambda$, any angle between 0 and 135 degrees will satisfy this condition and switch the loop back to its normal mode. Therefore the phase-switch switches when it should, but it also at times switches when it shouldn't.

As can be seen from Fig. 6.5, the testing circuit consists of two parts. The D-flip-flop and the D-latch form an event control circuit, while the two 710 comparators form a dual comparator [24] which determines whether hangup or phase lock has occured. The upper comparator is used to determine the occurence of phase-lock. Cos ϕ_{lock} is set to 27 degrees (see Chapter 5) and is connected to the negative terminal of the comparator. In the normal mode, $\cos\phi$ is connected to the positive terminal of the comparator. Output of this comparator will be HIGH if $\cos\phi$ is greater than or equal to $\cos\phi_{lock}$ that is, if ϕ is smaller than ϕ_{lock} and equals to LOW otherwise. In the switched mode, $-\cos\phi$ is connected to the positive terminal of the comparator. Output of this comparator will be HIGH if $-\cos\phi$ is greater than or equal to $\cos\phi_{lock}$, that is, if ϕ is smaller than $(180^{o} - \phi_{lock})$. On the other hand, the lower comparator is used to determine the occurence of hangup. Cos λ ($\lambda = 135^{o}$) is connected to the positive terminal of the comparator, therefore, output will be HIGH if ϕ is greater than λ in the normal mode or ϕ is smaller than $(180^{o}$ -

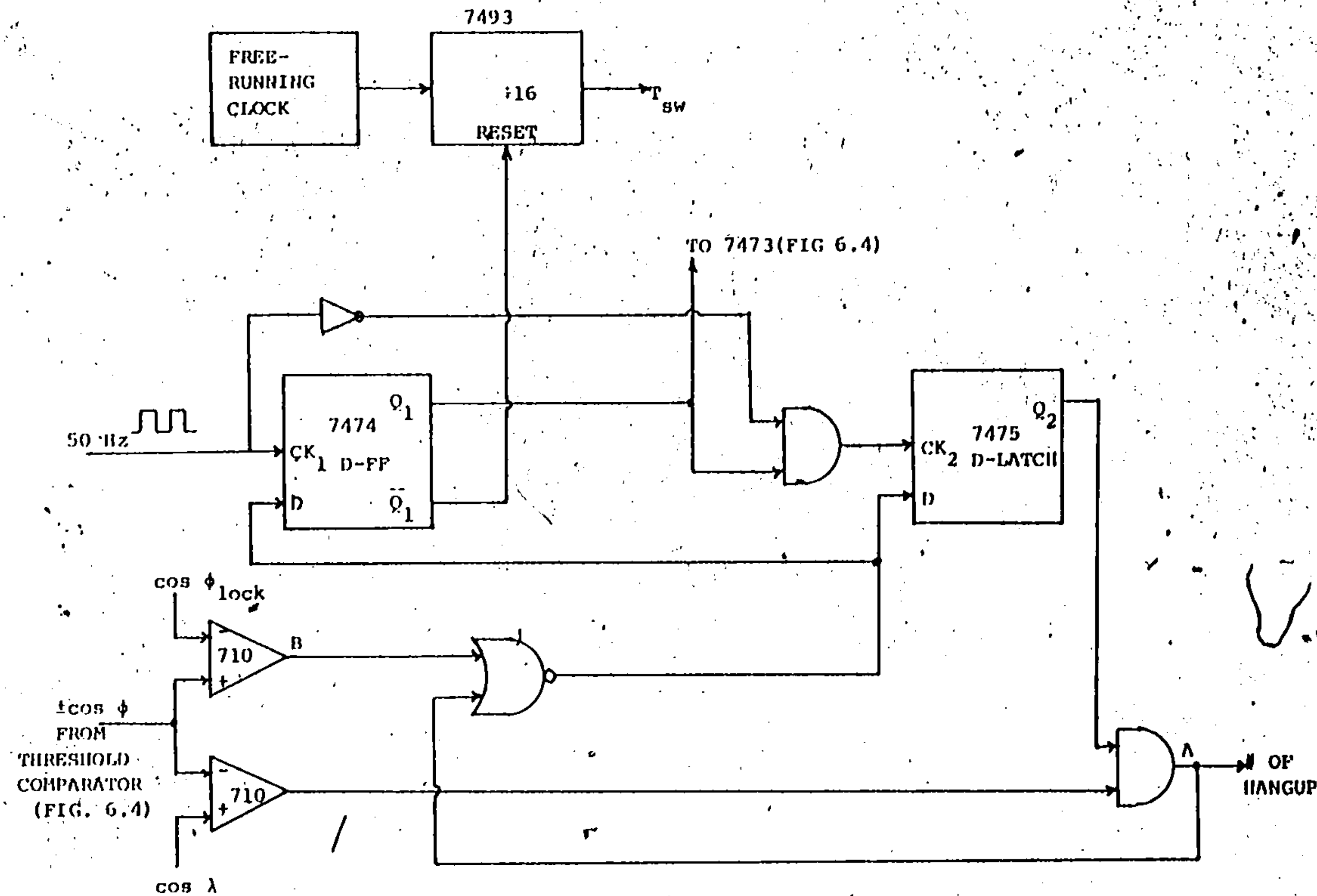

Figure 6.5 Testing circuit

$-\lambda$) in the switched mode and equal to LOW otherwise.

The function of the control circuit is threefold, first, to initiate and terminate a trial; second, to provide a timing pulse to enable the hangup counter after one loop time constant and third, to gate the switching time T_{sw}.

The system is initiated by a HIGH in CK_1 and D, as a result, Q_1 will be HIGH. After 0.01 seconds, CK_1 becomes LOW and CK_2, which is the AND ouptut of CK_1 and Q_1, is now HIGH. Q_1 remains HIGH although CK_1 goes to LOW because a D-flip-flop remembers its state before the clock goes to LOW. Since D and CK_2 are now both HIGH, Q_2 becomes HIGH, this enables the AND gate which controls the input to the hangup counter and now any occurence of hangup can then be recorded. An occurence of hangup results in a HIGH on line A (see Fig. 6.5). Output of the NOR gate, that is D, will therefore become LOW. As D goes to LOW, Q_1 will also go to LOW when it is clocked. Each trial can also be terminated by the occurence of phase-lock. After a trial has been initiated, occurence of a phase-lock will switch the output of the uper comparator to HIGH. As a result, D becomes ~~LOW~~ and then Q_1 will also be LOW when clocked and this will terminate the trial. The whole process will repeat again and again until 2^{17} trials have been performed. A timing diagram of the testing event is shown in Fig. 6.6.

The switching time T_{sw} is gated by a reset pulse from

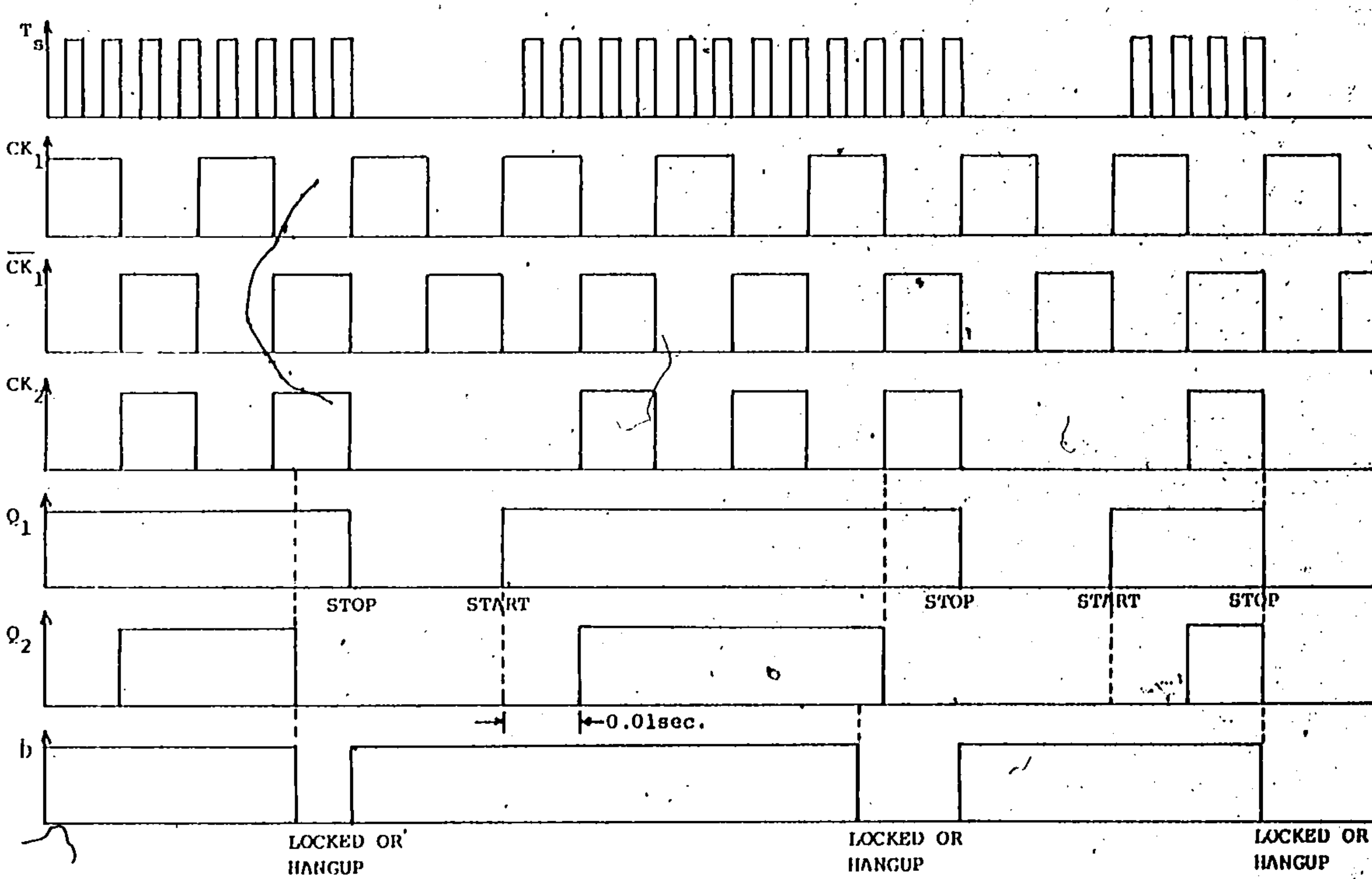

Figure 6.6 Timing diagram

the D-flip-flop $\bar{Q}$ output. The free-running clock has a variable frequency from 1778 Hz to 16 KHz, which when divided by 16 will give a switching time T_{sw} of 0.009 to 0.001 seconds. A frequency divider following the free-running clock is used to obtain an accurate delay between the reset pulse and the occurence of the first clock pulse at the toggle flip-flop input.

Details of the four-quadrant multiplier, two phase voltage-control oscillator and the 0 or π phase shifter can be found in [25] and [11].

6.4 Comparison of the Experimental and Simulation Results

The experimental results are shown in Fig. 6.7 and plotted against the simulation results in Fig. 6.8. Each result represents an average of five repeated measurements, each consists of 2^{17} trials.

It is interesting to note that all three curves revealed the same general shape, with a peak around 0.005 seconds and a dip around 0.003 and 0.001 seconds. This implies that a switching time between 0.001 to 0.003 seconds appears to be the best choice for this particular loop, while a switching time of 0.005 seconds should be avoided. Discrepancies between the 15 dB simulation and experimental curves can be explained by the fact that the noise source used in the simulation is almost perfectly Gaussian in

T_{sw}, sec	EXPERIMENTAL RESULTS LOOP SNR=15dB	SIMULATION RESULTS	
		LOOP SNR=6dB	LOOP SNR=15dB
0.001	0.032	0.04016	0.05882
0.002	0.041	0.00971	0.07031
0.003	0.046	0.01786	0.05976
0.004	0.038	0.04464	0.06796
0.005	0.083	0.1119	0.1327
0.006	0.042	0.08397	0.1282
0.007	0.040	0.07813	0.1102
0.008	0.049	0.07576	0.06723
0.009	0.044	0.07914	0.06818

Figure 6.7 Experimental and simulation results

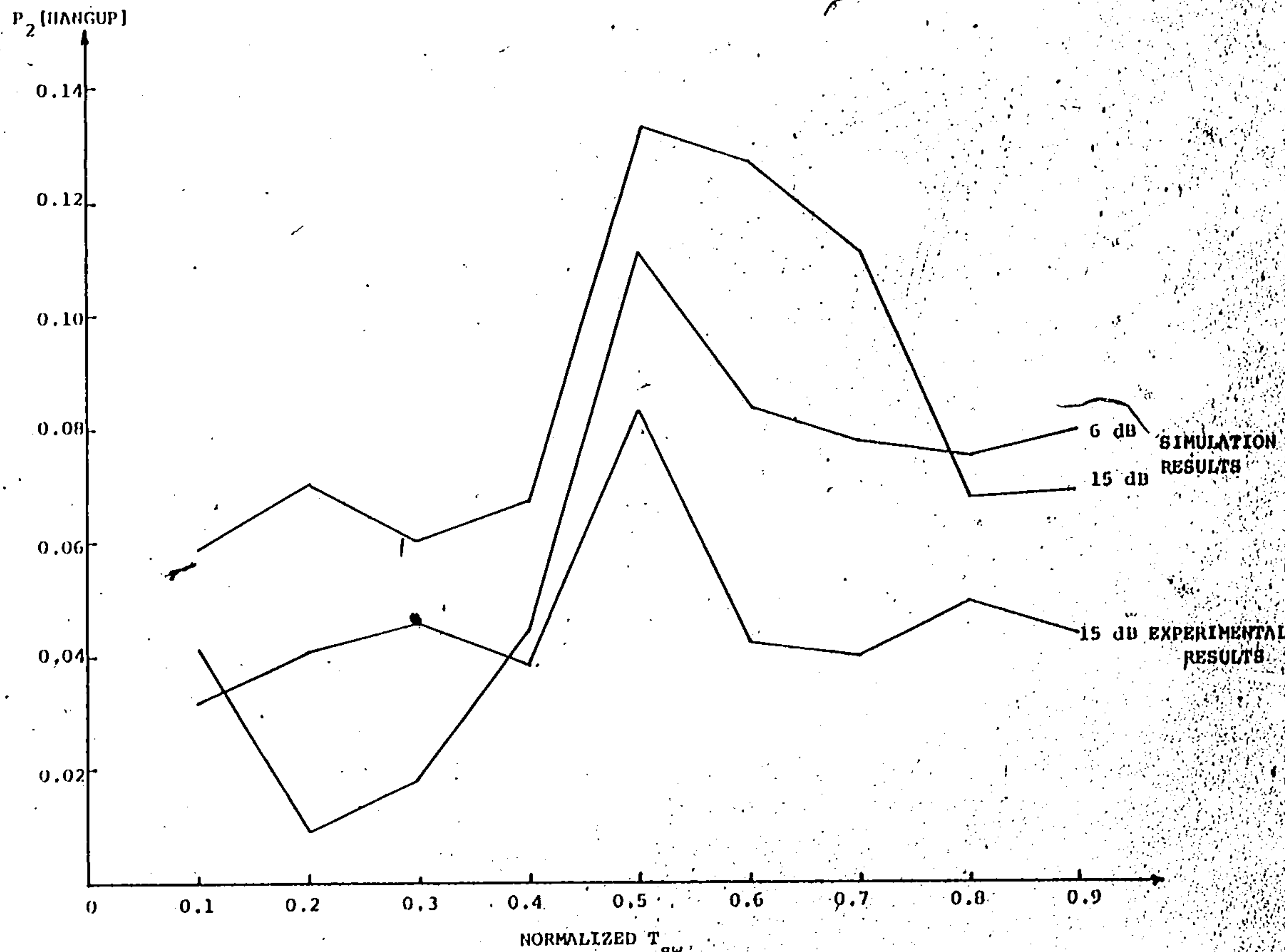

Figure 6.8 Experimental and simulation results

nature while the noise generator used in the experiment is not. Also, the accuracy of components, tuning of the circuits and other disturbances all perturb the experimental results to a certain extent. However, both methods have indicated that the limit-switched loop has greatly reduced the number of hangups.

It must be pointed out that the results obtained by these two methods represent the worst case with an initial phase error of 180 degrees. In real life, the initial phase errors are uniformly distributed and the probability of hangups should therefore be greatly lowered.

CHAPTER 7

CONCLUSIONS

7.1 Conclusion

It has been demonstrated in this thesis by simulation and by experimental results that the limit-switched loop offers a lower probability of hangup and a faster acquisition time than a conventional phase-locked loop.

In this thesis, the initial phase error input, the definition of hangup and the range of SNRs used in the simulation and experiments are so chosen as to obtain meaningful results without the necessity of performing a large number of trials. Because of these factors, results obtained represent the worst case. In practice, the initial phase inputs are randomly distributed. Also if phase-lock is required to be achieved within two or three loop time constants rather than one, the loop will be practically hangup-free after two loop time constants. In satellite communications, an input SNR of 15 to 20 dB is typical and can be achieved easily. This is equivalent to a loop SNR of 29 to 34 dB for this particular loop. The simulation results have shown that for a second-order loop with a loop SNR of 27 dB, the probability of hangup at one loop time constant is unmeasurably small. Therefore, higher performance is expected when the loop is used in a real system.

The loop used in this thesis is a low-frequency model. This is mainly because it is easier to simulate and to implement. A satellite communication system typically might have an IF centre frequency of about 140 MHz and an IF bandwidth of 70 MHz. Assuming a limit-switched loop with a noise bandwidth of 70 KHz is used to track the doppler shift, then with the switching time T_{sw} set equal to one-third of the loop time constant (which is within the optimum range of T_{sw} found in this thesis), a switching speed of 1.2 μ sec. is required. This switching speed is well below the gate delay limit of TTL logic, which is typically 6 to 33 nsec. and of that of CMOS logic, which is 25 to 35 nsec. Therefore it can be concluded that the limit-switched loop is not frequency sensitive. The limit-switched loop principle can also be extended to the Costas loop or QPSK carrier recovery loop, offering the same advantages.

A limit-switched loop outperforms a phase-locked loop, offering a shorter phase acquisition time and low probability of hangup with only a few additional circuits. However, with the rapid development of medium scale integration (MSI) and large scale integration (LSI) IC technology, the cost for producing a limit-switched loop can be expected to be the same as for a phase-locked loop. It is reasonable to conclude that a limit-switched loop can be used to replace a phase-locked loop where fast phase acquisition and low probability of hangup are required, without increasing the cost or complexity of the system.

APPENDIX A

REDUCTION OF THE FOKKER-PLANCK EQUATION

Equation (4.4) is rewritten here

$$(1+\tau_2 s)\ \{\tau_1 \frac{d^2x(t)}{dt^2} + \frac{dx(t)}{dt} + AK \sin [\tau_2 \frac{dx(t)}{dt}$$

$$+ x(t)] \cos S(U) + K\, n(t)\} = 0$$

Defining

$$L(x) \triangleq \tau_1 \frac{d^2x(t)}{dt^2} + \frac{dx(t)}{dt} + AK \sin [\tau_2 \frac{dx(t)}{dt} + x(t)] \cos S(U)$$

we then have to prove that

$$L(x) + Kn(t) = 0$$

is sufficient to characterize the solution of $\phi(t)$. Suppose

$$(1 + \tau_2 \frac{d}{dt})\ (L(x) + Kn(t)) = 0$$

and

$$L(x) + Kn(t) = \epsilon(t) \neq 0$$

Then we must have

$$\epsilon(t) + \tau_2 \dot{\epsilon}(t) = 0$$

or

$$\epsilon(t) = \epsilon_o \exp(-t/\tau_2)$$

If we define the initial conditions on x(0) such that

$$L[x(0)] + Kn(0) = 0 \qquad \text{(A.1)}$$

then $\varepsilon_o = 0 \rightarrow \varepsilon(t) = 0, \forall t$, contradicting the assumption that $\varepsilon(t) \neq 0$. And if $\dot{\varepsilon}(t) = 0, \forall t$, then we only have to solve the reduced equation

$$L(u) + Kn(t) = 0$$

Now we must show that there exists a $x(0)$ which is compatible with the initial condition on $\phi(t)$, that is, $\phi(0) = \dot{\phi}(0) = 0$.

Equation (A.1) is rewritten as

$$\tau_1 \frac{d^2x(0)}{dt^2} + \frac{dx(0)}{dt} + AK \sin\left[\tau_2 \frac{dx(0)}{dt} + x(0)\right] = -Kn(0) \quad (A.2)$$

and we than have

$$\phi(0) = 0 \rightarrow \tau_2 \frac{d^2x(0)}{dt^2} + x(0) = 0 \rightarrow \frac{dx(0)}{dt} = -\frac{1}{\tau_2} x(0) \quad (A.3)$$

$$\dot{\phi}(0) = 0 \rightarrow \tau_2 \frac{d^2x(0)}{dt^2} + \frac{dx(0)}{dt} = 0 \rightarrow \frac{d^2x(0)}{dt^2} = \left(\frac{1}{\tau_2}\right)^2 x(0) \quad (A.4)$$

Substituting (A.3) and (A.4) into (A.2), we have

$$\tau_1 \left(\frac{1}{\tau_2}\right)^2 x(0) - \frac{b}{\tau_2} x(0) + AK \sin[-x(0) + x(0)] = -Kn(0) \quad (A.5)$$

It can clearly be seen that there exists such a $x(0)$ which satisfies (A.5).

Last of all, we will have to show that $\phi(t)$ is independent of $x(0)$, which will complete the proof. From (4.3)

$$\phi(t) = \tau_2 \frac{dx(t)}{dt} + x(t) \tag{A.6}$$

Solving for x(t), we obtain

$$x(t) = x(0) \exp(-t/\tau_2) + \exp(-t/\tau_2) \int^t \phi(u) \exp(u/\tau_2)\, du \tag{A.7}$$

Defining

$$x_o(t) \triangleq \exp(-\tau/t_2) \int^t \phi(u) \exp(u/\tau_2)\, du$$

Using (A.7) and (A.8) in (A.6) yields

$$\phi(t) = -x(0) \exp(-t/\tau_2) + \tau_2 \frac{d}{dt} [\exp(-t/\tau_2) \int^t \phi(u)$$

$$\exp(u/\tau_2)\, dx + x(0) \exp(-t/\tau_2) + \exp(-t/\tau_2)$$

$$\int^t \phi(u/\tau_2)\, du = [1 + \tau_2 \frac{d}{dt}] x_o(t)$$

It can be seen that $\phi(t)$ does not depend on x(0). Therefore, the proof has been completed and the reduced equation completely characterises the original solution.

APPENDIX B

```
      PROGRAM HANGUP(INPUT,OUTPUT,TAPE5=INPUT,TAPE6=OUTPUT)
C
C  PROBABILITY OF HANGUPS IN SECOND ORDER LIMIT-SWITCHED LOOPS.
C  WITH F(S) = 1+A/S
C  SNR=15.0 DB
C
      DIMENSION VNOSIN(3000),VNOSQ(3000),VOF(3000),SUM(100)
      REAL NCOUNT,LAMDA,J1
      INTEGER FLAG
C
C     DEFINE CONSTANTS.
      NTRIAL = 100
      A = 0.0576
      AKK = 100.0
      FA = 50.0
      BL = (AKK+FA)/4.0
      FN = BL/3.35
      PLOCK = 0.47
      DELTAT = 0.00003
      TSET = 0.001
      SYNCT = 0.01
      TOTIME = 0.0
      NCOUNT = 0.0
      NTEST = 0
      PI = 4.0*ATAN(1.0)
      PHANG = PI*3.0/4.0
      LAMDA = PI*3.0/4.0
      P1 = 0.0
      P2 = 0.0
      P3 = 0.0
      P4 = 0.0
      WGN = 2.0*PI*900.0
      CON2 = 2.0*WGN*DELTAT/SQRT(2.0)
      CON1 = 1.0/(1.0+CON2)
      CON3 = (DELTAT*WGN)**2.0
      THRES = A*COS(LAMDA)
C
C     CLEAR ARRAYS.
      DO 50 M=1,100
      SUM(M)=0.0
   50 CONTINUE
      WRITE (6,700)
```

```
C
C     START THE SIMULATION FOR NTRIAL TIMES.
      DO 10 I = 1,NTRIAL
      N = I + 200
      PHI = PI
      PHIOP = PHI*180.0/PI
      T = 0.0
      TS= 0.0
      JO= 0.0
      IN = I + 10
      CALL RANGAU(VNOSIN,3000,IN,0.25)
      IN = IN + 1
      CALL RANGAU(VNOSQ,3000,IN,0.25)
      JTIME = SYNCT/DELTAT
      VOF(401) = 0.0
      VOF(402) = 0.0
C
C     START TRACKING UNTIL T-SYNCT,TIME TO TEST FOR HANGUP.
      FLAG =0
   11 DO 20 J = 1,JTIME
      L = J + 400
C
C     RESTRAINT THE ANGLES BETWEEN (-180,180) DEGREES.
      IF (SIN(PHI) .LT. 0.0) GO TO 33
      IF (COS(PHI) .LT. 0.0) GO TO 22
      PHI = ACOS(COS(PHI))
      GO TO 5
   22 PHI = PI/2.0+ASIN(ABS(COS(PHI)))
      GO TO 5
   33 IF (COS(PHI) .GT. 0.0) GO TO 44
      PHI = -(PI/2.0+ACOS(ABS(SIN(PHI))))
      GO TO 5
   44 PHI = -(ACOS(COS(PHI)))
C
C     START ITERATIONS
    5 J1 = JO+DELTAT*FA*AKK*(SIN(PHI)+VNOSIN(L)/A)
      PHIN = PHI-DELTAT*(J1+AKK*(SIN(PHI)+VNOSIN(L)/A))
      VIF = A*COS(PHI)+VNOSQ(L)
      VOF(L+2) = CON1*(-VOF(L)+2.0*VOF(L+1)+CON2*VOF(L+1)
     1           -CON3*(VOF(L+1)-VIF))

      U = VOF(L+2) - THRES
      T = TS+DELTAT
      PHI = PHIN
      JO = J1
C
C     CHECK FOR LOCKED CONDITION
      IF (ABS(PHI) .LE. PLOCK) GO TO 88
      IF(TS .LT. TSET) GO TO 20
      TS = 0.0
```

```
C
C     IF U IS .GE. 0.0,DON'T SWITCH.
      IF (U .GE. 0.0) GO TO 30
      IF ABS (PHI) .GT. LAMDA) GO TO 55
      P4 = P4 + 1.0
      GO TO 66
   55 P3 = P3 + 1.0
      GO TO 66
   30 IF (ABS(PHI) .GT. LAMDA) GO TO 77
      P2 = P2+1.0
      GO TO 20
   77 P1 = P1+1.0
      GO TO 20
   66 IF (PHI .GE. 0.0) GO TO 99
      PHI = -(PI+PHI)
      GO TO 20
   99 PHI = PI-PHI
   20 CONTINUE
C
C     CHECK FOR HANGUP CONDITION.
      GLAG = 1
      NTEST = NTEST + 1
      IF (PHI .LT. PHANG) GO TO 11
      NCOUNT = NCOUNT + 1.0
      DEG = PHI*180.0/PI
      WRITE (6,100) I
      WRITE (6,200) NCOUNT,DEG,T,U,PHIOP
      GO TO 11
   88 TOTIME = TOTIME+T
      IF (FLAG .EQ. 1) GO TO 60
      NTEST = NTEST + 1
   60 T = T*FN*100.
      DO 90 K =1,100
      IF ((T .LT. (K-1)) .OR. (T .GE. K)) GO TO 90
      SUM(K) = SUM(K)+1.0
   90 CONTINUE
   10 CONTINUE
C
      TTL = P1+P2+P3+P4
      P1 = P1/TTL
      P2 = P2/TTL
      P3 = P3/TTL
      P4 = P4/TTL
      WRITE (6,300) P3,P4,P1,P2
      AVTIME = TOTIME/NTRIAL
      PROB = NCOUNT/NTEST
      WRITE (6,400) PROB,AVTIME
      WRITE (6,500)
      DO 40 M=1,100
      PERCEN =0.0
```

```
      TIME = M/100.
      DO 80 KK =1,M
      PERCEN = PERCEN+SUM(KK)
   80 CONTINUE
      PERCEN = PERCEN*100.0/NTRIAL
      WRITE (6,600) TIME,PERCEN
   40 CONTINUE
C
  100 FORMAT(//" TRIAL NUMBER ",IF)
  200 FORMAT(" HANGUP NO. ",F5.0,4X,"AT ",E10.4,"DEGS. AND AT
     1 ",E10.4,"SEC."/" U= ",E10.4,4X,"INITIAL PHASE= ",
     2E10.4,"DEGS.")
  300 FORMAT (///" PROB. OF SWITCH WHEN SHOULD = ",E10.4/.
     1" PROB. OF SWITCH WHEN SHOULDN'T = ",E10.4/
     2" PROB. OF NON-SWITCH WHEN SHOULD = ",E10.4/
     3" PROB. OF NON-SWITCH WHEN SHOULDN'T = ",E10.4/)
  400 FORMAT (//" PROBABILITY OF HANGUPS = ",E10.4,5X,
     1"AVERAGE ACQ. TIME =",E10.4,"SECS.")
  500 FORMAT (///14X,"TIME,T,SECS.",10X,"PERCENTAGE OF ACQ.
     1TIME .LT. T")
  700 FORMAT (1H1,20X," SIMULATION OF SECOND ORDER LIMIT-
     1SWITCHED LOOP"/40X," SNR=15.0 DB"///)
  600 FORMAT(11X,F10.5,"/FN",18X,F10.4)
      STOP
      END
```

REFERENCES

[1] J.G. Puente, W.G. Schmidt, A.M. Werth, "Multiple Access for Commercial Satellites", Proceedings of the IEEE, vol. 59, pp. 218-229, February 1971.

[2] T. Sekimoto and J.G. Puente, "A Satellite Time-Division Multiple Access Experiment", IEEE Trans. Commun., vol. COM-16, pp. 581-588, August 1968.

[3] R.M. Hultberg, F.H. Jean, M.E. Jones, "Time Division Access for Military Communication Satellite", IEEE Trans. Aerosapce Electronic Syst., vol. AES-1, pp. 272-282, December 1965.

[4] O.G. Gabbard, "Design of a Satellite Time Division Access Burst Synchronizer", IEEE Trans. Commun., vol. COM-16, pp. 589-596, August 1968.

[5] O.G. Gabbard and P. Kaul, "Time-Division Multiple Access", Proceedings of EASCON, pp. 179-183, 1974.

[6] F.M. Gardner, "Hangup in Phase-Lock Loops", IEEE Trans. Commun., vol. COM-25, pp. 1210-1212, October 1977.

[7] F.M. Gardner, "Carrier and Clock Syncrhonization for TDMA Digital Communications", ESTEC Preliminary working Paper 733534 (Rev. 2), European Space Research Organization, Noordwijk, Netherlands, June 1974.

[8] F.G. Splitt, "Design and Analysis of a Linear Phase-Locked Loop of Wide Dynamic Range", IEEE Trans. Commun., vol. COM-14, pp. 432-440, December 1966.

[9] J.J. Spilker, "Digital Communications by Satellite", Englewood Cliffs, N.J.: Prentice-Hall, 1977.

[10] J.P. Frazier and J. Page, "Phase-Locked Loop Frequency Acquisition Study", IRE Trans. Space Electronics and Telemetry, vol. SET-8, pp. 210-227, September 1962.

[11] S. Mariuz, "The Limit-Switched Loop: an Improved Carrier Recovery Algorithm for Burst Mode Operation", CRL-47, June 1977.

[12] W.C. Lindsey, "Synchronization Systems in Communications and Control", Englewood Cliffs, N.J.: Prentice-Hall, 1973.

[13] A.J. Viterbi, "Principles of Coherent Communications", New York: McGraw-Hill, 1966.

[14] W.H. Tranter and R.E. Ziemer, "Principles of Communications: Systems, Modulation and Noise", Boston: Houghton Mifflin, 1976.

[15] J.E. Ohlson and A. Rutherford, "Transient Statistics of the First-Order Phase-Locked Loop", IEEE Trans. Commun., vol. COM-22, pp. 698-703, May 1974.

[16] G.E. Uhlenbeck and L.S. Ornstein, "On the theory of Brownian Motion", Phys. Rev., vol. 36, pp. 823-841, September 1, 1930.

[17] K.E. Dominiak and R.L. Pickholtz, "Transient Behaviour of a Phase-Locked Loop in the Presence of Noise", IEEE Trans. Commun., vol. COM-18, pp. 452-456, August 1970.

[18] D.R. Hummels, "Some Simulation Results for the Time to Indicate Phase Lock", IEEE Trans. Commun., vol. COM-20, pp. 37-43, February 1972.

[19] S.L. Goldman, "Second-Order Phase-Lock-Loop Acquistion Time in the Presence of Narrow-Band Gaussian Noise", IEEE Trans. Commun., vol. COM-21, pp. 297-300, April 1973.

[20] F.J. Charles and W.C. Lindsey, "Some Analytical and Experimental Phase-Locked Loop Results for Low Signal-to-Noise Ratios", Proceedings of the IEEE, vol. 54, September 1966.

[21] G.B. Clayton, "Linear Integrated Circuit Applications", London: McMillan Press Ltd., 1975.

[22] J. Millman and C. Halkias, "Integrated Electronics: Analog and Digital Circuits and Systems", New York: McGraw-Hill, 1972.

[23] R.C. Dorf, "Modern Control Systems", Mass: Addison-Wesley, 1974.

[24] W.G. Jung, "IC Op-Amp Cookbook", 1st edition, Indianapolis: H.W. Sams, 1974.

[25] Nonlinear Circuit Handbook. Engineering Staff of Analog Devices Inc., D.H. Sheingold, Ed. Norwood, Mass: Analog Devices Inc., 1976.